ENERGY LABORATORY

MASSACHUSETTS INSTITUTE
OF TECHNOLOGY

THE USE OF BURNABLE POISON TO IMPROVE URANIUM UTILIZATION IN PWRs

W. T. Loh
M. J. Driscoll
D. D. Lanning

DOE Contract No.DE-AC02-79ET34022 (Nuclear Engineering Department Report No. MITNE-250
Energy Laboratory Report NO. MIT-EL-82-014

May, 1982

DOE/ET/34022-3
MITNE-250
MIT-EL-82-014

THE USE OF BURNABLE POISON TO IMPROVE URANIUM UTILIZATION IN PWRs

W. T. Loh
M. J. Driscoll
D. D. Lanning

DOE Contract No.DE-AC02-79ET34022 (Nuclear Engineering Department Report No. MITNE-250 Energy Laboratory Report NO. MIT-EL-82-014

May, 1982

DOE/ET/34022-3

THE USE OF BURNABLE POISON TO IMPROVE URANIUM UTILIZATION IN PWRs

by

W. T. Loh
M. J. Driscoll
D. D. Lanning

Department of Nuclear Engineering

and

Energy Laboratory

Massachusetts Institute of Technology

Cambridge, Massachusetts 02129

Sponsored by:

U.S. Department of Energy

Division of Energy Technology

Under Contract No. DE-AC02-79ET34022

NOTICE

Printed in the United States of America

Available from:

National Technical Information Service
U.S. Department of Commerce
5285 Port Royal Road
Springfield, VA 22152

Distribution

R. Crowther
Project Manager
General Electric Company
175 Curtner Company
San Jose, California 95125

Dr. Peter M. Lang, Chief
LWR Branch
Division of Nuclear Power Development
US Dept. of Energy, Mail Stop B-107
Washington, D.C. 20545 (5 copies)

N. L. Shapiro
Manager, Advanced Design Projects
Combustion Engineering, Inc.
1000 Prospect Hill Road
Windsor, CT 06-95

W. L. Orr
Manager of Product Development Support
Nuclear Fuel Division
Westinghouse Electric Corp.
P.O. Box 355
Pittsburgh, PA 15230

Dr. Richard B. Stout
Nuclear Fuels Engineering Dept.
Exxon Nuclear
2101 Horn Rapids Road
Richland, W 99352

V. Uotinen
Project Manager
The Babcock & Wilcox Co.
P.O. Box 1260
Lynchburg, VA 24505

ABSTRACT

A methodology based on the linear reactivity model of core behavior has been developed and employed to evaluate fuel management tactics for improving uranium utilization in Pressurized Water Reactors in a once-through fuel cycle mode on a consistent basis. A major focus has been on the benefit of using burnable poison in conjunction with low-leakage fuel management schemes. Key features in the methodology, such as power weighting of batch reactivity values and correlation of neutron leakage effects with peripheral assembly power, were verified against results generated using detailed state-of-the-art computer analyses. A relation between batch power fraction and batch reactivity was derived from a 1½-group diffusion theory model, and similarly validated. These prescriptions have been used in two ways: to develop analytical models which allow quick scoping calculations; and, programmed into a code, to facilitate more rigorous applications.

The methodology has been applied to evaluate fuel management schemes of contemporary interest, such as the use of burnable poison to shape the power history profile, the use of low-leakage fuel loading patterns, and extended cycle length/burnup, and combinations of these individual schemes.

It was found that shaping of the power history profile in a low-leakage assembly pattern by means of burnable poison, even after accounting for the anticipated residual poison reactivity penalty, has the potential of increasing PWR discharge burnup, and hence uranium utilization by roughly 1%. The overall improvement in uranium utilization for a low-leakage loading over that for the current out-in/scatter scheme, was about 3.6% for current cycle lengths (3-batch, discharge burnup ~ 30,000 MWD/MT), and approximately 11.1% for extended cycle operation (3-batch, discharge burnup ~ 50,000 MWD/MT).

ACKNOWLEDGEMENTS

The work presented in this report has been performed primarily by the principal author, Wee Tee Loh, who has submitted substantially the same report in partial fulfillment of the requirements for the Ph.D. degree in Nuclear Engineering at M.I.T.

The principal author, in particular, wishes to thank Professor Allen F. Henry, Dr. Joseph Sefcik, Martin Plys, Christopher Hoxie, Thomas Downar, Eduardo Montaldo-Volachec, Ildo Sauer and Mushtaq Malik for their valuable comments and useful discussions concerning the physics and methodology employed in this work; and of course, his special thanks to Altamash Kamal who, during the last four years, has been a very good and helpful co-worker, and a fine friend.

The financial support provided by the U.S. Department of Energy (Division of Nuclear Power Development) which made this work possible is much appreciated. The assistance of Rachel Morton on computational problems is gratefully acknowledged. Computer services were provided by the facility at the M.I.T. Laboratory for Nuclear Sciences.

The authors would also like to express their appreciation for the cooperation of Dr. Edward Pilat of the Yankee Atomic Electric Company in facilitating the acquisition of descriptive data from publicly available documentation on the Maine Yankee Reactor. Although the information in this report is referred to as deriving from "Maine Yankee," it should not be considered as representing that actual system in its present or projected operating configuration, but as an idealization thereof. It should be noted that the results in this report have not been either reviewed or approved by the Yankee Organization.

Typing of the manuscript was most expertly done by Ms. Wynter Snow, with the assistance of Ms. Mia Saunders. Our thanks to them.

TABLE OF CONTENTS

TABLE OF CONTENTS (continued)

TABLE OF CONTENTS (continued-3)

TABLE OF CONTENTS (continued-4)

LIST OF FIGURES

LIST OF FIGURES (continued)

LIST OF FIGURES (continued-3)

LIST OF FIGURES (continued-4)

LIST OF TABLES

LIST OF TABLES (continued)

LIST OF TABLES (continued-3)

CHAPTER 1

INTRODUCTION

1.1 FOREWORD

There has been considerable interest of late in the achievement of higher fuel burnup in light water reactors due to a convergence of motivating factors: a desire to improve uranium utilization, particularly in view of the slower than anticipated implementation of fuel reprocessing and the delayed development of breeder reactors (due in part to a concern in some quarters over the attendent commerce in weapons-usable materials); and the interest by utilities in extending the length of the burnup cycle to increase plant capacity factor, reduce replacement energy costs, alleviate the impending shortage of spent fuel storage space, and decrease staff effort on reload licensing activities. In response to these concerns the U.S. Department of Energy (DOE) and the nuclear industry have collaborated to evaluate and prove-out modifications in LWR fuel design and fuel management strategy to permit the attainment of high burnup. MIT has participated in this program, sponsored by the DOE and its precursor, the Energy Research and Development Administration (ERDA), initially as part of the effort in support of the NASAP (Nonproliferation Alternative Systems Assessment Program) and INFCE (International Nuclear Fuel Cycle Evaluation) assessments, but most recently as part

of the DOE's LWR Technology Program for Improved Uranium Utilization.

Recent MIT work, including that reported here, has been concerned with the self-consistent evaluation of ways to facilitate the realization of high burnup and high neutron economy. A major focus of the present effort is on development of an optimum strategy for the use of a generalized burnable poison to alleviate the power peaking which typically characterizes high burnup assembly designs and core arrangements.

The present work is an extension of prior efforts at MIT [G-1, F-1, C-1, K-1, S-2], and, as with other recent efforts here and elsewhere, is limited to readily backfittable innovations applicable to the once-through mode of fueling. While cost of energy is the ultimate objective function for optimization, the subsidiary goal of improving natural uranium utilization will often suffice, since yellowcake accounts for on the order of half of the levelized lifetime fuel cycle cost projected for LWR's scheduled for startup in the mid-1980's [G-2].

The applications examined in this report are limited to PWRs since these reactors have captured two-thirds of the U.S. and one-half of the world markets for large central station nuclear units. Moreover the closely-related BWR accounts for the remaining one-third of the U.S. roster, and one-quarter of the world's. In addition the PWR has become the reactor of choice for many countries which originally selected other

types, such as the USSR, and very recently the United Kingdom, and for other nations just embarking on a nuclear power program, such as mainland China.

1.2 BACKGROUND AND PREVIOUS WORK

Over the past twenty years the discharge burnup of LWR fuel has risen steadily at a rate of nearly 1000 MWD/MT per year -- due in part to the inherently lower burnup of startup batches, but also to a growing emphasis on the attainment of higher steady state burnups [T-1]. The average of current performance specifications is approximately 31,000 MWD/MT. Steady state burnup can be related directly to uranium utilization efficiency. This parameter will be defined here as the total amount of electric energy produced per unit of natural uranium used [D-2]:

$$U\left(\frac{\text{kWh}}{\text{lb } U_3O_8}\right) = 9.231 \frac{(x_F - x_W)\,\eta B_{dis}}{(x_p - x_W)} \qquad (1.1)$$

where η is the net thermodynamic efficiency of the plant, MWe/MWth, which averages $\sim$ 0.32 for LWR's

B_{dis} is the discharge burnup (MWD/MT)

x_F is natural uranium feed enrichment, wt %

x_p is the reload batch enrichment, wt %

and x_W is the enrichment plant tails assay enrichment which typically is $\sim$ 0.2 wt %.

Thus the goal of higher burnup is a long standing one and great progress has been made, even if not widely heralded. The current focus on this goal should help insure continuance

of this historical trend.

Numerous studies completed over the last few years have shown that uranium utilization can be improved by a variety of strategies: extending burnup, subdividing the core into a larger number of staggered-reload batches, adopting low-leakage fuel reload arrangements, incorporating axial blankets, reoptimizing the lattice water-to-fuel ratio, introducing mechanical spectral shift, pin pulling and bundle reconstitution using smaller fuel assemblies, and by practicing routine coastdown. Table 1.1 summarizes the uranium conservation tactics envisioned for PWRs on a once-through fuel cycle and the potential ore savings estimated for each strategy. It must be pointed out that the total percentage savings in U_3O_8 are not directly additive, but cumulative amounts in the range of 15% (near-term) to 40% (long term) are projected.

The most effective near-term means of improving uranium utilization are to increase the discharge burnup, incorporate a larger number of in-core fuel batches and employ a modified (so-called "low-leakage") fuel management scheme, such as in-out-in, which reduces core neutron leakage. A substantial reduction, in the range of 10 to 20%, in yellowcake consumption can be achieved, if the discharge exposure of the fuel is increased to about 50,000 MWD/MT and the number of staggered in-core batches to five, as compared to current PWR designs and fuel management strategy, which use a three-batch out-in fuel management scheme and typically have discharge burnups of about 30,000 MWD/MT. Higher discharge burnup permits an

TABLE 1.1 POTENTIAL IMPROVEMENTS IN URANIUM UTILIZATION FOR PWRs ON A ONCE-THROUGH FUEL CYCLE

	OPTION	$\frac{NAT_U}{SAVINGS}$ (%)	REFERENCES	COMMENTS
1.	Extended Burnup and Increased Number of Batches	∿15	F-1,S-3, M-1,M-2	5-batch core with discharge burnup of ∿55,000 MWD/MT; risk of premature fuel failure must be considered
2.	Low-Leakage Fuel Management	∿ 3	M-1,S-3, S-4	Must cope with power peaking problem; if burnable poison is used, residual poison may negate savings
3.	Axial Blankets	∿ 2	K-1,M-1, S-3	Aggravates axial power peaking; may require poison or enrichment zoning
4.	Re-Optimizing Lattice Fuel-to-Moderator Ratio	2-3	R-1	For high burnup cores; depends on specifics of current core design
5.(a)	Continuous Mechanical Spectral Shift	10-15	S-2	May not be practical from an engineering standpoint
5.(b)	D_2O Spectral Shift	10-15	C-3,G-2	D_2O is expensive
6.	Mid-Cycle Pin Pulling and Bundle Reconstruction	∿10	S-2,R-1	Potential thermal-hydraulic problems; reduces plant capacity factor
7.	Routine Preplanned Coastdown	∿ 7	F-1,M-1, S-3,M-2, D-3	If coastdown to economic breakeven is considered instead of to the optimum, the uranium savings can be approximately doubled (as is the duration of coastdown)

annual refueling schedule to be maintained even with a lower fuel reload fraction. This will reduce the number of spent fuel assemblies discharged at the end of a cycle as well as over the lifetime of the plant and, therefore, decrease the requirement for shipping, handling, storage and disposal of spent fuel. There are other benefits offered by extended burnup. Separative work requirements are reduced and since there is less net plutonium production per unit of energy generated and a larger buildup of long-lived fission products and higher plutonium isotopes in the discharged fuel, the incentive for diversion will also be reduced.

The major disadvantages associated with this option are the increased potential for premature fuel failure at higher burnup, and the almost inevitable increase in power peaking. The main concerns relating to fuel failure at higher exposure in current LWR fuel are pellet-clad interaction, fuel-rod internal pressure due to fission gas release, changes in the structure and dimensions of the fuel and both internal and external cladding corrosion. Currently, extended burnup fuel-rod performance is being evaluated in several DOE-sponsored irradiation programs [L-1]. To date these projects have achieved assembly average burnups exceeding 40,000 MWD/MT, and burns to about 55,000 MWD/MT are currently being conducted [C-2]. In another program, fuel assemblies capable of achieving batch burnups in excess of 50,000 MWD/MT have been fabricated, and are in the process of being tested [A-1]. Data from these programs can provide the basis for further

improvements in fuel design and the required assurance to both vendors and utilities that high burnup fuel is ready for routine use.

As already noted, one disadvantage associated with the extended burnup option lies in the higher power peaking encountered (by about 10%) compared to that associated with current designs and fuel managements schemes [C-2]. This problem is attributable to the higher enrichment (hence reactivity) of the reload fuel. The large difference between the reactivity of the fresh fuel and fuel that has already received several cycles of exposure leads to correspondingly large differences in assembly power between the fresh and exposed batches, as well as large local flux and power gradients. This motivates the use of burnable poisons to suppress the local power, either by the insertion of discrete rods of lumped burnable poisons, or by admixture of burnable poison with the uranium dioxide fuel itself. Burnable poisons are also required to keep soluble boron concentrations at the beginning of cycle (BOC) sufficiently low to obtain an acceptable (slightly negative) moderator temperature coefficient of reactivity.

Higher discharge burnup also facilitates the implementation of a longer cycle (18 instead of 12 months) while keeping the number of feed assemblies the same. The basic incentive for this tactic is that one refueling outage is eliminated every three years, which permits a higher plant capacity factor, and thus significant savings in replacement power costs.

More efficient use of utility system outage maintenance teams can also be anticipated (including for example, lower lifetime radiation exposure and more tolerant scheduling constraints), and the increase in time between the reload licensing submittals will also result in potential savings in analysis and licensing costs [B-1]. This fuel management scheme employs reload fuel enrichments ranging from 3.6 w/o to 4.2 w/o to attain discharge burnups ranging from 36,000 MWD/MT to 45,500 MWD/MT [B-2]. Again burnable poison will be required to limit the concentration of soluble boron at BOC so that the moderator temperature coefficient of reactivity will be negative.

In the low-leakage fuel management scheme, fresh fuel assemblies are dispersed among older fuel assemblies in the core interior while once or twice burned low-reactivity fuel is placed on the core periphery in order to reduce radial neutron leakage from the core, in contrast to current PWR out-in/scatter fuel management strategy in which fresh fuel is loaded on the core periphery for the purpose of flattening the radial power profile. Ideally, by implementing this fuel management option, a further reduction in uranium requirements can be realized ($\sim$ 3%), because of the lower radial neutron leakage and because of the higher importance weighting of the high-reactivity fuel present in the core interior at the end of the cycle. However, when fresh fuel is placed in the core interior, severe power peaking problems can occur. This can be overcome by incorporating burnable poison into the fresh

fuel assemblies to limit the power density in these assemblies.

Leakage of neutrons from the core can be further reduced by employing axial blankets, comprised of natural or depleted uranium, at the top and bottom of the active core. This has the potential of improving uranium utilization since neutrons which would otherwise leak into the reflector and be lost through parasitic absorption, are captured instead in the fertile blanket material, producing additional fissile material. Studies [K-1, M-1, S-3] have shown that ore savings of about 3% can be achieved, but at the expense of a slightly higher axial power peaking factor. This problem can be solved using axial enrichment zoning and/or zoned axial poison.

All current LWRs have core lattice designs that were optimized under the assumption that spent fuel reprocessing and the recycling of recovered uranium and plutonium would be the normal mode of operation, under which circumstance high burnup is not as attractive. As a result, the lattices in use today may be slightly undermoderated (low water-to-fuel ratio). Hence a reactivity increment can be realized when the lattice is made a little wetter (for example, through the use of annular fuel or by decreasing the fuel rod diameter), thereby reducing the fissile inventory required to maintain criticality at the end of cycle, which translates into lower reload enrichment and yellowcake consumption. A wetter lattice, however, tends to have a less negative moderator temperature coefficient, particularly at BOC, and again one is led to use burnable poison in place of soluble poison.

There are other concepts which have the potential of improving uranium utilization: spectral shift through variation of coolant voids or inlet temperature, mechanical spectral shift (variation in lattice pitch), D_2O spectral shift, pin pulling and bundle reconstitution, using smaller fuel assemblies and routine pre-planned coastdown at the end of cycle. Although some of these options cannot be readily backfitted into current PWR designs, end-of-cycle coastdown or stretchout is already being practiced by a number of utilities [Q-1]. In this technique, insertion of positive reactivity to keep the reactor critical after the normal full power end of life has been reached is accomplished by reducing the coolant (and hence fuel) temperature to take advantage of the negative temperature (doppler) coefficient and/or by reducing the reactor power level (thus reducing both the xenon poisoning and fuel temperature), thereby extending the cycle length. In normal reactor operation, optional end-of-cycle coastdown has been used to obtain cycle flexibility; for example, should other units experience forced outages, refueling can be delayed through coastdown. Routine pre-planned coastdown on the other hand has the objective of lowering fuel cycle cost and minimizing uranium usage. This can be realized by reducing the feed enrichment enough to retain the original cycle length. However, either the plant capacity factor or its thermodynamic efficiency are below average in the latter stages of coastdown and the duration of the coastdown must thus be optimized. Utilities planning to adopt this technique routinely must

therefore weigh the above factors (U_3O_8 savings versus replacement power cost) to suit their needs.

The benefits, and indeed the perceived necessity, of using burnable poisons in conjunction with the different methods of improving uranium utilization in PWRs is clearly indicated by the preceding discussion, where burnable poisons were employed for power peaking control, criticality control and moderator temperature coefficient adjustment. However, it will be shown in the present work that there is still another dimension to the use of burnable poison: obtaining higher discharge burnup, and therefore better uranium utilization, through optimum power-shaping (i.e., creation of an improved power history trajectory). Important qualifications to this new aspect such as the effect of different reload patterns and the amount and effect of residual poison are addressed in chapters four and five of this report.

1.3 RESEARCH OBJECTIVES

In the many options available to improve uranium utilization and in particular, those which are retro-fittable to present generation PWRs, it is necessary to incorporate burnable poisons into the fuel assemblies to control power distribution (hence, holding power peaking below prescribed limits) and to keep the concentration of soluble poison at BOC sufficiently low to obtain an acceptable moderator temperature coefficient of reactivity. In this context, the identification of the objective of the present work becomes obvious, that is,

to evaluate the use of burnable poisons as a means to facilitate implementation of the improved design/management strategies discussed in the preceding section.

An evaluation of the benefits of burnable poisons can obviously be done on a case-by-case basis with the use of full-fledged state-of-the-art computer capabilities. The amount of detail involved makes this approach economically unappealing -- at least in preliminary scoping analyses. It also discourages generalization and the identification of global strategies. Moreover, it may prove to be difficult to make comparisons on an "all-else-being-equal" basis since this approach allows too much flexibility -- abetting the introduction of other changes which obscure the effect under study. On the other hand, too simplified a method may overlook small, but worthwhile improvements (or deleterious effects). To achieve the assigned goal of evaluating the use of burnable poisons on a strategic level, a simple model which has a sound theoretical basis will be developed. In a way, the model is an extension as well as a refinement of screening methods previously developed at MIT [S-2], which were found to be capable of evaluating the effects of small changes in core design and fuel management schemes on a consistent basis. The present methodology, although evolved from the linear reactivity model of core behavior, utilizes an improved version which has a better theoretical basis, and one which is more thoroughly benchmarked against results generated with detailed state-of-the-art computer analyses.

Although many aspects of PWR core design and fuel management are addressed in the present work, the most important subtask was to determine the optimum (maximum discharge burnup) power history trajectory of a fuel batch obtainable using burnable poison and to debit the compensatory penalty in discharge burnup caused by residual poison. These results will provide core designers with a clearer picture of the "best attainable" poison performance against which specific designs can be evaluated.

1.4 ORGANIZATION OF REPORT

The work presented in this report is organized as follows. Chapter two provides an outline of the state-of-the-art computer codes used in this research together with the reactor system and lattice model employed in the calculations. A short discussion on the selection of burnable poisons and the characteristics of candidate poisons is also included in this chapter.

Chapter three deals with the linear reactivity model (LRM) of core behavior. Significant improvements in and additions to LRM methodology are presented. Key features of the extended LRM methodology such as leakage, and power sharing among fuel batches are discussed. A power split relation is derived using "group-and-one-half" diffusion theory, to supplant the purely empirical relations used by prior authors. Application of the LRM to obtain analytical estimates of the discharge burnup for a variety of reactivity-burnup histories

concludes the chapter.

In Chapter Four, the methodology is extended to compute discharge burnup numerically, using a computer code, DISBURN, developed for this purpose. Some important features of the code will be presented. The code will also be applied to evaluate various fuel management strategies, and the analytical results obtained in Chapter Three are compared and normalized to more precise numerically computed results.

Finally, the economic impact of using burnable poison with regard to the residual poison penalty and the radial power flattening effect of burnable poison are briefly discussed.

Chapter Five summarizes the present study: the development of the methodology and the results obtained therefrom. Recommendations for future work are also made.

Several Appendices are included containing data supporting the work reported in the main text. A listing of the code DISBURN together with a sample problem run are included here.

CHAPTER 2

METHODS AND MODELS

2.1 INTRODUCTION

In-core fuel management analysis relies heavily upon reactor physics calculations. The major objective of these neutronic calculations is the accurate prediction of pertinent core parameters such as reactivity, reaction rates (thus, power density) and isotopic compositions at all in-core locations and at all time. Equipped with this information, plant operators and reactor designers can make appropriate management decisions pertaining to the operation and design of the reactor plant. Although well developed and sophisticated computer codes are available to perform very detailed and thus very accurate neutronic analyses of the reactor core (using hundreds of energy groups, thousands of spatial mesh intervals and very small time increments), technical and economic constraints such as the size of today's computers and the cost associated with running long programs forbid exclusive reliance on such efforts. Fortunately, less comprehensive state-of-the-art computer programs and methodology can often provide acceptably accurate results for the purposes of reactor fuel management. Even further, simple models of the type developed in the present work can provide results which are useful on a global scale, at the sacrifice of local detail.

The computer programs employed in the present work were primarily the LEOPARD and PDQ-7 codes. They were used either individually or in combination to generate results against which the models developed and deployed in this research are tested. These codes were, and still are in widespread use [A-2, C-4, S-5], and they have been benchmarked against extensive experimental data. Moreover, previous workers at MIT: namely, Fujita [F-1], Correa [C-1] and Sefcik [S-2] have accumulated extensive experience with these same codes, and have shown that for applications similar to those of present concern, the codes are sufficiently accurate. A brief description of these well-documented codes will be presented in this chapter.

Recent interest in the use of burnable poisons to facilitate the implementation of improved uranium utilization tactics has accelerated the development of more powerful computational techniques, such as transport and collision probability methods. This progress is due in part to the cumulative increase in computer memory and speed realized over the past decade. Besides being able to handle highly shielded absorbers in lumped form or admixed with the fuel, codes employing transport and collision probability methods can also deal simultaneously with a number of adjacent cells within an assembly (for example, fueled cells, water holes, control rod channels, etc.). A representative example is Combustion Engineering's DIT program [J-1]. The Electric Power Research Institute (EPRI) has, under its Advanced Recycle Methodology

Program (ARMP), several computer codes of similar capabilities: EPRI-CELL, CPM and MICBURN [E-1]. In the present work we are interested in the generic behavior of burnable poisons, rather than the specific details which such codes provide. Hence we will only review typical results published by others to establish overall patterns of reactivity behavior in assemblies containing burnable poison.

2.2 COMPUTER CODES

In this section, a brief description of the computer codes used in the present work, LEOPARD and PDQ-7, will be given.

The LEOPARD code [B-3] calculates the spectrum and neutron multiplication factor, and generates few group (2 or 4) cross sections for a LWR unit fuel cell or a supercell (cell plus an extra region). The unit cell consists of fuel, gap, metallic cladding and moderator, and, in the case of a supercell, an extra region representing fuel assembly water holes, control rod sheaths, spacer grids and inter-assembly water gaps [see Fig. 2.1]. The code can also perform zero dimensional depletion calculations in which the neutron spectrum (and appropriate few group cross sections) are recomputed after each depletion time step. The microscopic cross section library for the version of LEOPARD used in this work (EPRI-LEOPARD) is derived from the ENDF/B-IV data set and only geometrical dimensions, temperatures, pressures, material compositions and the corresponding number densities, and burnup

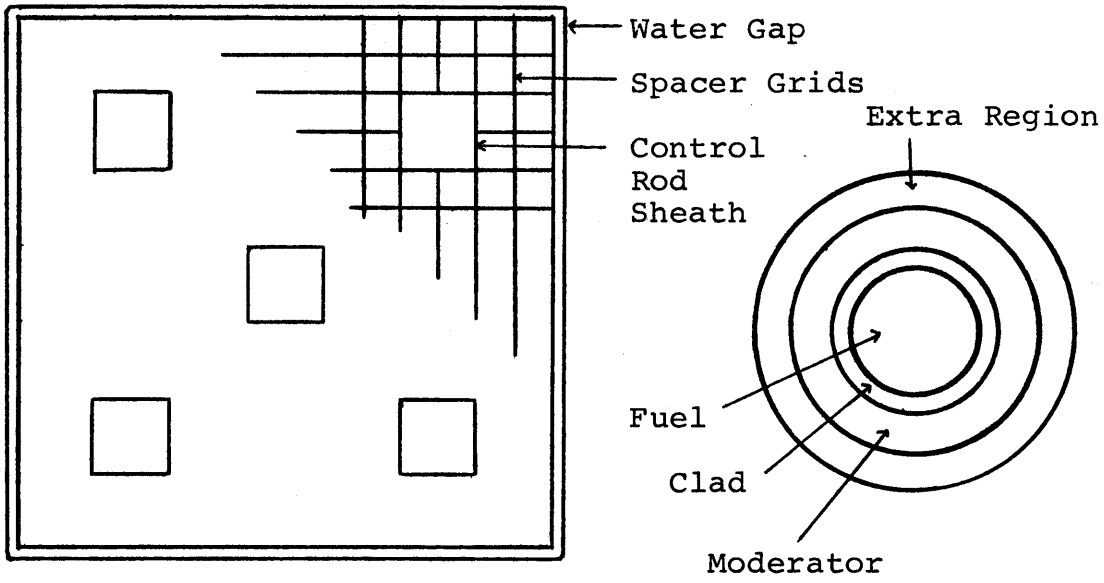

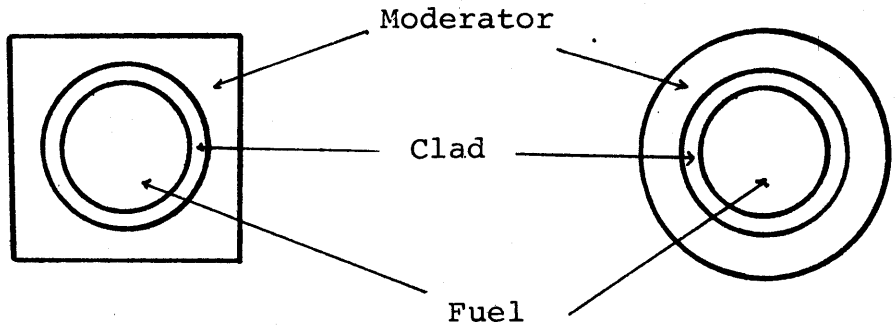

Fig. 2.1 LEOPARD Geometrical Representation

time-steps (for depletion calculations) are required as user input by the code.

The LEOPARD code uses the MUFT [B-4] subprogram to calculate the fast and empithermal region spectrum (in 54 groups) while SOFOCATE [A-3] handles the thermal spectrum (with 172 energy groups) using the Wigner-Wilkin treatment. As both MUFT and SOFOCATE execute homogeneous medium calculations, the cell heterogeneity is corrected for through the use of fast advantage factors, thermal disadvantage factors and an iteratively adjusted resonance self-shielding factor. The code also permits optional use of the Mixed Number Density (MND) approach [B-5], which employs a boundary condition of neutron activation continuity rather than flux continuity.

An option is provided in LEOPARD to adjust the cross section of the single non-saturating fission product used in the code to allow for differences in fuel type by inputing a scaling factor. In the present research, a value of 0.84 [M-3] was used for typical PWR uranium oxide fuel and a value of 1.26 was employed in cases involving plutonium enriched fuel [S-6].

The LEOPARD code and its companion cross section library have been extensively benchmarked at MIT by Garel [G-3] and Correa [C-1]. Garel has tested the code against critical and exponential experiments for 63 cases of slightly-enriched-uranium (U-235/U-238) light water lattices and 42 plutonium-enriched uranium oxide light water cases. On the other hand Correa concentrated his work on tight pitch U-233/ThO_2,

Pu/ThO_2 and $U\text{-}235/UO_2$ lattices. Table 2.1 summarizes the results obtained by these two previous workers at MIT. For lattices of interest to the present work (that is, $U\text{-}235/UO_2$ lattices with and without soluble boron), the $|\overline{\Delta k}|$ was found to be ± 0.012. This result is sufficiently accurate for the type of work we are interested in here. Finally, in a recent study an assessment was made of LEOPARD and two other newer codes, and LEOPARD was found to be in better agreement with experimental results than the other codes [L-2].

The PDQ-7 code [C-5] solves the multigroup diffusion equations in one, two or three dimensions. The eigenvalue solution to the equations can be obtained in rectangular, cylindrical, spherical or hexagonal geometry. Although this code allows up to five energy groups, only two energy groups were used in the present work; no depletion calculations were done using the code.

In PDQ-7 the diffusion equation is solved by discretizing the energy variable and finite-differencing (central) the spatial part of the equation over a constant (or variable) mesh interval. The one dimensional equations are solved using the Gauss elimination technique and the two dimensional equations are solved using a single-line cyclic semi-iterative procedure. For three dimensional problems, a block Gauss-Seidel procedure is used. However, only two dimensional analyses were done in the present work.

The calculational flow path linking the LEOPARD and PDQ-7 codes is shown in Fig. 2.2. The LEOPARD code can be used to

TABLE 2.1 SUMMARY OF LEOPARD BENCHMARK COMPARISONS

FUEL:	$U\text{-}233/ThO_2$ (1)	$U\text{-}235/ThO_2$ (1)	$U\text{-}235/UO_2$ (1)	U-235/U (1)	$U\text{-}235/UO_2$ (2)	Pu/UO_2 (2)
ε (w/o)	3.00	3.78-6.33	3.00-4.02	0.7-1.5	1.3-4.1	1.5-6.6
F/M	0.01-1.00	0.11-0.78	0.23-2.32	0.15-1.69	0.1-1.3	0.1-0.9
(H+D)/U-238 (or/Th-232)	3.4-403.	4.7-36.	1.31-14.6	0.8-5.7	2.9-1.3	3.5-39.0
ϕ_1/ϕ_2	0.3-21.	1.7-23.	2.4-50.	1.3-12.	1.6-12.	1.2-20.
D_2O (%)	0.-99.34	0.-81.96	0.-89.14	---	---	---
Boron (PPM)	---	---	---	---	0.-3400.	---
$\bar{k}$	1.003	1.009	0.998	1.006	1.003	1.018
$\pm\Delta k$	0.012	0.016	0.006	0.011	0.012	0.014
# of cases	16	16	26	82	63	42

(1) Reference C-1

(2) Reference G-3

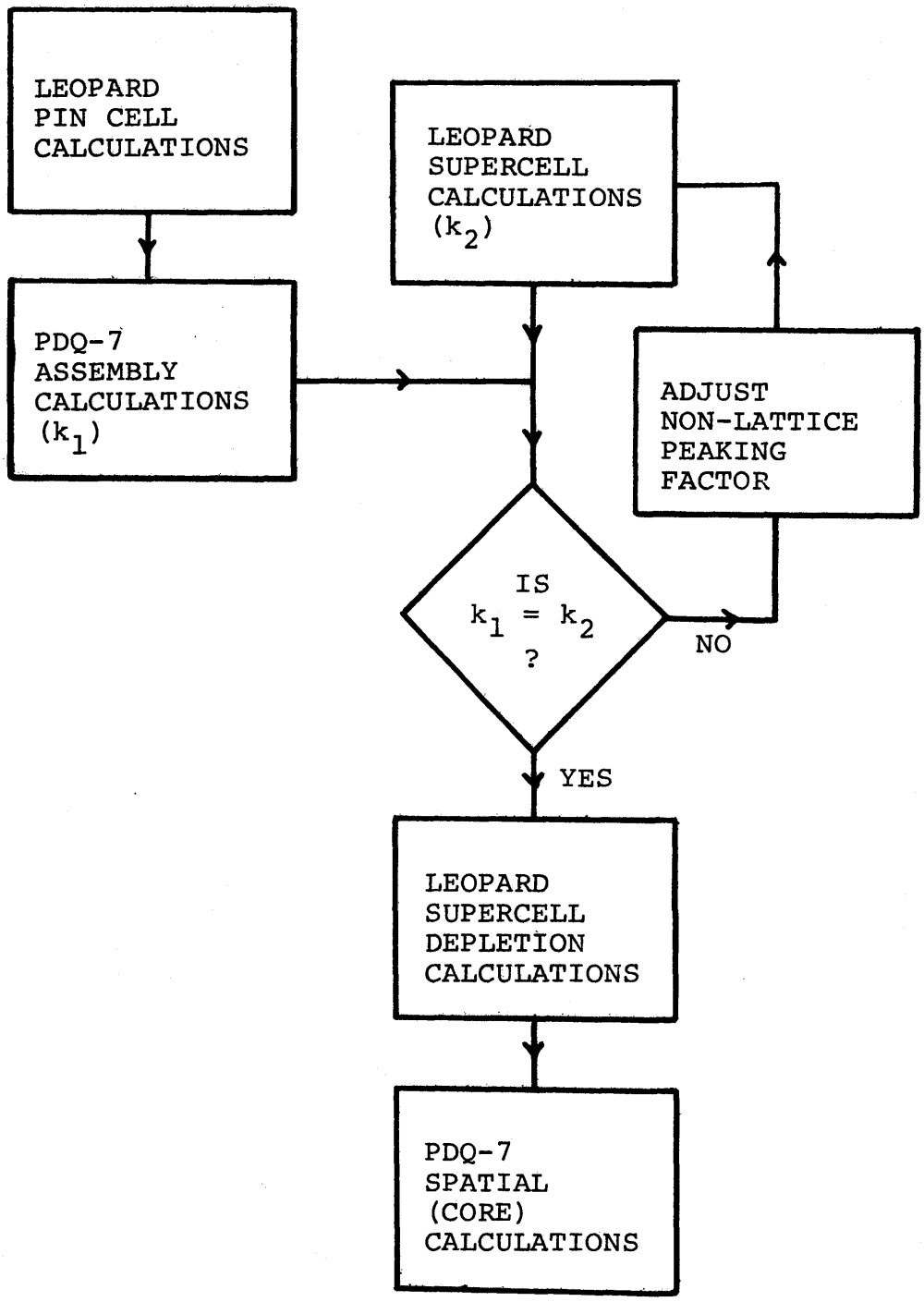

Fig. 2.2 Calculational Flow Path

carry out simulated full-assembly calculations by correctly specifying the non-lattice fraction ('extra' region of the supercell) and its corresponding non-lattice power peaking factor. Fig. 2.2 shows how this is done, by adjusting the non-lattice peaking factor to match PDQ-7 whole-assembly calculations.

2.3 REACTOR MODELS AND LATTICES

In the present work it was considered essential, in the interests of realism, to have a specific reactor design to serve as a reference case in the establishment of relevant design parameters. The Maine Yankee PWR system was selected because of the fact that it is a large modern PWR (designed by Combustion Engineering, Inc.) which is currently operating and, more importantly, the reactor fuel design characteristics and other information vital to this study were readily available in publicly available information supplied by the Yankee Atomic Electric Co., which manages the operation of the reactor. Although the information in this report is referred to as deriving from "Maine Yankee," it should not be considered as representing that actual system in its present or projected operating configuration, but as an idealization thereof. It should also be noted that the results in this report have not been either reviewed or approved by the Yankee organization. Table 2.2 briefly summarizes the Maine Yankee reactor's key core parameters, and Tables 2.3 and 2.4 list the geometrical dimensions, the thermodynamic

TABLE 2.2 MAINE YANKEE REACTOR CORE PARAMETERS [S-7]

ITEM	VALUE	UNITS
Rated Thermal Power	2630	MWth
Rated Electric Power	840	MWe
Fuel Management	3-batch, out-in/scatter	
Equilibrium Discharge Burnup	33,000	MWD/MT
Power Density	80.85	kw/liter
Initial System Pressure	2250.0	psia
Average Linear Heat Rate (102% of Nominal)	6.35	kw/ft.
Nominal Coolant Bulk Temperature	576.4	°F
Fuel Rod Array	14 x 14	
Fuel Rod Pitch	0.580	inches
Pellet OD	0.3765	inches
Clad Material	Zircaloy-2	
Clad OD	0.440	inches
Clad ID	0.384	inches

TABLE 2.3 VOLUME FRACTIONS OF VARIOUS MAINE YANKEE SUPERCELL CONSTITUENTS

	REGION			
	Pellet	Clad[1]	Moderator	Extra
CONSTITUENT				
UO_2	1.0000	0.0	0.0	0.0
Zircaloy-2	0.0	0.907475	0.012124	0.087651
Light Water	0.0	0.0	0.986144	0.912349
Chromium	0.0	0.0	0.000330	0.0
Nickel	0.0	0.0	0.000909	0.0
Manganese	0.0	0.0	0.000006	0.0
Iron	0.0	0.0	0.000478	0.0
Carbon	0.0	0.0	0.000001	0.0
Aluminum	0.0	0.0	0.000008	0.0

(1) Volume fractions do not add to unity due to the presence of the fuel-clad gap in this region.

TABLE 2.4 REQUIRED DIMENSIONAL, THERMODYNAMIC AND NEUTRONIC PARAMETERS USED FOR THE MAINE YANKEE SUPERCELL

PARAMETER	VALUE
"Resonance" Temperature (°F)	1232.0
Pellet Temperature (°F)	1232.0
Clad Temperature (°F)	630.4
Moderator Temperature (°F)	576.4
Geometrical Buckling (cm^{-2})	7.319×10^{-5}
Non-Lattice Peaking Factor	1.16
Pellet Outer Radius (in)	0.18825
Clad Outer Radius (in)	0.220
Clad Inner Radius (in)	0.1920
Pitch (in)	0.580
Power (fraction of full power)	1.0

PARAMETER	VALUE
Non-Lattice Fraction	0.115166
H_2O Pressure (Psia)	2250.0
H_2O Density (g/cc)	1.0*
Fuel Theoretical Density Fraction	0.92
Power Density (Watts/cm^3)	80.8574
Fission Product Absorption Cross-Section Scale Factor	0.84

* The code adjusts the density to correspond to the specified moderator temperature

and the neutronic parameters required to describe this reactor in a LEOPARD supercell calculation, that is, a simulated full-assembly calculation.

2.4 BURNABLE POISON MODELING

Incorporation of burnable poison into the fuel assemblies for the purpose of facilitating the implementation of certain uranium utilization improvement techniques (for example, extended burnup and/or low-leakage fuel management schemes) can be done in two ways: homogeneously mixing the burnable poison with the uranium oxide fuel; or in the heterogeneous form of poison pins placed in fuel rod locations (lattice shims) or in control rod guide tubes (water-hole shims). There are advantages and disadvantages associated with both methods of incorporating the burnable poison within the fuel assemblies, and these two options are both in use.

The selection of material for burnable poisons and the way in which they can be incorporated within the fuel lattice are governed by several considerations: acceptable total reactivity worth, depletion rate, good corrosions resistance in water, resistance to radiation damage, ease of fabrication, compatibility with clad and/or fuel, manufacturability, material cost, etc. From a neutronic standpoint, the ideal burnable poison should have a depletion characteristic such that relatively uniform depletion of the poison throughout the operating cycle is maintained and complete destruction of the high cross section isotopes occurs just before the end of

cycle. This would compensate for the linear loss in reactivity of the freshly-loaded fuel as a function of burnup, and leave a negligible shim residual at the end of cycle. The amount of residual poison present at EOC is of concern since the discharge burnup (hence, the uranium utilization) can be significantly affected.

Researchers [F-2, L-3] over the past several years have studied a number of elements, particularly those with high microscopic thermal absorption cross sections (> 10^3 barns), as potential candidates for burnable poisons. The two elements which are considered leading candidates for use as burnable poison in PWRs are boron and gadolinium. Extensive experience with these elements has been accumulated over many years of reactor operation: boron in the form of B_4C has been employed as control material in both PWRs and BWRs, boron in alumina or a pyrex-type glass has been used to poison startup cores, and gadolinium burnable poison (in the form of Gd_2O_3 mixed with UO_2 fuel) has been used in BWRs. In recent years, the DOE and the nuclear industry have embarked on a number of programs which include gadolinium and boron burnable poison design development, demonstration of high burnup poison fuel for PWRs, analytical modeling of burnably-poisoned fuel burnup, poisoned fuel pin/assembly modeling, comparison of analytical and experimental results, and the like.

Preliminary studies [H-3] have shown that gadolinia admixed with UO_2, and boron in the form of borosilicate rods, deplete at a relatively uniform rate (i.e., with an essentially

linear reactivity vs. exposure characteristic) over an operating cycle, and leave a small residual at the end of cycle. Figures 2.3 and 2.4 show typical curves of the reactivity versus burnup behavior of burnable-poison-load PWR fuel assemblies. For the purpose of this work, a simple depletion model of a generalized burnable poison, consistent with such results, will be adopted: that is, a poison material is postulated which burns out at a uniform rate over a cycle and leaves a small residual at the EOC. Figure 2.5 illustrates this model. An important subtask of this work is to determine the optimum shape (slope and intercept) of the reactivity-burnup trace with respect to maximization of fuel burnup.

2.5 CHAPTER SUMMARY

In this chapter a brief description was presented of the computer codes (LEOPARD and PDQ-7) employed in the present research. The manner in which the codes are linked together in computations performed for this work was also outlined. The LEOPARD code was determined to be sufficiently accurate for the type of work to be done here. The Maine Yankee reactor system was chosen as the reference system because it is a modern, operating PWR, and information pertaining to this system was readily available. Finally, a simple generic depletion model of burnable poison (consistent with results obtained from more sophisticated computer calculations) in a fuel assembly was defined.

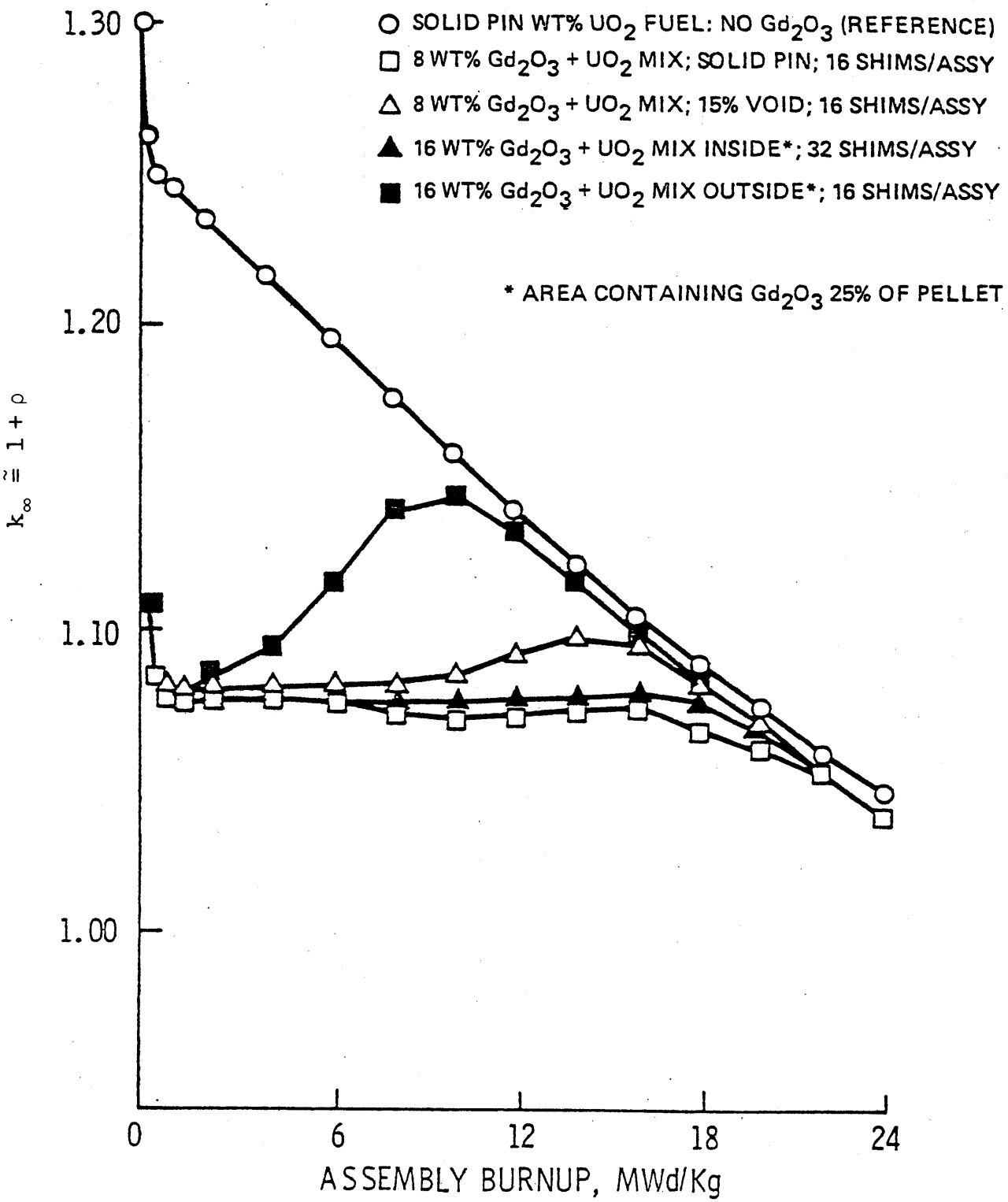

Fig. 2.3 k_∞ versus Burnup for Gadolinia-Poisoned Assemblies (From Ref. [H-3]

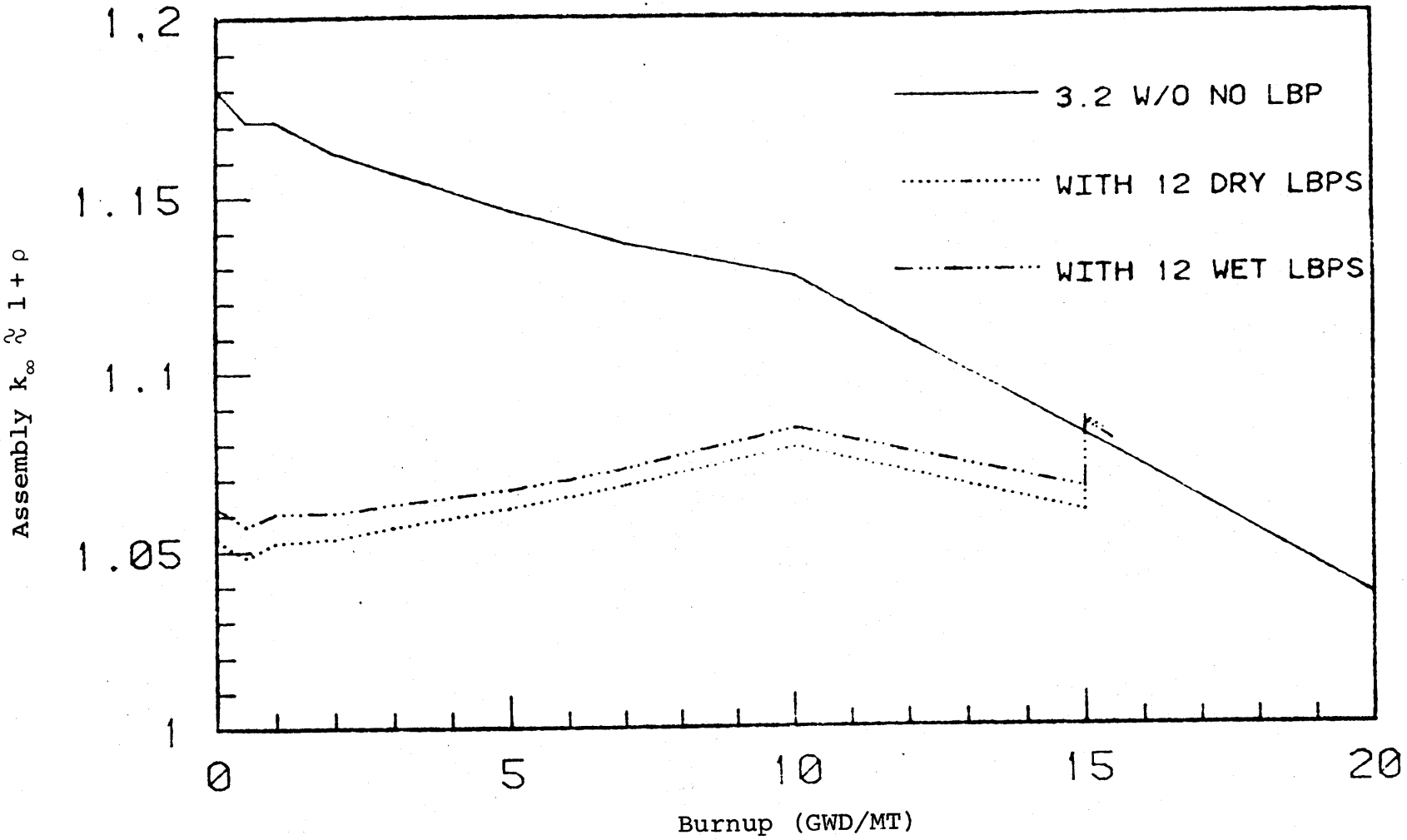

Fig. 2.4 k_∞ versus Burnup for Boron-Poisoned Assemblies (From Ref. [H-4])

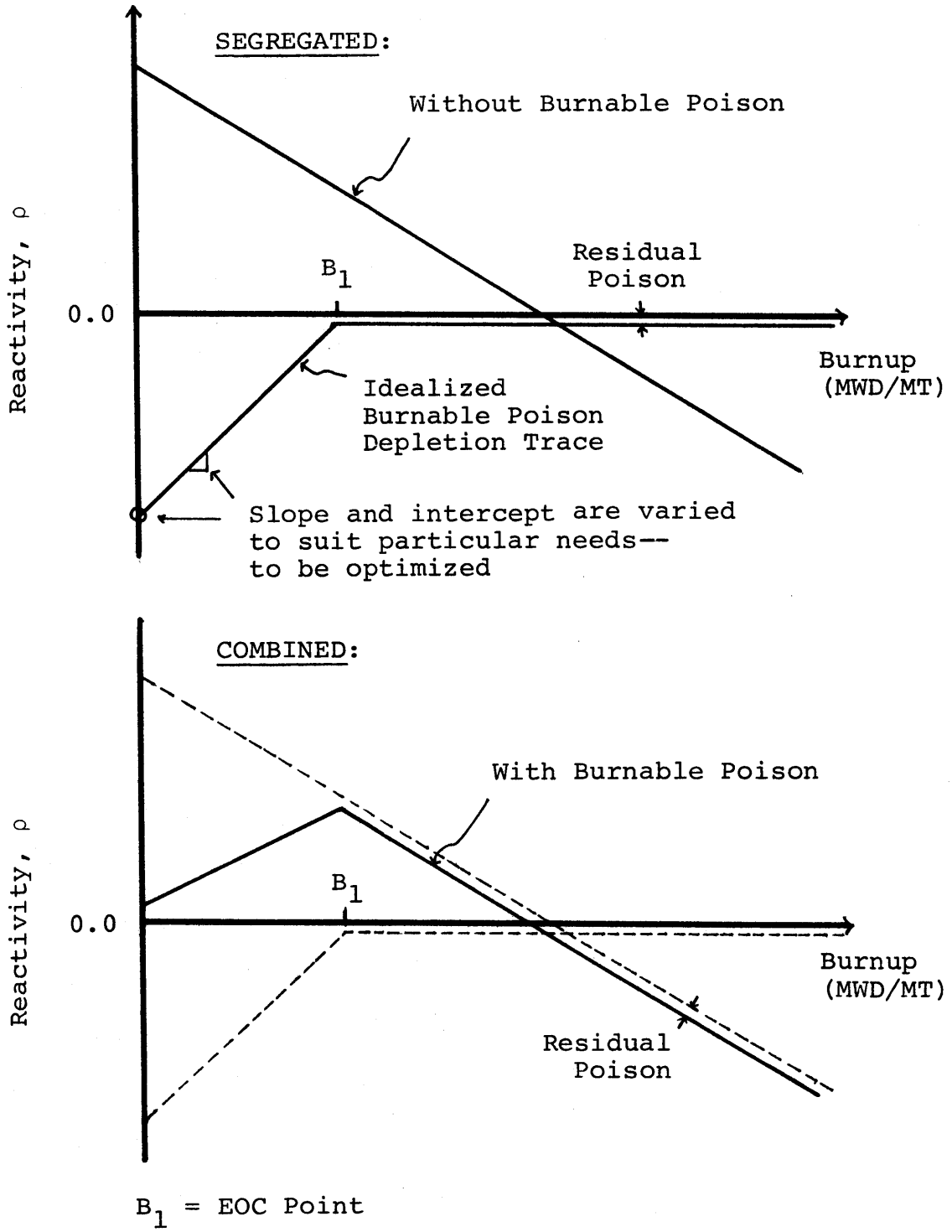

Fig. 2.5 Generic ρ versus Burnup Trace for Assembly with Burnable Poison

CHAPTER 3

LINEAR REACTIVITY MODEL METHODOLOGY

3.1 INTRODUCTION

The linear reactivity model (LRM) is based on the observation that the reactivity, ρ, of a PWR fuel assembly (embedded in a lattice of similar assemblies) decreases linearly as a function of burnup. With this model one can determine in-core fuel management parameters such as the reactivity contribution of a fuel assembly or batch of assemblies after a certain in-core residence time. Having this information the cycle and discharge burnups of the fuel can be computed. Elementary versions of this approach have been employed for approximate analyses and pedagogical purposes for some time now. Since greater accuracy is required in the present work, other important, and newer additions to the methodology will be included here: power weighting of the reactivity, and explicit treatment of the core leakage in the radial direction. Since both of these key features have been discussed in some detail in prior MIT work by Sefcik [S-2], only a brief summary description will be given in this chapter. More attention will be given to the final component in the LRM methodology, the relation used to estimate the sharing of power among in-core fuel batches. Prior empirical prescriptions will be replaced by one derived from the "group-and-one-half" model of

neutron behavior. Verification of this relation for both interior and peripheral fuel assemblies will be presented.

Finally, an analytical model permitting computation of the discharge burnup for various cases of fuel management schemes of contemporary interest will be developed.

3.2 THE LINEAR REACTIVITY MODEL

The eigenvalue (λ) obtained by solving the neutron diffusion equation for a core lattice is, on a physical basis, the neutron multiplication factor (k) of that assembly. It has been observed that the k of a typical PWR fuel assembly/lattice, with fuel enrichment in excess of roughly 2.0 w/o, varies, approximately, linearly with burnup [G-3]. However, the reactivity (ρ) of the fuel assembly/lattice, defined as

$$\rho = \frac{k-1}{k} = 1 - \frac{1}{k} \qquad (3.1)$$

has been found to be a much more linear function of burnup than k. In fact, Sefcik [S-2] has shown that for the Maine Yankee supercell reference lattice with enrichment variations ranging from 1.5 w/o U-235 to 4.34 w/o U-235, the linear least squares curve-fits of ρ versus burnup (150-50,000 MWD/MT) gave an average coefficient of determination (R^2) of 0.995 (i.e., only 0.5% of the variance is not accounted for by the correlation) compared to an average R^2 value of 0.9898 for linear fit of k versus burnup. Figure 3.1 shows the plots of ρ versus burnup for the Maine Yankee supercell with

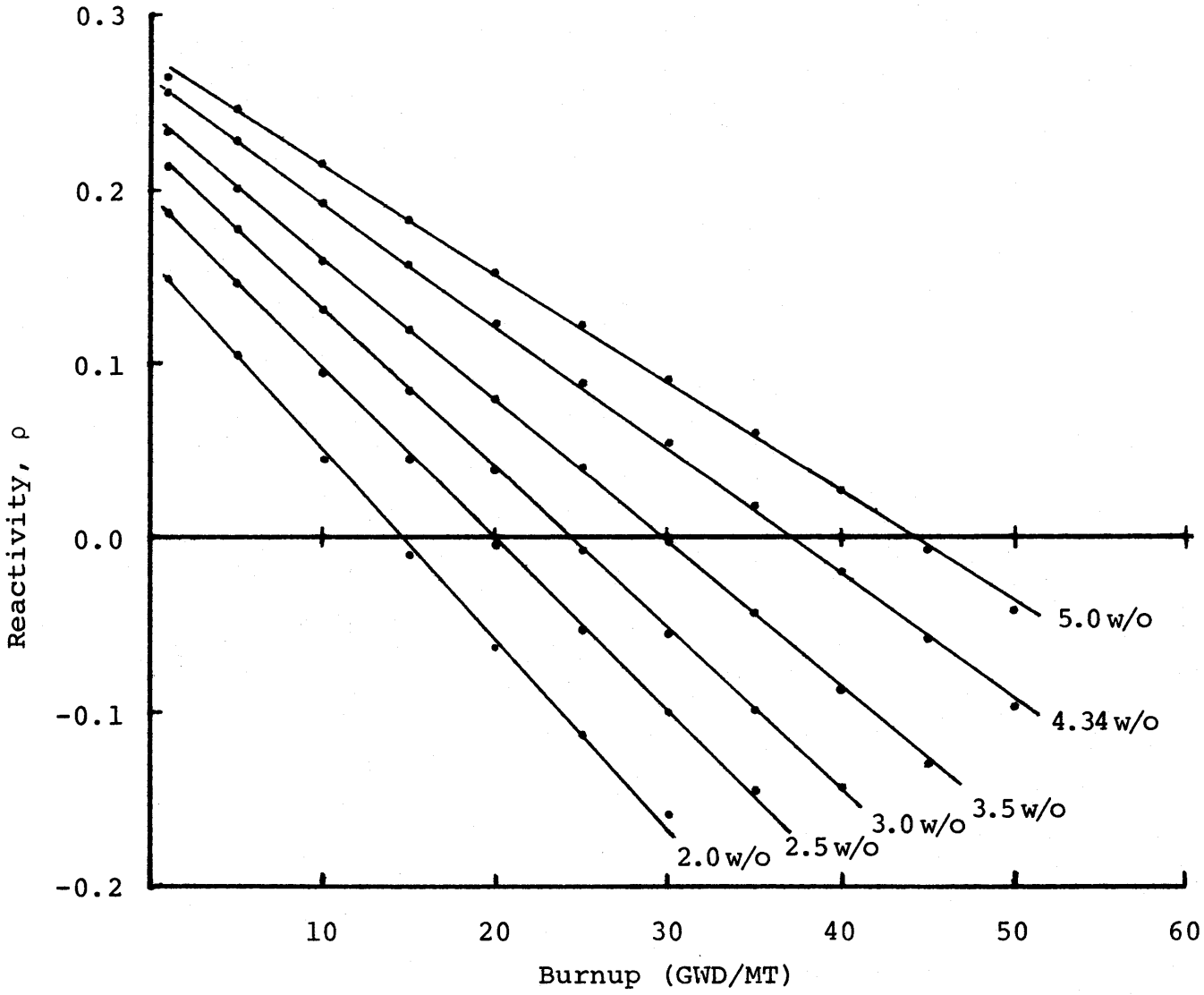

Fig. 3.1 Reactivity versus Burnup for the Main Yankee Supercell with Different Fuel Enrichments

different fuel enrichments. Although not shown in the figure, there is a sharp drop in the reactivity during the first 150 MWD/MT for each curve due to the buildup of the xenon and samarium fission product poisons to their saturation levels. Omitting this initial transient, then, for a particular curve, we can write,

$$\rho = \rho_o - AB \tag{3.2}$$

where ρ_o is the extrapolated beginning of life reactivity (i.e., at B=0),

A is the slope of the curve, $(MWD/MT)^{-1}$,

and B is the burnup, MWD/MT.

In a simple application of the linear reactivity model relevant to the present work, the discharge burnup ($B_{dis,n}$) of an n-batch core under steady-state refueling conditions will be determined as follows. Neglecting leakage for the moment, and assuming that the core has a fixed thermal power rating and there is equal power sharing among the fuel batches (of fixed size), the freshest batch will be burned to $(B_{dis,n})/n$ at the end of cycle, the next older batch to $(2B_{dis,n})/n$, etc. The system reactivity of the combination of the fuel batches is obtained by algebraic averaging of the EOC reactivity of each batch,

$$\rho_1 = \rho_{on} - A \cdot \frac{(B_{dis,n})}{n}$$

$$\rho_2 = \rho_{on} - A \cdot \frac{(2B_{dis,n})}{n} \qquad (3.3)$$

$$\vdots \qquad \vdots \qquad \vdots$$

$$\rho_n = \rho_{on} - A \cdot \frac{(nB_{dis,n})}{n}$$

- -

System reactivity $\rho_{sys} = \frac{1}{n}\sum_{i=1}^{n}\rho_i = \frac{1}{n}\left(n\rho_{on} - A \cdot (B_{dis,n}) \cdot \frac{n(n+1)}{2n}\right)$ (3.4)

At the EOC, $\rho_{sys} = 0$ (reactivity-limited EOC condition), and Eq. (3.4) can be rearranged to give

$$B_{dis,n} = \left(\frac{2n}{n+1}\right)\frac{\rho_{on}}{A} \qquad (3.5)$$

For a one-batch (n=1) core, the discharge burnup is given by

$$B_{dis,1} = \frac{\rho_{o1}}{A} \qquad (3.6)$$

When the one-batch core has the same discharge burnup as the n-batch core ($B_{dis,1} = B_{dis,n}$), the reload reactivity (hence, reload enrichment) of the latter will be lower than that of the former:

$$\rho_{on} = \left(\frac{n+1}{2n}\right)\rho_{o1} \qquad (3.7)$$

Or alternatively, if the reload reactivity is the same ($\rho_{on} = \rho_{o1}$), an n-batch core can be driven to a higher burnup:

$$B_{dis,n} = \left(\frac{2n}{n+1}\right) B_{dis,1} \tag{3.8}$$

The above results (Eqs. 3.5 to 3.8) were obtained based on the linearity of the $\rho(B)$ trace of a fuel lattice. However, the EOC reactivity balance approach of Eq. (3.3) can be extended to evaluate the discharge or cycle burnup of a reactor core whose fuel lattice/assembly reactivity varies non-linearly with burnup (for example, the natural uranium fuel of the heavy water moderated CANDU reactor). This is discussed in Appendix A. Similarly, the approach can be employed to compute the burnup of fuel batches in subsequent cycles following different types of perturbation from the steady state condition, such as changes in cycle length due to an early unscheduled shutdown of the reactor or due to coastdown, and changes in reload enrichment or batch fraction [D-2]. In the present work, however, the focus will remain on the steady state or equilibrium cycle of the reactor.

3.2.1 ρ VERSUS BURNUP CURVES FOR DIFFERENT FUEL TYPES

In the preceding section a case has been made for the use of the linear reactivity model for current PWR fuel (i.e., UO_2 slightly enriched with U-235). While the present study deals exclusively with this fuel in a once-through fueling mode, it is of interest to inquire whether the LRM is applicable to

other fuel types in similar lattices, since the commercialization of spent-fuel reprocessing will lead to the use of other fissile isotopes (U-233, Pu-239 and Pu-241) and the other major fertile species, Th-232, in LWR fuel. The results will also provide valuable insight into the nature of the physical properties contributing to or detracting from the linearity of $\rho(B)$.

Several Maine Yankee supercell depletion calculations using all possible combinations of fissile and fertile materials were performed. The isotopic compositions of the fissile material used in these computations corresponds to those one would obtain from the reprocessing of current LWR spent fuel. Table 3.1 gives the compositions of these fissile constituents. Figures 3.2 and 3.3 show the reactivity versus burnup curves for the different fuel types, and Table 3.2 gives the coefficients of determination (R^2) for the linear least squares curve-fits of the $\rho(B)$ traces, and other relevant parameters. Except for the Pu/ThO_2 system the results confirm the validity of applying the LRM methodology to different fuel types. For Pu/ThO_2 the methods of appendix A could be used to improve the accuracy of the linear model or to show that it is precise enough for a given application.

The departure from linearity of the Pu/ThO_2 system $\rho(B)$ trace can be attributed to the "Phoenix Effect" which involves the conversion of fertile Pu-240 by neutron capture into fissile Pu-241. Plutonium discharged from a typical PWR has a high concentration of Pu-240 (here, approximately 26% by

TABLE 3.1 ISOTOPIC COMPOSITION OF PLUTONIUM- AND U-233-ENRICHED FUEL

FUEL TYPE	ISOTOPE	WEIGHT FRACTION
1. Plutonium Enriched:	Pu-239	0.5422
	Pu-240	0.2596
	Pu-241	0.1394
	Pu-242	0.0588
2. U-233 Enriched:*	U-233	0.9064
	U-234	0.0808
	U-235	0.0128

* U-236 is neglected

TABLE 3.2 RESULTS OF LINEAR CURVE-FITTING OF THE $\rho(B)$ TRACES FOR THE DIFFERENT FUEL TYPES

FUELS:	$U\text{-}233/UO_2$	$U\text{-}235/UO_2$	Pu/UO_2	$U\text{-}233/ThO_2$	$U\text{-}235/ThO_2$	Pu/ThO_2
Fissile Enrichment (ε w/o)	3.15	3.00	3.08	2.94	3.23	3.34
Extrapolated BOL Reactivity, (ρ_o)	0.30609	0.22340	0.09450	0.22003	0.11586	0.06566
Slope (A, MWD/MT^{-1})	-9.299E-6	-9.266E-6	-3.883E-6	-1.074E-5	-6.394E-6	-3.270E-6
R^2	0.999987	0.999968	0.998288	0.998959	0.999483	0.975308

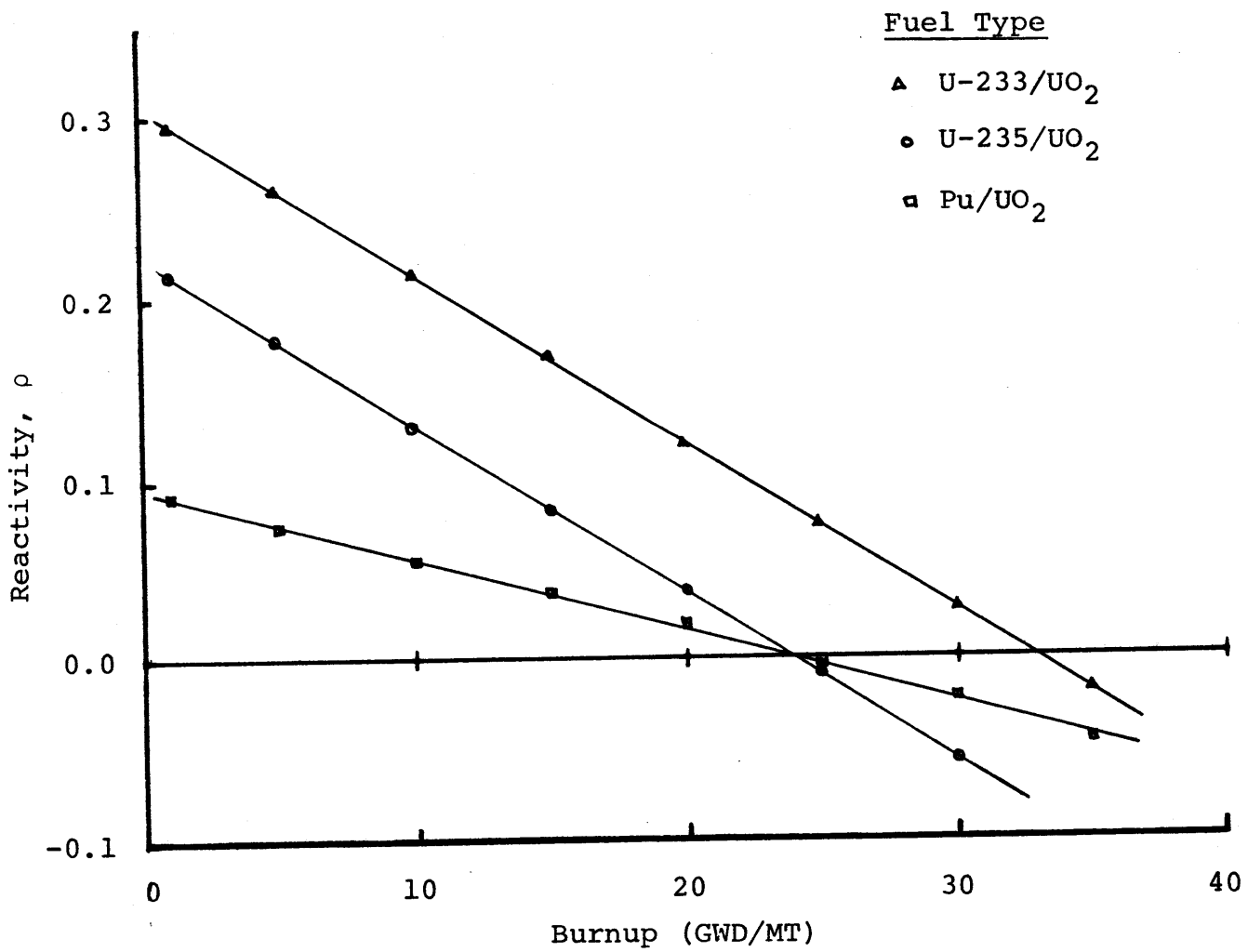

Fig. 3.2 Reactivity versus Burnup for Various Fissile Materials in UO_2

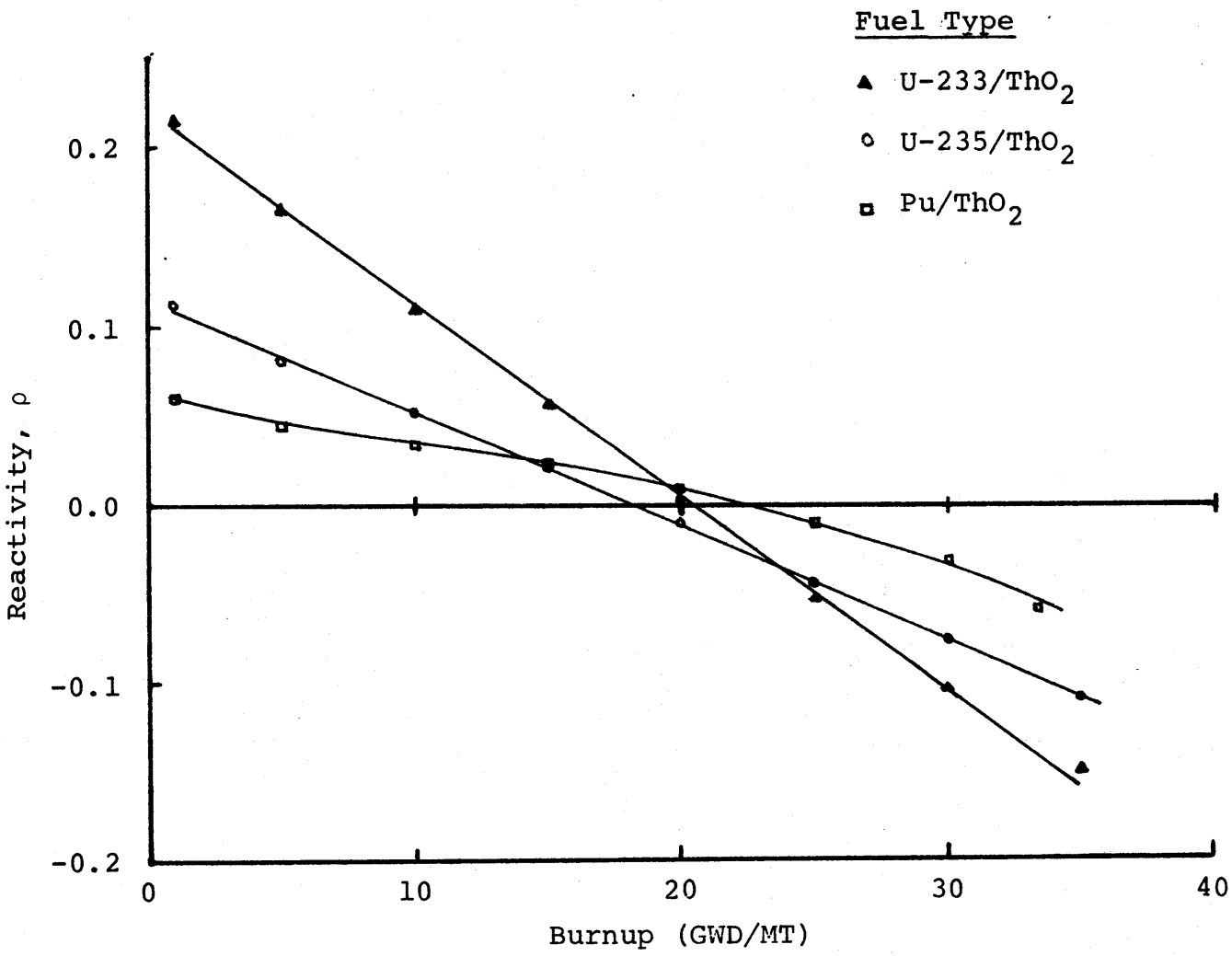

Fig. 3.3 Reactivity versus Burnup for Various Fissile Materials in ThO_2

weight. The Pu-240 isotope has a large, sharp resonance at 1.05 eV and thus behaves like a self-shielded burnable poison to thermal neutrons. The production of the high-worth fissile isotope Pu-241, coupled with the depletion of the "burnable poison" Pu-240, provides extra reactivity which effectively 'flattens' the $\rho(B)$ trace of the Pu/ThO_2 system [H-2]. The above explanation for the non-linear behavior of the Pu/ThO_2 system $\rho(B)$ trace was confirmed by making a similar supercell depletion calculation using pure Pu-239 as the fissile material. The resulting reactivity versus burnup curve was much "steeper" and much more linear (with $R^2 = 0.995$).

3.2.2 A CONTRIBUTION TO THE DEBATE AS TO WHY $\rho(B)$ IS LINEAR

Although researchers in the field of PWR nuclear fuel management have recognized the linearity of the $\rho(B)$ curve for a core lattice/assembly and have made good use of this empirical observation, no physical explanation has been advanced to account for this phenomenon. Through the process of induction, an attempt is made here to better understand the cause for this linear behavior.

For the $U\text{-}235/UO_2$ lattice system, a major reactivity penalty comes from the accumulation of fission products with burnup. The reactivity loss due to fission product buildup is given by (using a one-group model)

$$\rho_{FP} = \frac{C_{FP}}{\nu F} \qquad (3.9)$$

where F is the fission rate which, for constant power level operation, is approximately, a constant,

$$= [\, N_{25}\sigma_f^{25} + N_{49}\sigma_f^{49} \,] \cdot \phi$$

and C_{FP} is the capture rate in the fission products

$$= N_{FP} \cdot \sigma_c^{FP} \cdot \phi$$

But $$N_{FP} \simeq 2F \cdot t \qquad (3.10)$$

where $F \cdot t$ is the total fissions, and the relatively small effect of fission product transmutation is neglected [A-4].

Therefore, the reactivity loss due to fission products is given by,

$$\rho_{FP} = \frac{2F \cdot t \cdot \sigma_c^{FP} \cdot \phi}{\nu F}$$

$$= \left(\frac{2\sigma_c^{FP}}{\nu} \right) \cdot \phi \cdot t$$

$$\simeq (\text{constant}) \cdot \phi \cdot t \qquad (3.11)$$

Since, as is well known, ϕ increases with time (to maintain a constant power level as fissile fuel depletes), we would expect ρ_{FP} to increase at a greater than linear rate with t.

But, the results from LEOPARD calculations, as shown in Fig. 3.4, indicate that there is a continuous readjustment of the spectrum by the lattice to produce changes in the spectrum-averaged cross sections (and to a lesser extent, ν), such that the loss in reactivity due to fission products, ρ_{FP}, is caused to be a linear function of time (burnup). This prompts the speculative suggestion that an underlying physical principle may govern the behavior of neutrons in a steady state LWR lattice parallel to Le Chatelier's principle in physical chemistry! In any event, the linearity is a fortunate convergence of several complicated adjustments in lattice neutronics—not readily explained in simplistic terms: as already noted, the same effect is observed in other fuel types, ruling out the attribution of this linear behavior to some unique properties of a particular fissile/fertile species.

3.3 OTHER KEY FEATURES OF LRM METHODOLOGY

To improve the accuracy of the linear reactivity model, some of its constraining conditions had to be relaxed. Equal power sharing among fuel batches and the neglect of neutron leakage from the reactor core, are perhaps the only two important assumptions made in the previous derivations, which do not reflect the actual behavior of pressurized water reactor cores. In this section the correct algorithm for combining the reactivity of fuel batches in a core, to account for unequal power sharing characteristics of these batches will be formulated, and leakage of neutrons from the reactor core will

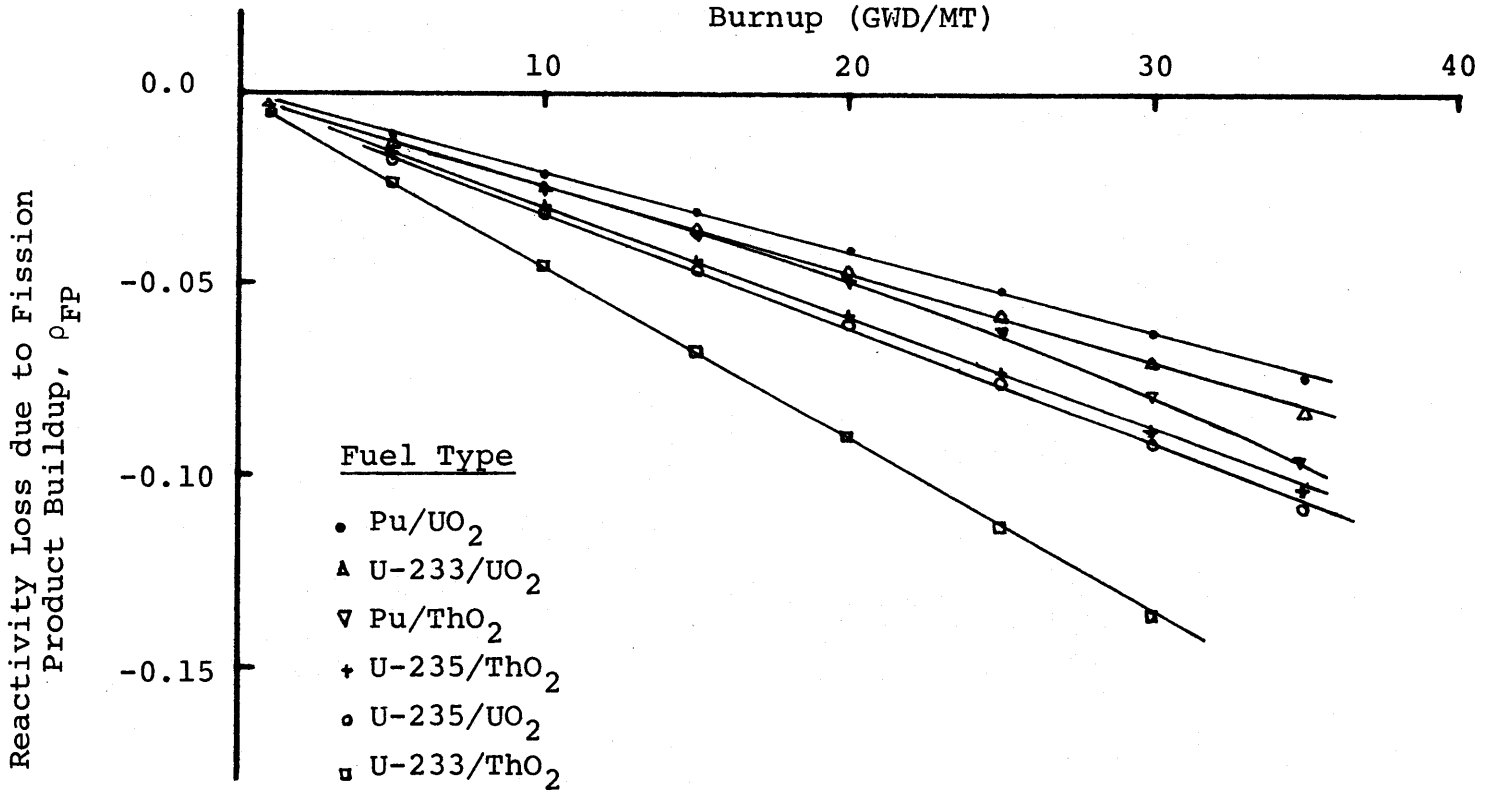

Fig. 3.4 Reactivity Loss Due to Fission Product Buildup versus Burnup for Different Fuel Types

also be included in the methodology.

3.3.1 POWER WEIGHTING

The equal power sharing approximation assumes that the total thermal power in the reactor core, at any time, is contributed by all the fuel batches (of the same size) in equal proportion. But, intuitively we expect a fresh batch of fuel (of higher reactivity worth) to run at a higher power level than an older fuel batch. The first step in accounting for this added realism is to develop a power-reactivity weighting algorithm.

Consider a large reactor core with no leakage of neutrons and having n fuel regions (assemblies or batches). The reactivity of an individual fuel region, i, can be defined in terms of the neutron production rate by fission, νF_i, and neutron destruction rate by absorption, A_i

$$\rho_i = \frac{\nu F_i - A_i}{\nu F_i} \tag{3.12}$$

The system reactivity is thus,

$$\rho_{sys} = \frac{\sum_{i=1}^{n} (\nu F_i - A_i)}{\sum_{i=1}^{n} \nu F_i} \tag{3.13}$$

Using Eq. (3.12) to eliminate A_i in Eq. (3.13) yields:

$$\rho_{sys} = \frac{\sum_{i=1}^{n} \nu F_i \rho_i}{\sum_{i=1}^{n} \nu F_i} \tag{3.14}$$

We now assume that the average amount of thermal power generated is directly proportional to the total fission neutron production rate, and that this quantity does not vary significantly with the burnup status (i.e., composition) of the fuel. This assumption is valid if the ratio of the average energy released per fission (κ) to the average number of neutrons released per fission (ν) is a constant. Figure 3.5 shows that the variation of (κ/ν) with burnup is very slight in Maine Yankee supercell depletion calculations. Hence:

$$\rho_{sys} = \frac{\sum_{i=1}^{n} q_i \rho_i}{\sum_{i=1}^{n} q_i} \tag{3.15}$$

where q_i is the thermal power associated with fuel region i. Total core power Q is given by

$$Q = \sum_{i=1}^{n} q_i \tag{3.16}$$

If we define the normalized thermal power fraction f_i as

$$f_i = \frac{q_i}{\sum_{i=1}^{n} q_i} = \frac{q_i}{Q} \tag{3.17}$$

such that

$$\sum_{i=1}^{n} f_i = 1 \tag{3.18}$$

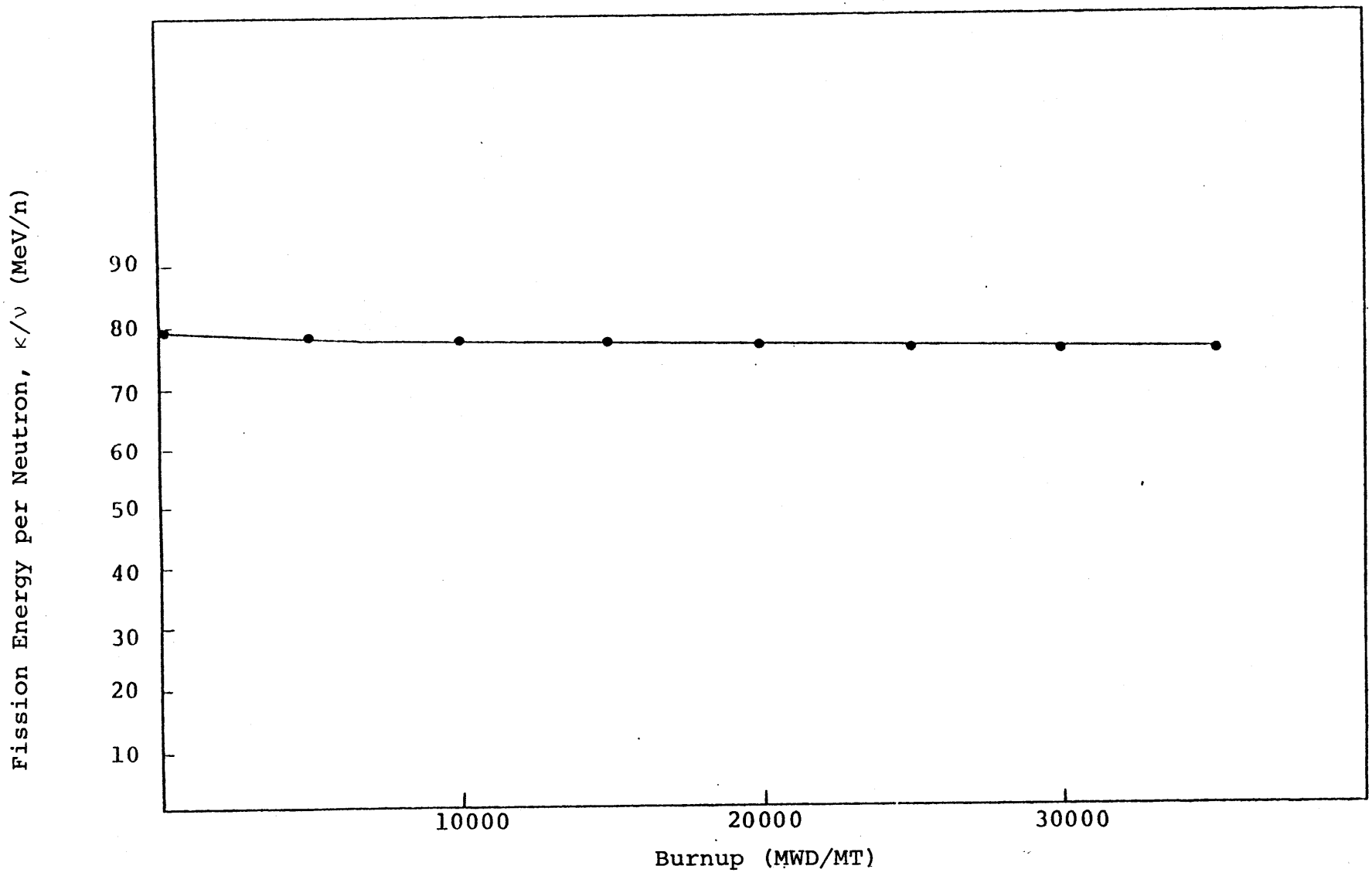

Fig. 3.5 Average Energy Release per Fission Neutron (κ/ν) as a Function of Fuel Burnup [S-2]

then Eq. (3.15) can be rewritten:

$$\rho_{sys} = \sum_{i=1}^{n} f_i \rho_i \tag{3.19}$$

Sefcik [S-2] has tested this equation (expressed in terms of the neutron multiplication factor, k) against PDQ-7 results generated for a two-region (i=2), zero current boundary condition problem. Good agreement ($\Delta k_{sys} < 0.4$ %) was found between the eigenvalues calculated using Eq. (3.19) and those computed by the PDQ-7 code, supporting the use of Eq. (3.19) for present purposes. The approximate value of this relation should be noted, however: in addition to assuming κ/ν is invariant, the preceding development implies that the infinite medium reactivity also characterizes assemblies surrounded by non-identical neighbors -- an inexact prescription because of inevitable changes in the neutron spectrum, particularly near the assembly periphery. The consequences of power weighting can now be realized by redoing the reactivity balance for an n-batch, steady state core. Assuming that the cycle burnup for a given batch, i, is proportional to its average power level $\bar{f}_i$:

$$\begin{aligned}
\rho_1 &= \rho_o - AB_{dis}\bar{f}_1 \\
\rho_2 &= \rho_o - AB_{dis}(\bar{f}_1+\bar{f}_2) \\
&\vdots \\
\rho_n &= \rho_o - AB_{dis}(\bar{f}_1+\bar{f}_2+\ldots+\bar{f}_n)
\end{aligned} \tag{3.20}$$

At the end of cycle (reactivity-limited condition), and assuming that the corresponding thermal power fraction of batch i is given by f_i:

$$\rho_{sys} = 0 = \sum_{i=1}^{n} f_i \rho_i \tag{3.21}$$

Expanding the equation, we get

$$\rho_{sys} = 0 = \rho_o - AB_{dis}\left[\sum_{i=1}^{n}\sum_{j=1}^{i} f_i \bar{f}_j\right] \tag{3.22}$$

or

$$B_{dis} = \frac{\rho_o}{A\left[\sum_{i=1}^{n}\sum_{j=1}^{i} f_i \bar{f}_j\right]} \tag{3.23}$$

The term with a double summation in the denominator (designated as the "cycle schedule index" (CSI) by Sefcik [S-2] reduces to $\left(\frac{n+1}{2n}\right)$ if we assume that the power fractions for the batches remain constant over a cycle

$$f_i = \bar{f}_i \tag{3.24}$$

and that there is equal power sharing among the batches

$$f_i = f_{i+1} \qquad i = 1, 2, \ldots, n-1 \tag{3.25}$$

In addition, it can be shown that the condition of equal

power sharing as expressed in Eq. (3.25) results in the minimum value of the CSI when Eq. (3.24) is also imposed and hence the "maximum" discharge burnup. Although the preceding development suggests the objective of achieving a uniform burnup rate, it should be pointed out that this goal is not attainable in practice. A fresh fuel batch having large positive reactivity inherently tends to have higher power, and hence cycle burnup, than those older fuel batches having low or negative reactivity. Fortunately, because Eq. (3.24) is not necessarily true, the use of burnable poison for power/reactivity suppression can lead to higher discharge burnups than the flat power result. This is discussed in the next chapter.

It is important to note that the effects of unequal power sharing are not large; for example, the difference in discharge burnup between a $(\frac{1}{3}, \frac{1}{3}, \frac{1}{3})$ set of f_i and a $(\frac{1}{2}, \frac{1}{3}, \frac{1}{6})$ pattern is only 4 %.

Finally, it should be noted that the f_i appear in a dual role: as the parameters determining the cycle-by-cycle burnup history of a given batch, and as the parameters defining the power level of all batches in the core during a given cycle. The CSI accounts for the effect of non-uniform core power distribution among the fuel batches. This index will be expressed more explicitly once the appropriate functional dependence of f_i on ρ_i is established.

3.3.2 LEAKAGE OF NEUTRONS

Accounting for neutron leakage from a reactor core is an important improvement to the linear reactivity model since approximately 3 % to 4 % of the neutrons are lost via leakage in a normal pressurized water reactor operated with a conventional out-in/scatter fuel management scheme. This will allow a more accurate determination of the core reactivity (and hence, the discharge burnup) using the LRM approach.

The neutrons leaking from the core are parasitically absorbed in the structures surrounding the core (such as the core barrel, thermal shields, grids, etc.). The absorption of neutrons in the ex-core regions can be incorporated into the system reactivity expression by introducing the term A_R which is defined as the neutron absorption rate in the non-fuel, ex-core regions. The system reactivity of a steady state core having n fuel regions (assemblies/batches) can therefore be written as:

$$\rho_{sys} = \frac{\left[\sum_{i=1}^{n} (\nu F_i - A_i)\right] - A_R}{\sum_{i=1}^{n} \nu F_i}$$

$$= \left[\sum_{i=1}^{n} f_i \rho_i\right] - \frac{A_R}{\sum_{i=1}^{n} \nu F_i} \qquad (3.26)$$

where νF_i and A_i are the neutron production rate by fission and the neutron absorption rate in the fuel region i, respectively; ρ_i is the reactivity of fuel region i, and f_i is

its thermal power fraction. The term $\frac{A_R}{\sum_{i=1}^{n} \nu F_i}$ is associated with leakage and thus can be characterized as the leakage reactivity, ρ_L. Equation (3.26) can therefore be written as:

$$\rho_{sys} = \left[\sum_{i=1}^{n} f_i \rho_i\right] - \rho_L \qquad (3.27)$$

and the corresponding discharge burnup:

$$B_{dis} = \frac{\rho_o - \rho_L}{A\left[\sum_{i=1}^{n} \sum_{j=1}^{i} f_i \bar{f}_j\right]} \qquad (3.28)$$

If A_R is the total ex-core absorption rate, then ρ_L will include the radial as well as the axial leakage of neutrons from the core. However, for the purpose of this research, the radial and the axial component of the leakage reactivity are assumed to be "decoupled," i.e., separable -- changes in one will not affect the other.

Neutrons leaking from the core are primarily those of the fast group (since thermal leakage is approximately an order of magnitude smaller) and this leakage is essentially dependent upon the shape of the source. If we consider a fuel region of total length 2L with a source shape which is symmetrical about the centerline/origin, then the leakage reactivity (fraction of neutrons leaking out of the edge of the fuel region) is given by:

$$\rho_L = \frac{\int_0^L J(x,L)\ \psi(x)\ dx}{\int_0^L \psi(x)\ dx} \tag{3.29}$$

where $\psi(x)$ is the source shape and the neutron current at L (the edge) due to a source at x

$$J(x,L) = \frac{-\ D d\phi(x,L)}{dx} \tag{3.30}$$

The flux kernel (flux at L due to source at x) $\phi(x,L)$ is given by (plane geometry approximation):

$$\phi(x,L) = \frac{M}{2D} \exp\ [-\ \frac{(L-x)}{M}] \tag{3.31}$$

where D is the coefficient of diffusion, and
M^2 is the migration area.

Equation (3.29) can thus be written as

$$\rho_L = \frac{\int_0^L \frac{1}{2} \exp\ [-\ \frac{(L-x)}{M}]\ \psi(x)\ dx}{\int_0^L \psi(x)\ dx} \tag{3.32}$$

However, the treatment of leakage developed thus far is only applicable to the leakage of neutrons in the axial direction since the source shape in this direction is readily characterized throughout the in-core residence of the fuel. On the other hand, the radial source shape is more complex, varying with the fuel loading pattern. Therefore a different approach is taken to account for radial leakage, as will be discussed later in this section.

In a PWR core, the axial source shape is cosine $[\psi(x) = \psi_o \text{Cos}\ (\frac{\pi x}{2L})]$ at the beginning of life and flat with drooping ends $[\psi(x) \simeq \psi_o\ (1 - \exp\{-\frac{(L-x)}{M}\})]$ by the end of a typical in-core cycle. Since the reactivity balance of greatest interest is at end of cycle (EOC) the EOC source shape should be employed to evaluate the leakage reactivity in the axial direction. Thus

$$\rho_L = \frac{\int_o^L \frac{1}{2} \exp\ [-\frac{(L-x)}{M}] \cdot \psi_o[1-\exp\{-\frac{(L-x)}{M}\}]\ dx}{\int_o^L \psi_o[1-\exp\{-\frac{(L-x)}{M}\}]\ dx}$$

$$\simeq \frac{1}{4[(\frac{L}{M})-1]} \qquad (3.33)$$

Using representative values for a PWR of the core half-height, L = 175.0 cm, and the migration length, M = 7.5 cm, the axial leakage reactivity is approximately 0.0112.

Closer inspection of the flux kernel indicates that the leakage effect is most prominent in the last few migration (diffusion) lengths of the fuel material. This implies that, in the context of a core, neutrons leaking from it are predominantly from within two or three migration lengths of the core periphery. This suggests an approach for handling radial leakage, that is, the the correlation of radial leakage reactivity with core assembly peripheral power since PWR assemblies are approximately 2M ≃ 15 cm wide. We can thus express the radial leakage reactivity as:

$$\rho_L = \alpha f_{per} \tag{3.34}$$

where f_{per} is the cumulative power fraction of the peripheral assemblies

and α is a constant which depends upon the particulars of a given reactor design.

The correlation expressed by Eq. (3.34) agrees well with the results of PDQ-7 calculations for a CE System 80 PWR, as shown in Fig. 3.6 [K-2]. Similar analyses were done by Sefcik [S-2] for the Maine Yankee reactor, again using PDQ-7 static computations. Here, by successively shuffling four fuel batches in the core between the periphery and the interior, the peripheral power was varied. Fresh fuel loaded on the core periphery produces the highest power fraction, whereas cycle four fuel on the core periphery gives the lowest power fraction case. The results are shown in Fig. 3.7.

3.4 POWER SPLIT RELATION AMONG BATCHES

In the preceding section, the power-weighting scheme for combining the reactivity of fuel batches in a core, and prescriptions accounting for neutron leakage were incorporated into the LRM methodology. However, the remaining component necessary for the implementation of the LRM methodology in a complete and rigorous fashion is the power sharing relationship among the fuel batches in the PWR core. Although the power fractions of the fuel regions (assemblies/batches) can be determined using detailed computer analysis, a simple

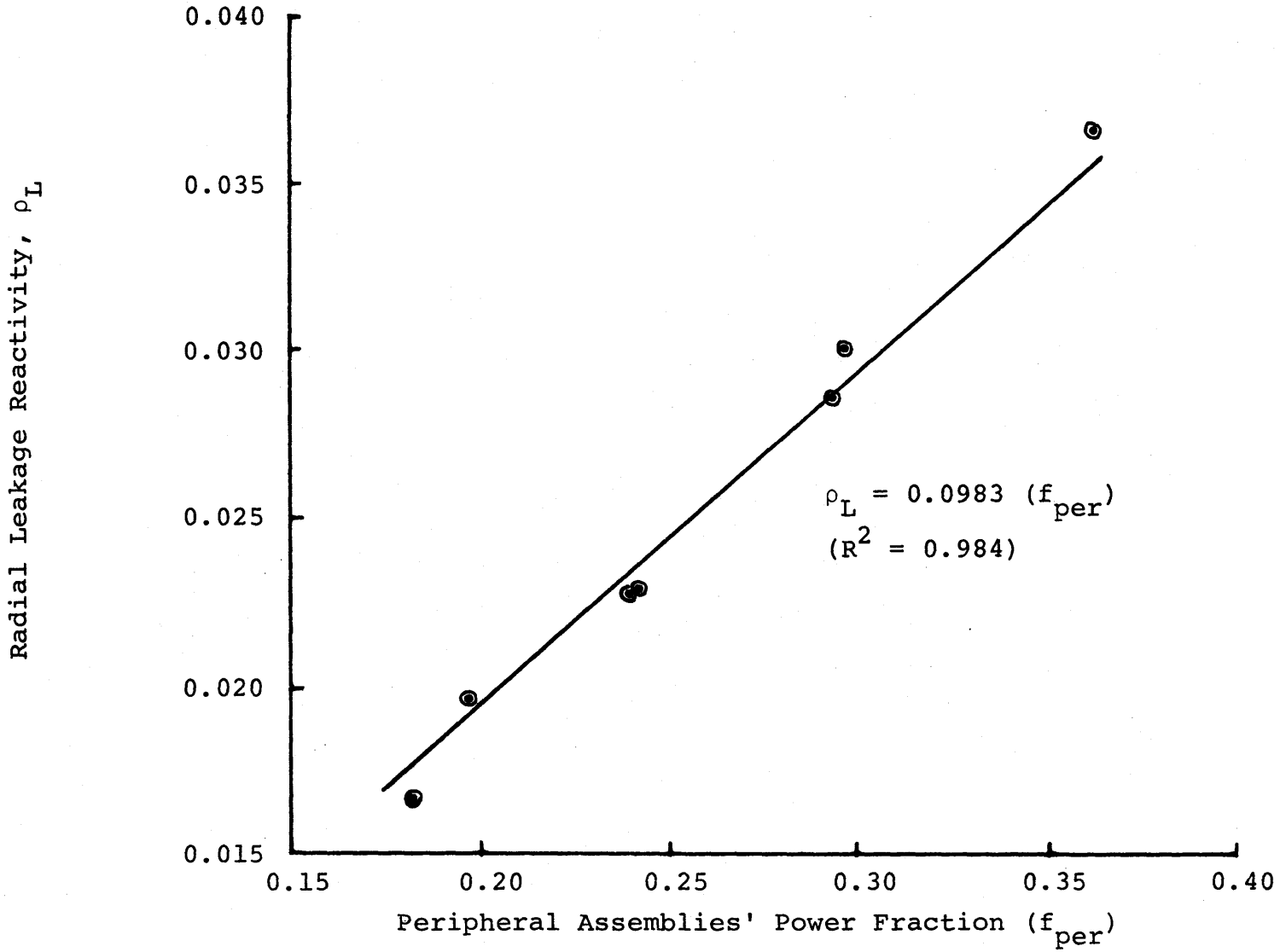

Fig. 3.6 Radial Leakage Reactivity vs. Peripheral Assemblies' Power Fraction

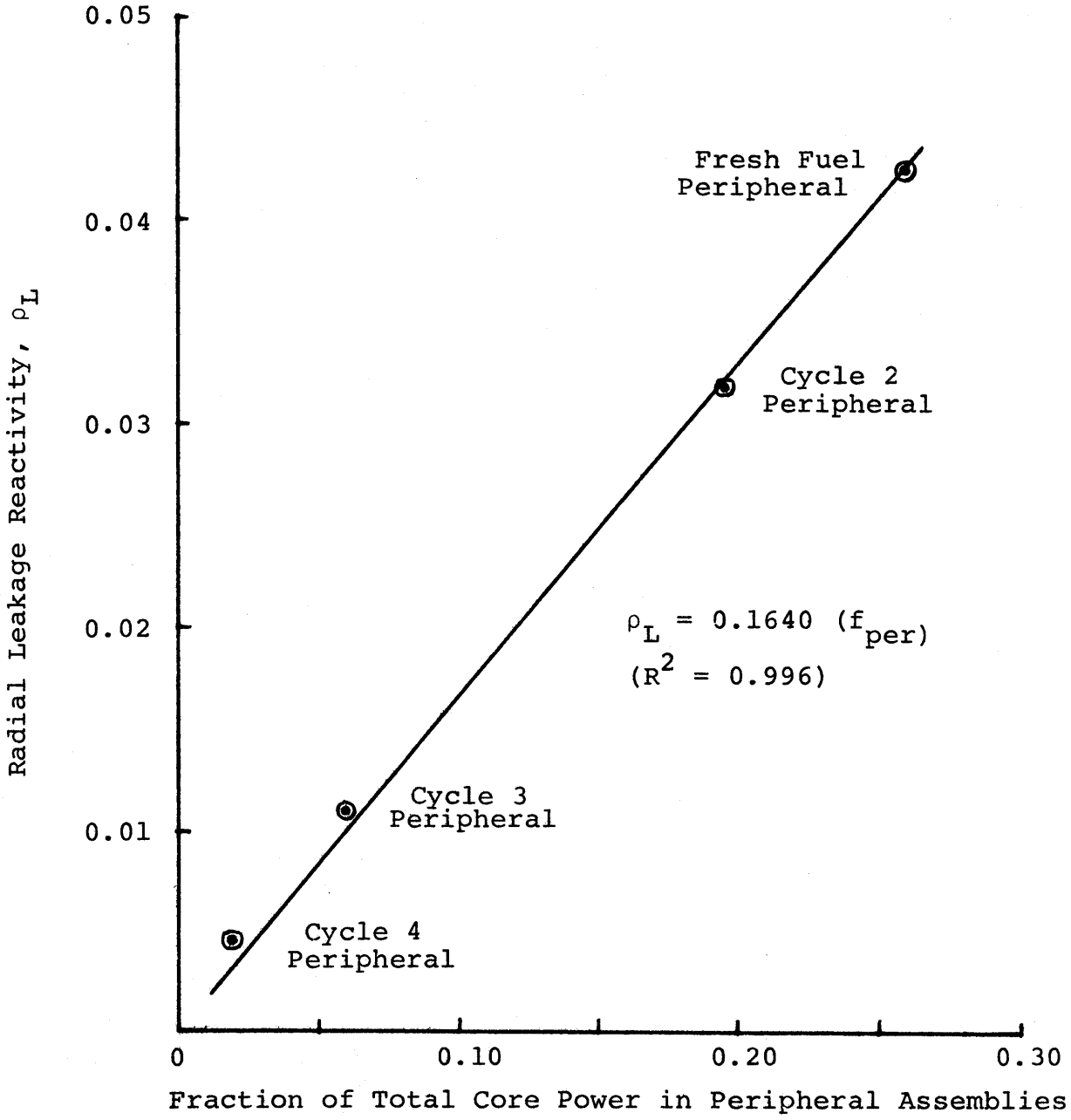

Fig. 3.7 Radial Leakage Reactivity for M.Y. Reactor vs. Fraction of Core Power Generated in Peripheral Assemblies

power sharing relation which has a sound theoretical basis will be employed in this research. Empirical power sharing algorithms have been proposed in the past [S-2], for example:

$$f_i \propto \left(\frac{1}{1-\rho_i}\right)^{\theta} \tag{3.35}$$

where f_i and ρ_i are the power fraction and the reactivity of the fuel region i, respectively, and θ is an empirical exponent. Here we will show that relations of this type can be put on a theoretically sound basis.

Using the "group-and-one-half" theory, the power split equation used in this work will be derived. The equation will be verified using results from PDQ-7 calculations of a nine-bundle, zero-current boundary condition problem as well as those from quarter-core analyses.

3.4.1 DERIVATION OF POWER SPLIT EQUATION

The two-group theory requires the solution of the coupled fast and thermal group diffusion equations:

<u>fast group</u> (> 0.6 ev)

$$\underset{\text{leakage}}{-D_1\nabla^2\phi_1} + \underset{\text{absorption}}{\Sigma_{a1}\phi_1} + \underset{\text{down-scatter}}{\Sigma_{12}\phi_1} - \underset{\text{fission source}}{\frac{1}{k}(\nu\Sigma_{f1}\phi_1 + \nu\Sigma_{f2}\phi_2)} = 0 \tag{3.36}$$

thermal group

$$- D_2\nabla^2\phi_2 + \Sigma_{a2}\phi_2 - \Sigma_{12}\phi_1 = 0 \qquad (3.37)$$

leakage absorption in-scatter

where k is the eigenvalue (the neutron multiplication factor) and Σ_{12} is the macroscopic downscatter cross section from group one to group two.

In the "group-and-one-half" model of core neutronics, the thermal neutrons are absorbed at the point of removal from the fast group, or equivalently, the thermal leakage, which is an order of magnitude smaller than the fast leakage, is neglected ($\nabla^2\phi_2 \simeq 0$). Equation (3.37) thus becomes

$$\Sigma_{a2}\phi_2 = \Sigma_{12}\phi_1 \qquad (3.38)$$

Equations (3.36) and (3.38) can be manipulated into an equivalent one-group model for the fast group flux; for a critical medium (k=1) we have:

$$\nabla^2\phi_1 + \frac{1}{M^2}\left(\frac{\rho}{1-\rho}\right)\phi_1 = 0 \qquad (3.39)$$

where M^2 is the migration area

$$= D_1 / (\Sigma_{12} + \Sigma_{a1})$$

and ρ is the local reactivity

$$= (k_\infty - 1)/k_\infty$$

The local thermal power density can be written as

$$q''' = \kappa\Sigma_{f1}\phi_1 + \kappa\,\Sigma_{f2}\phi_2 \tag{3.40}$$

where κ is the energy released per fission. Substituting ϕ_2 from Eq. (3.38) into Eq. (3.40) we have

$$q''' = \kappa\left[\,\Sigma_{f1} + \frac{\Sigma_{f2}\Sigma_{12}}{\Sigma_{a2}}\,\right]\phi_1 \tag{3.41}$$

The two group value of the local eigenvalue k_∞ is given by

$$k_\infty = \frac{\nu\Sigma_{f1}}{\Sigma_{a1}+\Sigma_{12}} + \frac{\Sigma_{12}}{\Sigma_{a1}+\Sigma_{12}} \cdot \frac{\nu\Sigma_{f2}}{\Sigma_{a2}} \tag{3.42}$$

The local thermal power density can therefore be written as

$$q''' = \frac{\kappa}{\nu}\,(\Sigma_a+\Sigma_{12})\;k_\infty\phi_1$$

$$= \left(\frac{\kappa}{\nu}\right)\left(\frac{D_1}{M^2}\right)\;k_\infty\phi_1 \tag{3.43}$$

Assuming that κ, D_1 and M^2 do not vary with position, substitution of Eq. (3.43) into Eq. (3.39) yields:

$$\nabla^2\left(\frac{f}{k_\infty}\right) + \frac{1}{M^2}\left(\frac{\rho}{1-\rho}\right)\left(\frac{f}{k_\infty}\right) = 0 \tag{3.44}$$

where f is the normalized local power fraction

$= Vq'''/Q$,

V is the nodal volume,

and Q is the total core power.

The Laplacian in Eq. (3.44) can be approximated as the difference between the local value and the average of its surroundings, in which case Eq. (3.44) can be rewritten:

$$\frac{\left(\frac{V_i}{V_s}\right)\left(\frac{\bar{f}}{k_\infty}\right)_s - \left(\frac{f}{k_\infty}\right)_i}{\gamma h^2} + \left(\frac{1}{M}\right)^2 \rho_i f_i = 0 \qquad (3.45)$$

where h is the size of the node -- in our case the width of an assembly,

γ is a constant,

and subscripts i and s denote the node and its surroundings (here the sum of 8 nodes), respectively.

Solving Eq. (3.45) for the power fraction in node i gives:

$$f_i = \frac{\left(\frac{V_i}{V_s}\right)\left(\frac{\bar{f}}{k_\infty}\right)_s}{1 - \theta\rho_i} \qquad (3.46)$$

where $\theta = \left(1 + \frac{\gamma h^2}{M^2}\right)$

here treated as a constant, since we are concerned primarily with PWR cores.

Equation (3.46) constitutes the power-sharing algorithm required in the LRM methodology. For a group of assemblies

(usually a fuel reload batch) in a critical core, we will use the form:

$$f_i = \frac{\bar{f}}{1 - \theta\rho_i} \tag{3.47}$$

where $\bar{f}$ is the average power fraction for an aggregation of assemblies of the size in question (for example, $\bar{f} = \frac{1}{n}$ for an n-batch core).

An important constraint which the power split relation must comply to is

$$\sum_{i=1}^{n} f_i = 1 \tag{3.48}$$

or

$$\sum_{i=1}^{n} (f_i - \bar{f}) = \sum_{i=1}^{n} (f_i - \frac{1}{n}) = 0 \tag{3.49}$$

Substituting Eq. (3.47) for f_i, we have

$$\sum_{i=1}^{n} \left[\left(\frac{\frac{1}{n}}{1 - \theta\rho_i} \right) - \frac{1}{n} \right] = \sum_{i=1}^{n} \frac{1}{n} \left[\frac{1 - (1 - \theta\rho_i)}{1 - \theta\rho_i} \right]$$

$$= \sum_{i=1}^{n} \theta \left(\frac{\frac{1}{n}}{1 - \theta\rho_i} \right) \rho_i$$

$$= \theta \sum_{i=1}^{n} f_i\rho_i = 0 \tag{3.50}$$

Since θ is a constant, we will have

$$\sum_{i=1}^{n} f_i \rho_i = 0 \qquad (3.51)$$

This equation can be recognized as the power-weighted prescription for core reactivity averaging, which was independently derived in the previous section (3.3.1) using the definition of reactivity. Hence Eq. (3.47) is a compatible power split formulation.

Finally, suppose we perturb the reactivity locally, say, in region i; the change in the local reactivity ($\Delta\rho_i$) affects the global reactivity according to (Taylor series expansion):

$$\Delta\bar{\rho} \simeq \sum \left(\frac{\partial \bar{\rho}}{\partial \rho_i}\right) \cdot \Delta\rho_i \qquad (3.52)$$

Application of the power split relation (Eq. 3.47) gives:

$$\begin{aligned} \Delta\bar{\rho} &\simeq \sum \frac{\partial}{\partial \rho_i} \{f_i \rho_i\} \Delta\rho_i \\ &= \sum \frac{\partial}{\partial \rho_i} \left\{ \frac{\frac{1}{n}}{1-\theta\rho_i} \cdot \rho_i \right\} \Delta\rho_i \\ &= \frac{1}{n} \sum \left\{ \frac{1}{(1-\theta\rho_i)^2} \right\} \Delta\rho_i \end{aligned} \qquad (3.53)$$

or,

$$\Delta\bar{\rho} \simeq n \sum f_i^2 \cdot \Delta\rho_i \qquad (3.54)$$

Hence the power split relation given by Eq. (3.47) generates the familiar source-squared weighting typical of perturbation

theory methods. This is another argument favoring the use of this form of the power sharing algorithm.

Note that to a first order expansion, the power sharing prescription may be written in many forms:

$$f = \frac{\bar{f}}{1 - \theta\rho} \simeq f(1 + \theta\rho) \tag{3.47b}$$

$$\simeq \bar{f}\left(\frac{1}{1-\rho}\right)^{\theta} \equiv \bar{f}k^{\theta} \tag{3.47c}$$

The last expression is in fact the form deduced by Sefcik [S-2] on purely empirical grounds; the first expression, which is linear in ρ, will prove useful in analytic applications to be discussed later. Also see Appendix E for adddi-tional discussion.

3.4.2 VERIFICATION FOR INTERIOR ASSEMBLIES

The power split relation given by Eq. (3.47) is compatible with several powerful constraints imposed on the linear reactivity model methodology development. However, verification of this power sharing algorithm using results generated from detailed computer analysis is necessary, so as to evaluate the accuracy with which the algorithm describes a specific or generic reactor core environment. Conditions in the interior of the core are considered first, and application of the power split equation to the core peripheral assemblies is featured in the next section.

In the interior of a PWR core (i.e., excluding the peripheral ring of assemblies), the fuel assemblies with higher reactivity

are normally surrounded with low reactivity fuel assemblies to achieve power flattening. This well shuffled core pattern can be represented by the configuration and boundary conditions shown in Fig. 3.8. To test the power split relation given by Eq. (3.46), a series of PDQ-7 calculations were performed with three successive constant values of k_2 (0.9, 1.0, 1.2) and the values of k_1 were varied over a wide range of enrichments, burnups, fuel-to-moderator ratios and boron concentrations. Figure 3.9 shows the plot of $\left[\left(\frac{V_1}{V_2}\right)\left(\frac{\overline{f}}{k_\infty}\right)_2\right] / f_1$ versus $\rho_1 = 1 - \frac{1}{k_1}$. Plotted in this manner, the slope of the curve is just the constant θ. While the linearity of the relationship is evident, the data scatters significantly (linear fit $R^2 = 0.831$), in particular the data points segregate according to the value of k_2. If only $k_2 = 1.0$ data is selected the agreement is considerably improved: $R^2 = 0.952$. This is not altogether unexpected and can be explained by the fact that the majority of the data points do not correspond to a critical configuration -- a condition imposed on the derivation of the power split equation. Otherwise the agreement must be considered good in view of the large variation in assembly properties considered.

A more appropriate set of data for the verification of the power split equation can be obtained from whole core analyses. Moreover, a value for the constant θ (See Eq. 3.47) which characterizes the particular core in question can be determined. This parameter is required in the application of the LRM methodology for the purpose of fuel management stra-

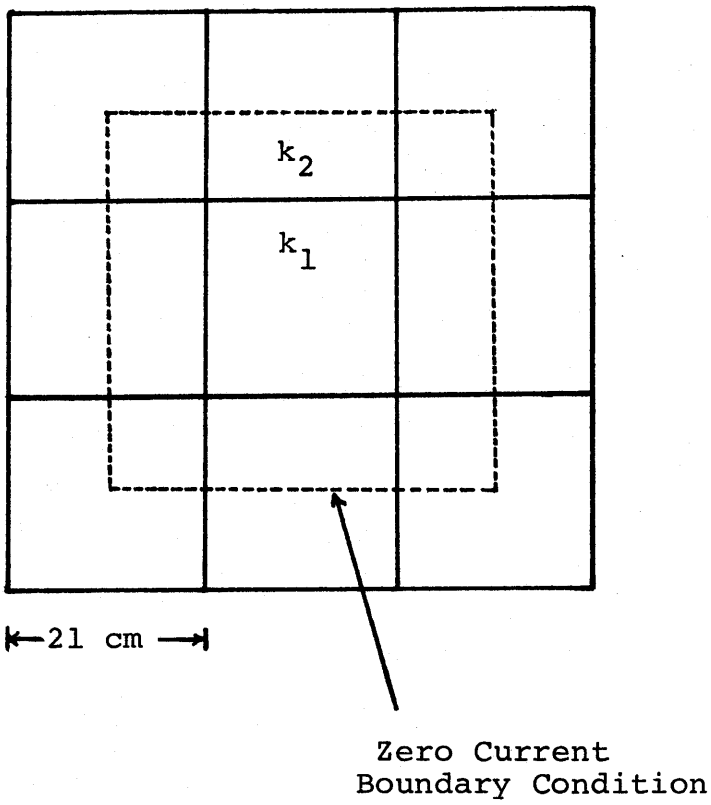

Fig. 3.8 Assembly Configuration for the Verification of the Power Split Relation (3 x 3 Bundles)

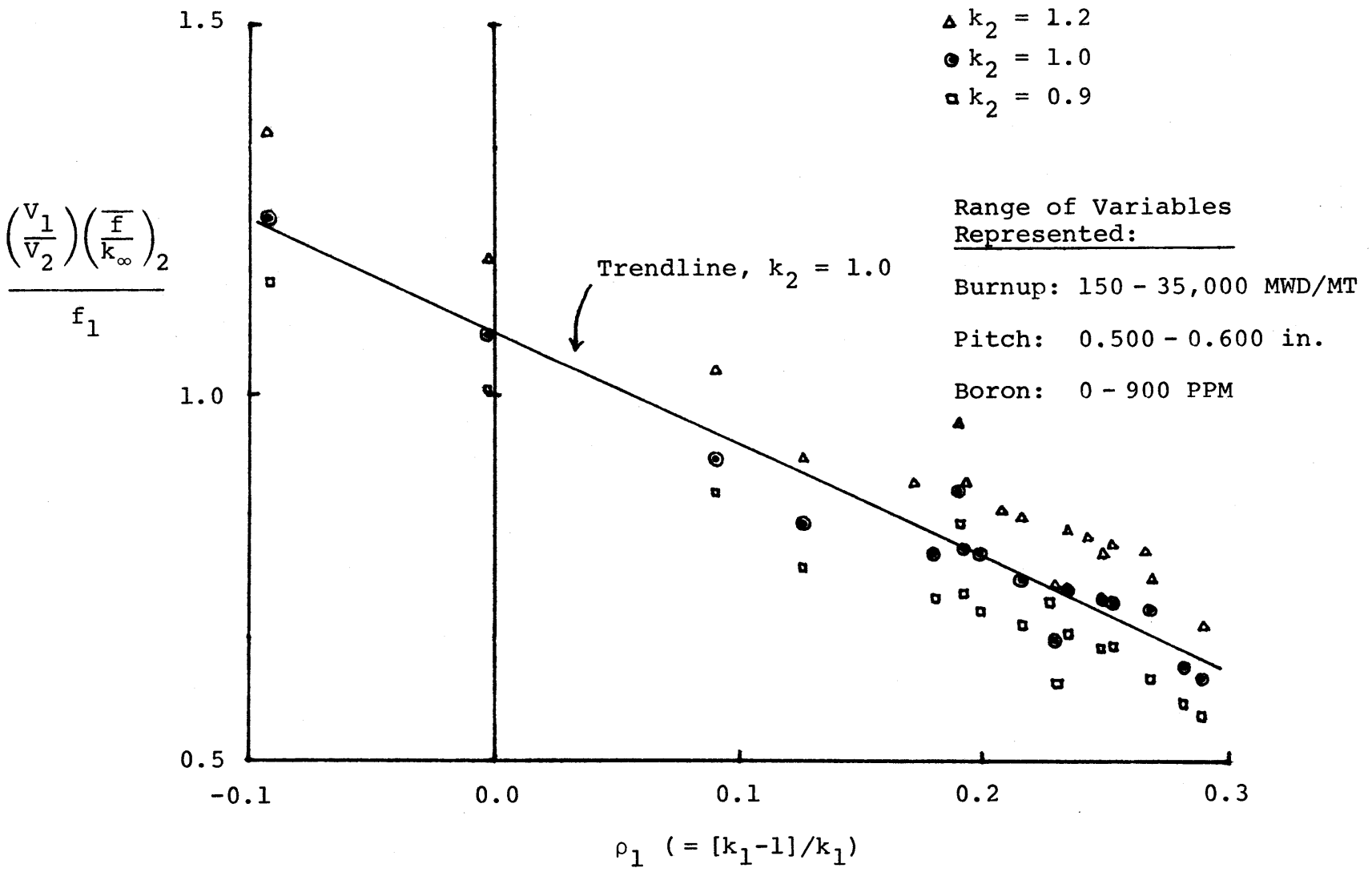

Fig. 3.9 Power Fraction-Reactivity Correlation for a 3 x 3 - Bundle Problem

tegy evaluation.

The two reactor system designs used in this context are the Maine Yankee cycle-four reload design and a representative CE System-80™ core design. The core maps together with the assemly k and its relative power for these two designs are shown in Figs. 3.10 and 3.11. The inverse of the interior assembly powers $(q/\bar{q})^{-1}$ as a function of the assembly reactivity ρ values are plotted in Figs. 3.12 and 3.13 for the Maine Yankee and System-80™ core designs, respectively. The wide scatter among assembly data is evident from the figures. The reason for this observation is similar to that given for the results of the 3 x 3 fuel bundle configuration analyses. However, for the present purpose it is more relevant to plot the data for assemblies grouped into a batch. Moreover, on the batch basis, the criticality constraint assumed in the derivation of the power split equation is more nearly satisfied. Figure 3.14 shows the results for the Maine Yankee cycle 4 reload core design. The best-fit line can be described by the equation

$$\left(\frac{q_{batch}}{q_{average}} \right)^{-1} = \left(\frac{f_{batch}}{\bar{f}} \right)^{-1} = 0.98 - \theta \rho_{batch} \qquad (3.55)$$

The constant θ has a value of 1.42. The coefficient of determination (R^2) for this plot is 0.988. Equation (3.55) can be rewritten as:

$$f_{batch} \simeq \frac{\bar{f}}{1 - \theta \rho_{batch}} \qquad (3.56)$$

k / $q/\bar{q}$								
						1.194 0.689	1.194 0.949	
				1.194 0.698	1.194 0.927	1.194 1.101	0.909 0.952	1.134 1.324
			1.194 0.843	1.138 1.153	0.934 0.891	0.928 0.943	1.139 1.280	0.935 1.062
		1.194 0.840	1.138 1.284	0.936 0.987	1.088 1.148	1.003 0.986	0.906 0.937	1.036 1.080
	1.194 0.696	1.138 1.152	0.936 0.991	1.075 1.200	1.016 1.040	0.917 0.935	1.103 1.179	1.011 1.097
	1.194 0.920	1.934 0.833	1.089 1.150	1.016 1.045	0.932 0.916	1.109 1.161	0.912 0.896	1.075 1.152
	1.195 1.087	0.928 0.931	1.003 0.972	0.917 0.929	1.110 1.161	1.908 0.914	1.082 1.090	1.006 1.010
1.194 0.680	0.909 0.936	1.140 1.251	0.896 0.791	1.103 1.158	0.912 0.889	1.082 1.090	0.910 0.832	1.037 0.907
1.195 0.934	1.139 1.300	0.935 1.039	1.036 1.049	1.011 1.078	1.075 1.041	1.006 1.005	1.036 0.905	0.908 0.734

Fig. 3.10 Core Map for Maine Yankee Cycle 4 Redesign [S-2]

k $q/\bar{q}$								
						1.174 0.694	1.170 0.958	
				1.173 0.772	1.169 0.995	1.168 1.123	0.900 0.878	1.137 1.338
			1.169 0.923	1.135 1.278	0.975 1.038	0.901 0.856	1.138 1.295	0.900 0.966
		1.169 0.923	1.135 1.306	0.956 1.064	1.137 1.280	0.919 0.816	0.905 0.839	1.139 1.267
	1.173 0.771	1.135 1.277	0.956 1.063	0.970 0.956	0.901 0.819	0.926 0.817	0.986 0.923	0.908 0.830
	1.169 0.994	0.975 1.037	1.137 1.279	0.901 0.819	0.041 1.071	1.055 1.133	1.025 1.067	1.012 1.043
	1.168 1.121	0.901 0.854	0.919 0.815	0.926 0.816	1.055 1.132	1.040 1.120	0.901 0.860	1.069 1.158
1.174								
0.694	0.900	1.138	0.905	0.988	1.025	0.901	1.054	1.012
1.170	0.875	1.292	0.837	0.922	1.063	0.852	1.138	1.085
0.956	1.137	0.900	1.139	0.906	1.024	1.040	1.024	0.896
	1.334	0.963	1.264	0.828	1.053	1.095	1.102	0.877

Fig. 3.11 Core Map for Combusion Engineering System-80™ Core [W-1]

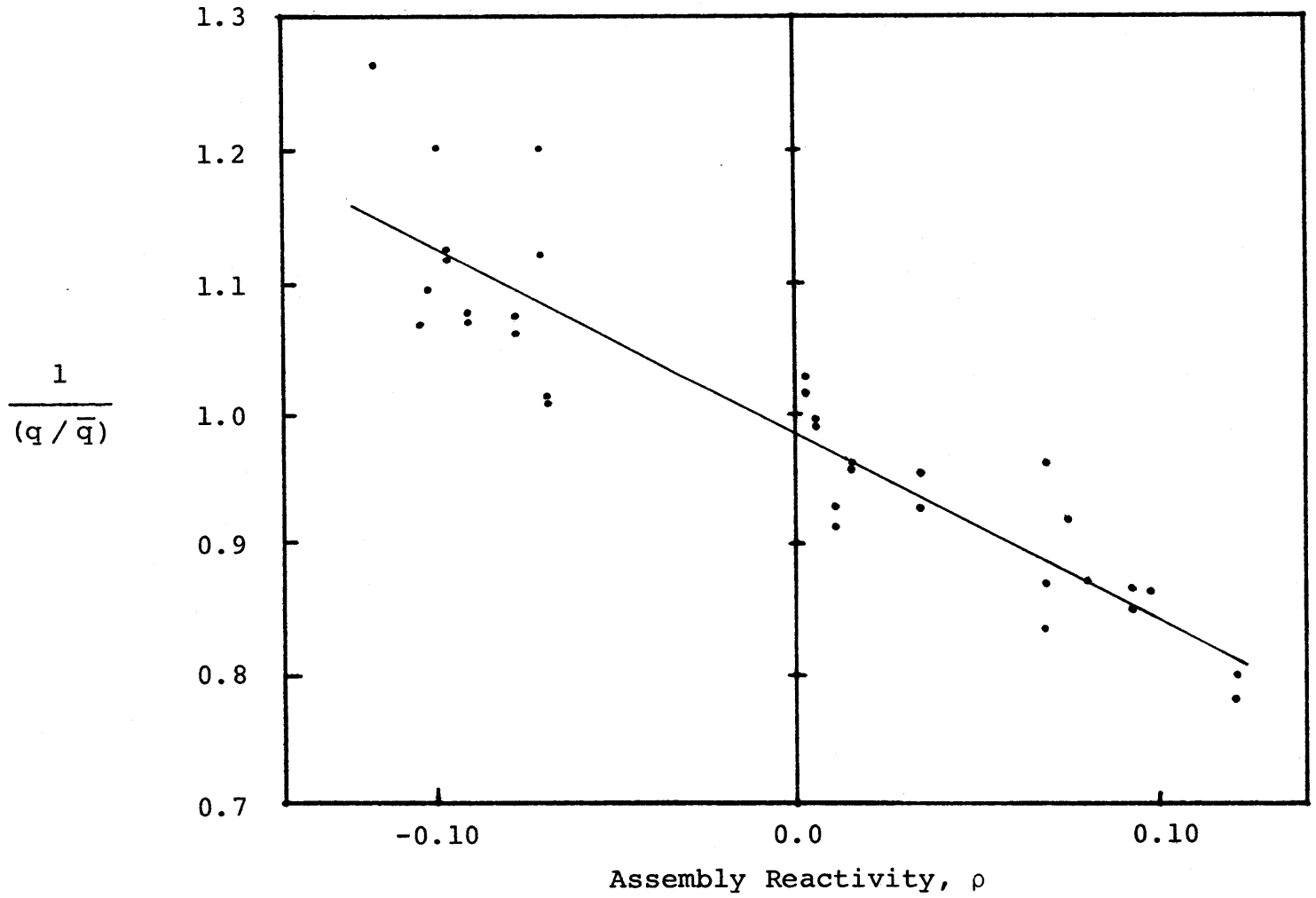

Fig. 3.12 Reciprocal Assembly Power vs. Assembly Reactivity for Interior Assemblies in the Main Yankee Cycle 4 Reload Design

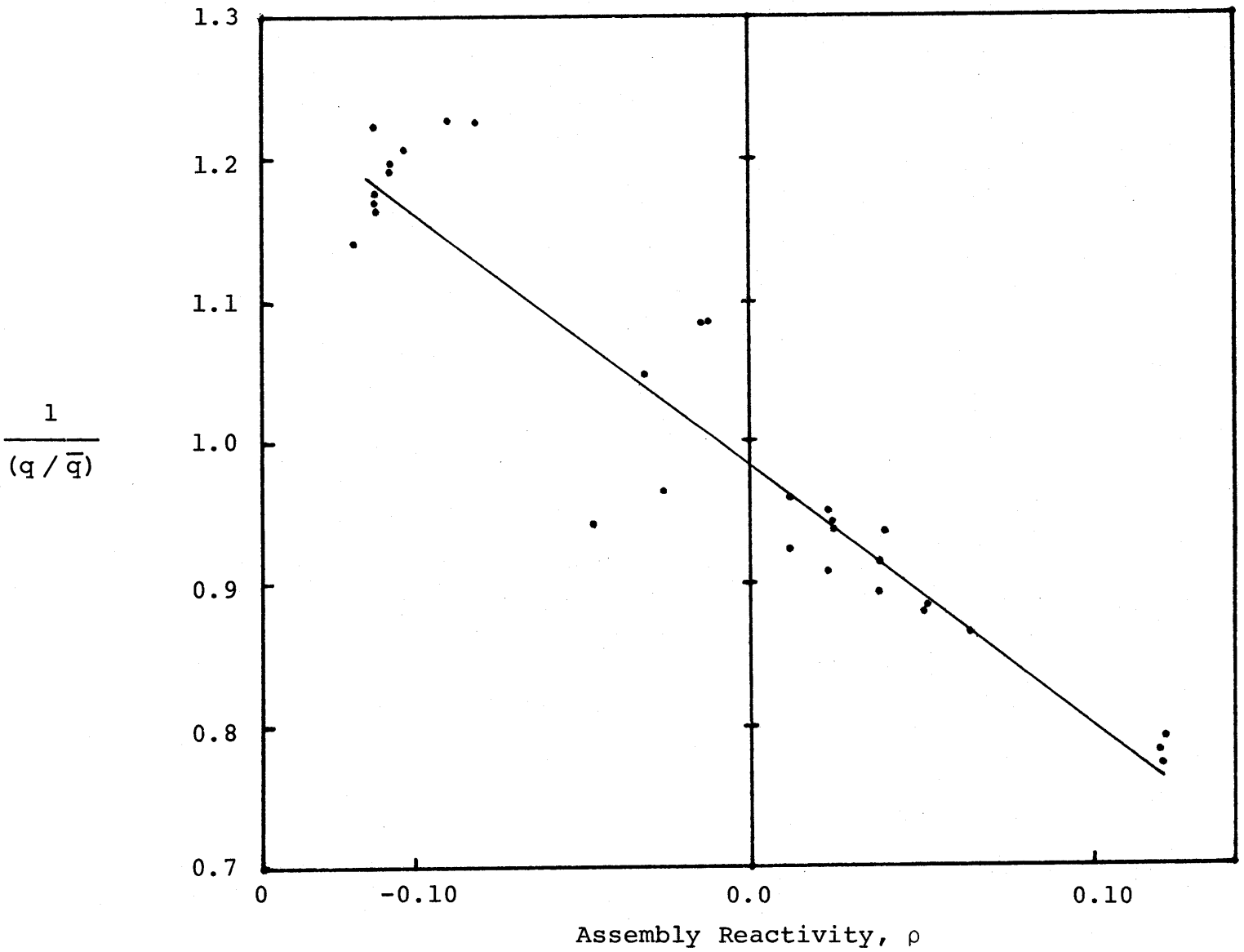

Fig. 3.13 Reciprocal Assembly Power vs. Assembly Reactivity for Interior Assemblies in a Representative C-E System 80™ Core

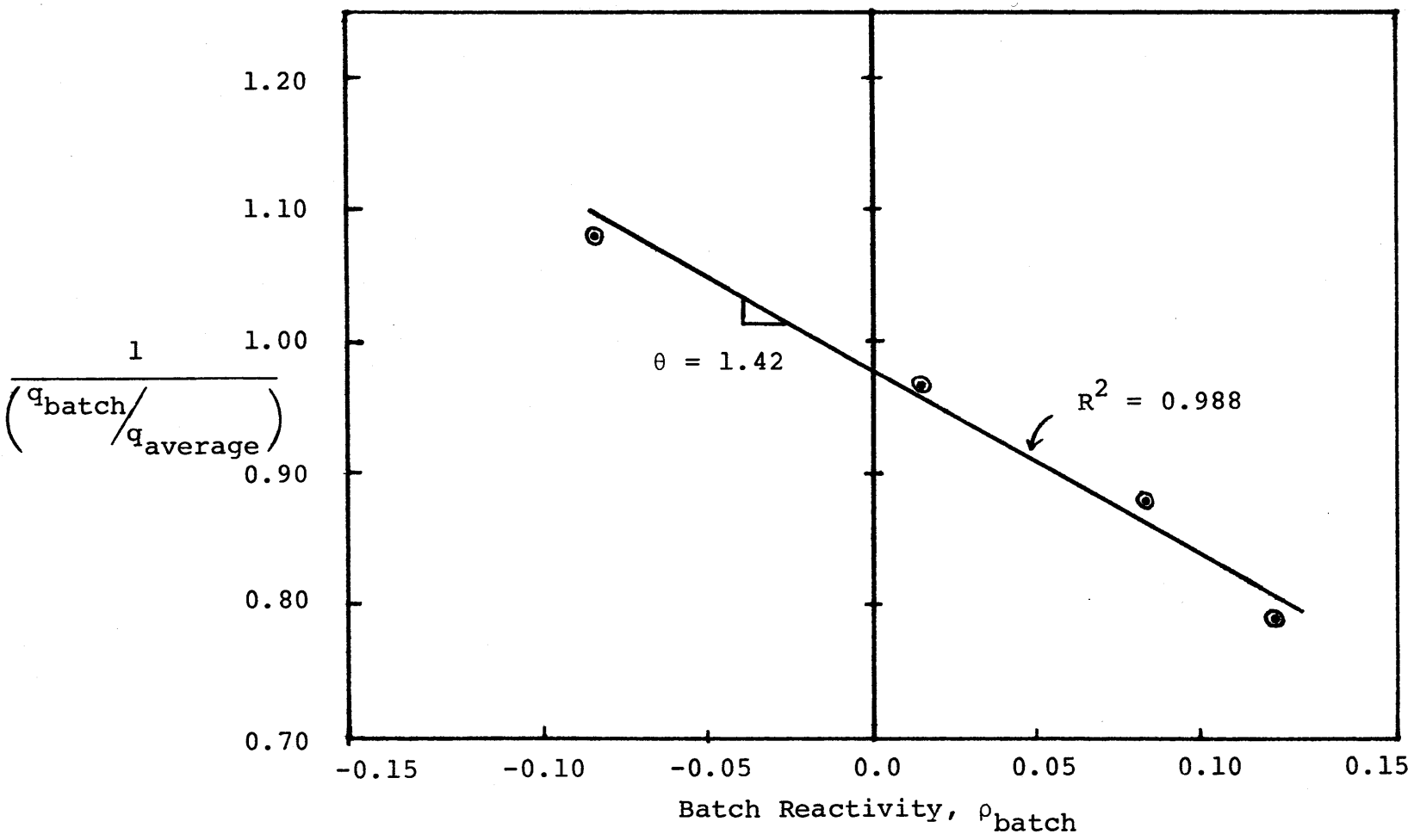

Fig. 3.14 Regression Line of Power vs. Reactivity for Main Yankee Fuel Batches

which corresponds exactly to the power split relation given in Eq. (3.47). A similar analysis for the System-80^{TM} core yielded a θ value of 1.81 with an R^2 value of 0.972. The plot for the batch power versus batch reactivity of this core is shown in Fig. 3.15. Thus, even though individual assembly power cannot be predicted accurately, the batch-wise power splits can be calculated to the level of accuracy required for detailed fuel management analysis.

3.4.3 TREATMENT OF PERIPHERAL ASSEMBLIES

In the derivation of the algorithm for the power sharing relation among assemblies, the implicit assumption in the assemblies' arrangement is that the test assembly is completely surrounded by other fuel assemblies. Such an assembly configuration is representative of the assemblies in the interior of the core. However, assemblies situated at the periphery of the core have one or two of their sides bordered by non-fuel regions of coolant and structure. The power split relation which has been developed so far can be extended to include these peripheral assemblies.

We have shown in the previous section that the leakage reactivity, ρ_L, of the assemblies placed at the core periphery can be correlated to the peripheral power fraction f_{per}:

$$\rho_L = \alpha f_{per} \tag{3.57}$$

where α is a constant.

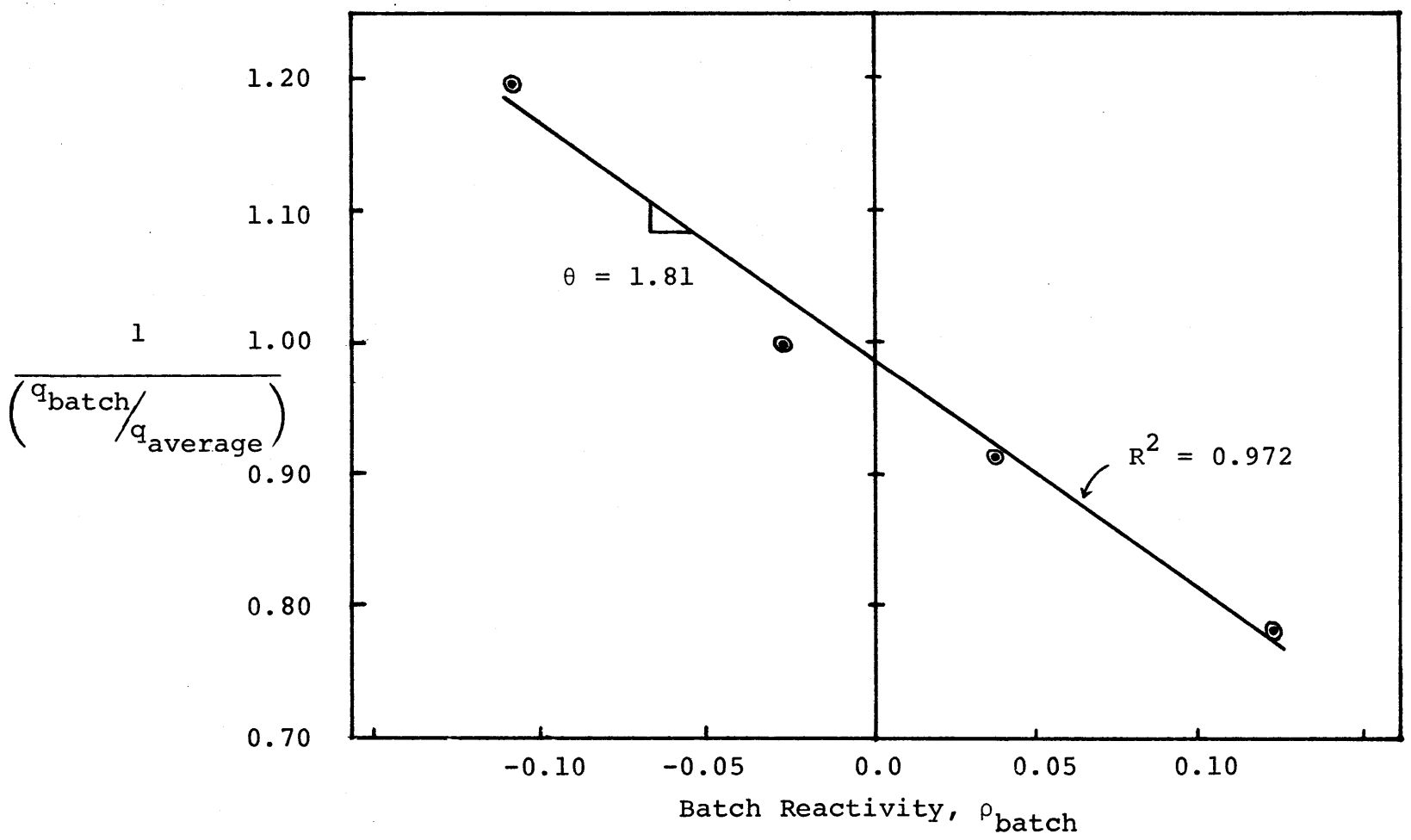

Fig. 3.15 Regression Line of Power vs. Reactivity for C-E System-80™ Fuel Batches

This equation can be rewritten in terms of fuel batches in the peripheral locations:

$$\rho_L = \alpha \sum_{i=1}^{m} f_i \tag{3.58}$$

where $\sum_{i=1}^{m} f_i = f_{per}$ is the power fraction of the core's peripheral batches, m in number. The system reactivity of a steady state core with n fuel batches (m of which are on the core periphery) and leakage reactivity ρ_L has been shown to be

$$\rho_{sys} = \sum_{i=1}^{n} f_i \rho_i - \rho_L \tag{3.59}$$

At the end of cycle, $\rho_{sys} = 0$, and substituting Eq. (3.58) for ρ_L into Eq. (3.59) yields:

$$\sum_{i=1}^{n} f_i \rho_i = \alpha \sum_{i=1}^{m} f_i \tag{3.60}$$

or

$$\sum_{i=1}^{n-m} f_i \rho_i + \sum_{i=1}^{m} f_i \rho_i = \alpha \sum_{i=1}^{m} f_i$$

Interior Batches — Peripheral Batches

$$\sum_{i=1}^{n-m} f_i \rho_i + \sum_{i=1}^{m} f_i (\rho_i - \alpha) = 0 \tag{3.61}$$

The power split equation which is compatible with this power-weighted prescription for core reactivity averaging is

$$f_i = \frac{\bar{f}}{1 - \theta(\rho_i - \alpha)} \tag{3.62}$$

where $\alpha = \begin{cases} \alpha & \text{for peripheral batches} \\ 0 & \text{for interior batches} \end{cases}$

One of the key constraints this proposed power split relation must satisfy is the summation of batch power fractions to unity, or equivalently,

$$\sum_{i=1}^{n} f_i - 1 = 0 = \sum_{i=1}^{n} (f_i - \frac{1}{n}) \tag{3.63}$$

This is the same as writing (substituting and reorganizing the f_i from Eq. 3.62):

$$\sum_{i=1}^{n} \left[\frac{\frac{1}{n}}{1-\theta(\rho_i-\alpha)} - \frac{1}{n} \right] = 0 \tag{3.64}$$

or,

$$\underbrace{\sum_{i=1}^{n-m} \left[\frac{\frac{1}{n}}{1-\theta\rho_i} - \frac{1}{n} \right]}_{\text{Interior Batches}} + \underbrace{\sum_{i=1}^{m} \left[\frac{\frac{1}{n}}{1-\theta(\rho_i-\alpha)} - \frac{1}{n} \right]}_{\text{Peripheral Batches}}$$

$$= \sum_{i=1}^{n-m} \frac{1}{n} \left[\frac{1-(1-\theta\rho_i)}{1-\theta\rho_i} \right] + \sum_{i=1}^{m} \frac{1}{n} \left[\frac{1 - \{1-\theta(\rho_i-\alpha)\}}{1-\theta(\rho_i-\alpha)} \right]$$

$$= \theta \sum_{i=1}^{n-m} \left[\frac{\frac{1}{n}}{1-\theta\rho_i} \cdot \rho_i \right] + \theta \sum_{i=1}^{m} \left[\frac{\frac{1}{n}(\rho_i-\alpha)}{1-\theta(\rho_i-\alpha)} \right]$$

$$= \theta \sum_{i=1}^{n-m} f_i\rho_i + \theta \sum_{i=1}^{m} f_i(\rho_i-\alpha) = 0 \qquad (3.65)$$

Since θ is a constant, Eq. (3.65) can be rewritten as

$$\sum_{i=1}^{n-m} f_i\rho_i + \sum_{i=1}^{m} f_i(\rho_i-\alpha) = 0 \qquad (3.66)$$

which is the power-weighted prescription for core reactivity averaging given earlier in Eq. (3.61).

3.5 AN ANALYTICAL MODEL FOR DISCHARGE BURNUP

The LRM methodology has now been sufficiently developed to permit the accurate computation of the discharge burnup for various cases of fuel management strategies of contemporary interest. An analytical model will be developed in this section and an automated procedure which numerically calculates the discharge burnup based on the LRM methodology is described in the next chapter. The computer program developed for this purpose can easily handle cases which are too difficult to be modeled in a closed analytical form. In addition, the numerical results obtained are used to check and normalize the analytical ones.

An approximation is required to facilitate the analytical derivation of discharge burnup equations for different power history trajectories. To first order, the power split relation given by Eq. (3.56) becomes

$$f_{batch} = \bar{f}(1 + \theta\rho_{batch}) \tag{3.67}$$

This linearized version of the power split equation fits core map data equally well, and this is testified to by the plots shown in Figs. 3.16 and 3.17 for the CE System-80™ core design and the Maine Yankee cycle 4 reload design, respectively.

Consider the reactivity versus burnup trace shown in Fig. 3.18. For an n-batch steady-state core, and with the assumption that the average power fractions remain constant over a given cycle,

$$\begin{aligned}
\rho_1 &= \rho_o - A \cdot B_c \cdot \bar{f}_1/\bar{f} \\
\rho_2 &= \rho_o - A \cdot B_c \cdot (\bar{f}_i + \bar{f}_2)/\bar{f} \\
&\vdots \\
\rho_n &= \rho_o - A \cdot B_c \cdot (\bar{f}_1 + \bar{f}_2 + \cdots + \bar{f}_n)/\bar{f}
\end{aligned} \tag{3.68}$$

where $\bar{f}_i$ is the average power fraction of batch i,

$\bar{f}$ is the core-average power fraction $= \frac{1}{n}$

and B_c is the cycle average burnup.

The approach is to weight Eq. (3.68) at the end of cycle using the power split relation given by Eq. (3.67), and then set the system reactivity equal to zero:

$$\rho_{sys} = \sum_{i=1}^{n} f_i\rho_i = 0 \tag{3.69}$$

Now, from Eq. (3.67), which applies when the core environment

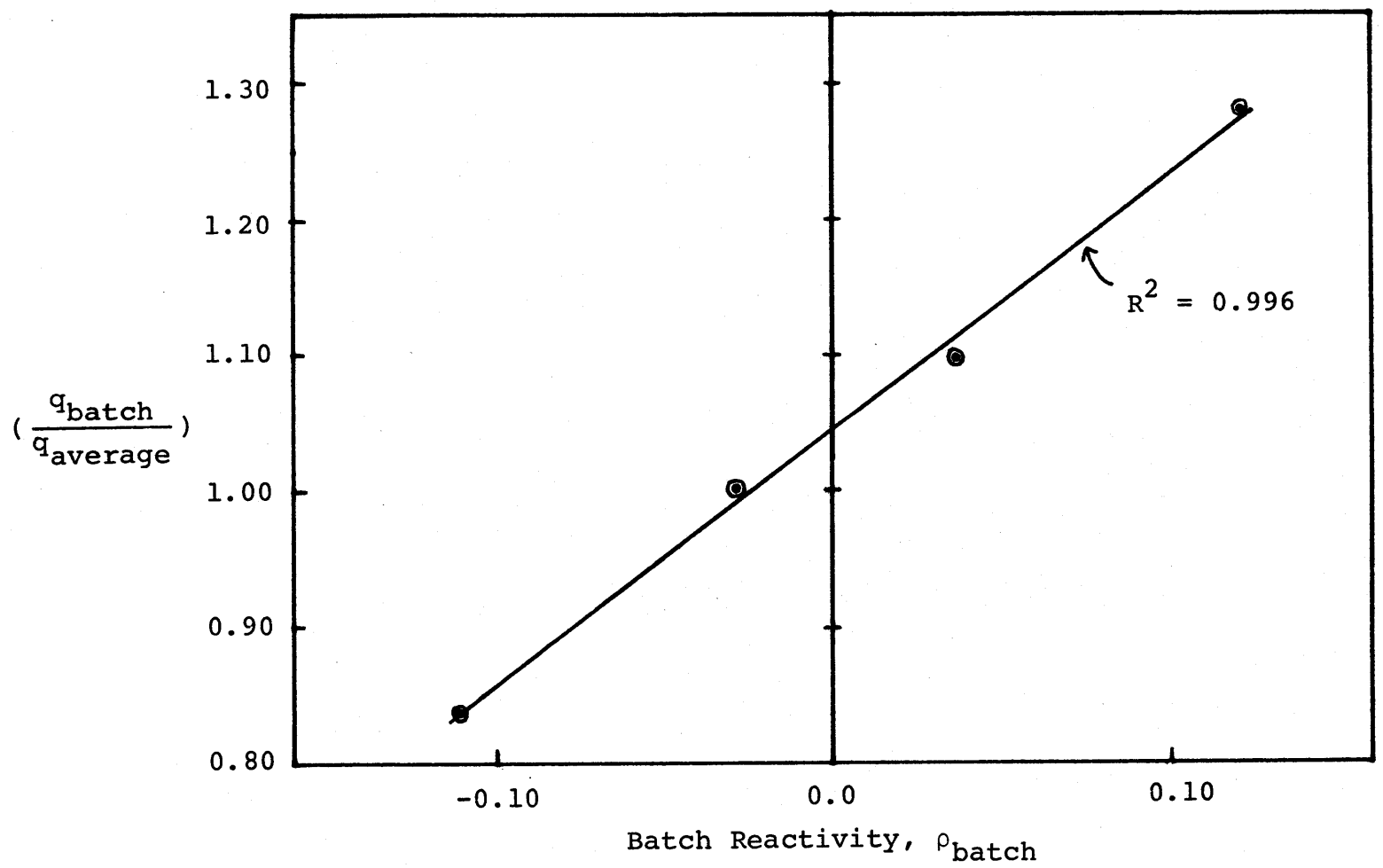

Fig. 3.16 Linearized Power versus Reactivity Correlation for C-E System-80™ Fuel Batches

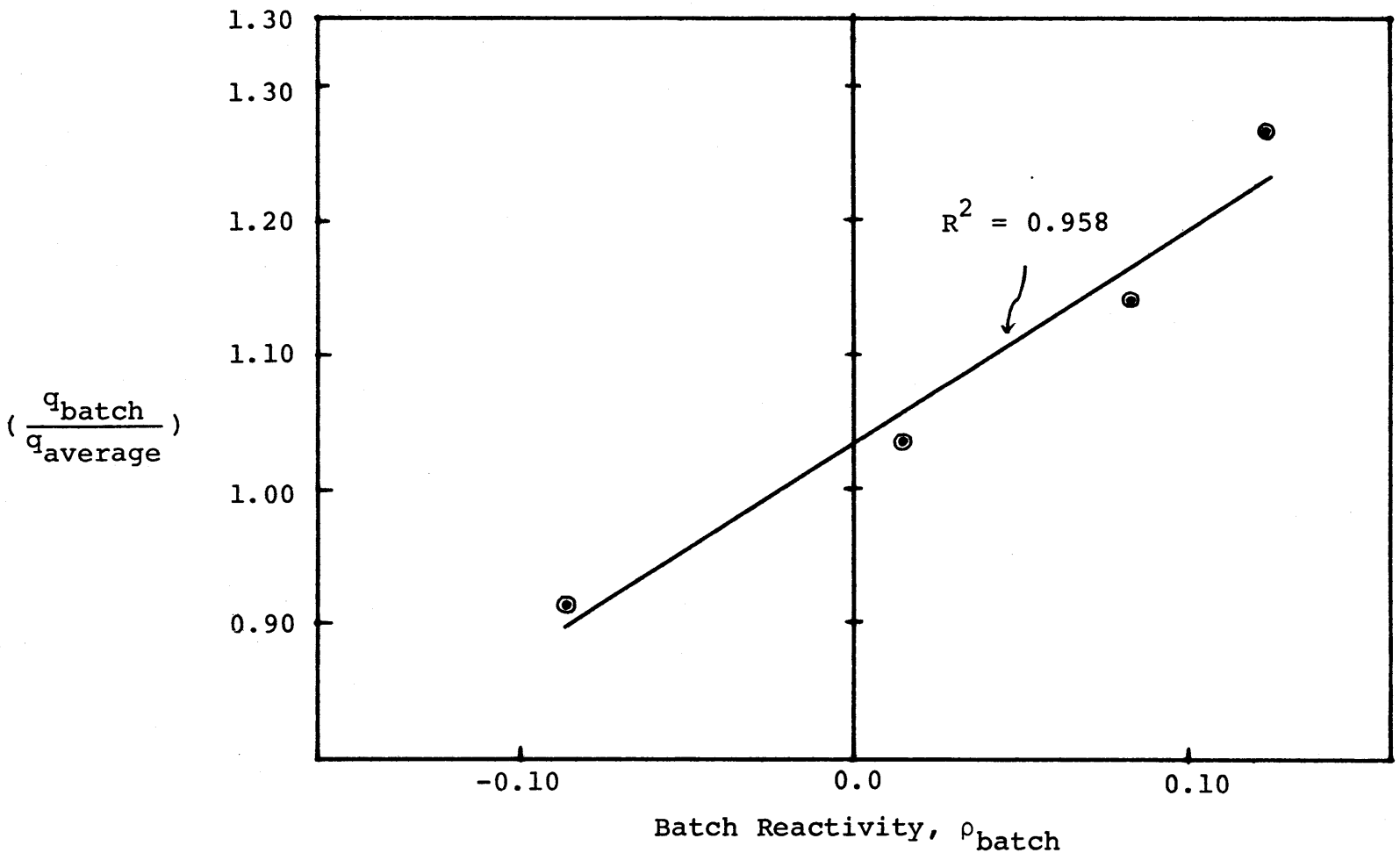

Fig. 3.17 Linearized Power versus Reactivity Correlation for Maine Yankee Fuel Batches

is critical, we can write

$$\bar{f}_i = \bar{f}(1 + \theta\bar{\rho}_i) \tag{3.70}$$

And, for the j^{th} batch

$$\bar{f}_i + \bar{f}_2 + \cdots \bar{f}_j = j\bar{f}(1 + \theta\bar{\bar{\rho}}_j) \tag{3.71}$$

where $\bar{\bar{\rho}}_j$ is the average over the in-core history to date, that is,

$$\bar{\bar{\rho}}_j = \frac{\bar{\rho}_1 + \bar{\rho}_2 + \cdots + \bar{\rho}_j}{j}$$

$$= \frac{1}{j} \sum_{i=1}^{j} \bar{\rho}_i \tag{3.72}$$

But the correct expression for $\bar{\bar{\rho}}_j$ to be used is that in a poisoned core. This implies that the reactivity values must be reduced by (to a good approximation) the cycle average control poison penalty. To determine the poison adjusted reactivity values, we must first get an estimate of the batch reactivity. Using the equal power sharing approximation, the reactivity of batch i at the end of cycle is

$$\rho_i = (1 - \frac{2i}{n+1})\rho_o \tag{3.73}$$

The cycle average reactivity for batch i, is thus

$$\bar{\rho}_i = \frac{1}{2}(\rho_{i,BOC} + \rho_{i,EOC})$$

$$= \frac{1}{2}[\ \rho_o(1 - 2\frac{(i-1)}{n+1}) + \rho_o(1 - \frac{2i}{n+1})\ ]$$

$$= (\ \frac{n+2}{n+1} - \frac{2i}{n+1}\ )\ \rho_o \qquad (3.74)$$

Substituting this equation into Eq. (3.72), the average reactivity of batch j over its entire in-core history to date, becomes,

$$\bar{\rho}_j = \frac{1}{j} \sum_{i=1}^{j} (\ \frac{n+2}{n+1} - \frac{2i}{n+1}\ )\ \rho_o$$

$$= \frac{1}{j}\ [\ (\ \frac{n+2}{n+1}\ )j - (\ \frac{2}{n+1}\ )\ \frac{j(j+1)}{2}\ ]\ \rho_o$$

$$= [\ (\ \frac{n+2}{n+1}\ ) - (\ \frac{j+1}{n+1}\ )\ ]\ \rho_o \qquad (3.75)$$

From this expression, we can determine the cycle average excess reactivity which must be suppressed using soluble poison:

$$\bar{\bar{\rho}}_n = [\ (\ \frac{n+2}{n+1}\ ) - (\ \frac{n+1}{n+1}\ )\ ]\ \rho_o$$

$$= \frac{\rho_o}{(n+1)} \qquad (3.76)$$

This is also the cycle average poison which must be subtracted from all the reactivity values. The poison adjusted average reactivity of batch j over its in-core residence to

date, is therefore

$$\vec{\rho}_j = \bar{\bar{\rho}}_j - \bar{\bar{\rho}}_n$$

$$= \left(\frac{n}{n+1} - \frac{j}{n+1} \right) \rho_o \qquad (3.77)$$

A power-weighted reactivity balance gives (from Eqs. 3.68, 3.69, 3.70, 3.73 and 3.77):

$$\sum_{i=1}^{n} f_i \rho_i = 0 = \rho_o \bar{f} \{ n + \theta \sum_i \rho_i \}$$

$$- A \cdot B_c \cdot \bar{f} \sum_i [1 + \theta (1 - \frac{2i}{n+1})] \cdot i \cdot$$

$$[1 + \theta (\frac{n}{n+1} - \frac{i}{n+1}) \rho_o] \qquad (3.78)$$

Expanding and rearranging Eq. (3.78) and noting that when $\theta = 0$ the discharge burnup for the flat power case is

$$B_o = \frac{2n}{n+1} \left(\frac{\rho_o}{A}\right) = nB_{co} \qquad (3.79)$$

where B_{co} is the cycle average burnup for the equal power sharing case.

We will obtain, after considerable algebra:

$$\frac{B}{B_o} = \left[1 + (\theta \rho_o)^2 \frac{(n-1)}{3(n+1)^2} \right]^{-1} \qquad (3.80)$$

or

$$B = B_o / (1+\varepsilon) \tag{3.81}$$

The factor ε, being a positive number in this case, gives an estimate of the penalty in discharge burnup due to the unequal sharing of power among the fuel batches. As expected, ε will approach zero as n becomes large, for fixed $(\theta\rho_o)$. This simply means that one can approach an equal power sharing condition if the number of reload batches is sufficiently large. However, it must be noted that ε is only a second order effect, and as will be seen, thus is rather small (< 1%).

Using the same approach, equations similar in form to Eq. (3.81) can be derived for the different power history trajectories shown in Fig. 3.19. The $\rho(B)$ trace designated case 4 in Fig. 3.19 is a limiting case which has been identified for assessment vis-à-vis burnable poison control, namely a core controlled entirely by burnable poison in the fresh fuel without the need for soluble poison. In this particular case, we can show that (see Appendix B) the beginning-of-life reactivity of a batch of fuel is equal to its end-of-life reactivity. Or equivalently, the BOC reactivity of the poisoned fresh fuel, $\rho_{1,BOC}$ is equal to the EOC reactivity of the oldest batch of fuel $\rho_{n,EOC}$. The results are summarized in Table 3.3.

Although the effect of leakage or permanent poison shim was not explicitly modeled in the analytical derivation of the discharge burnup, it can be accounted for through its

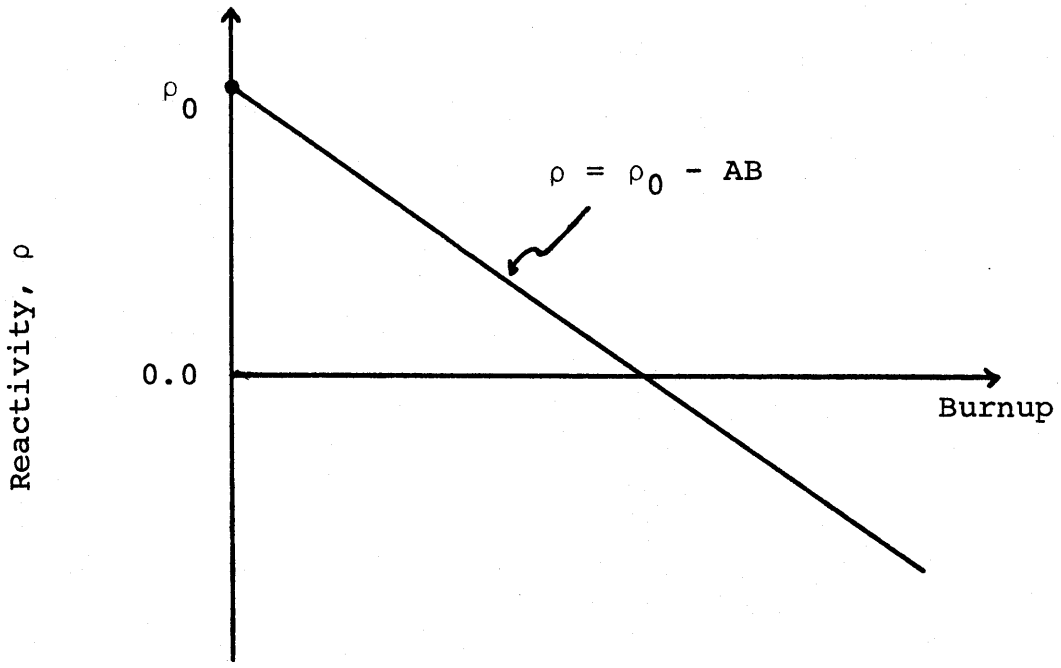

Fig. 3.18 Reactivity versus Burnup Curve for a Fuel Assembly or Assemblies in a Batch

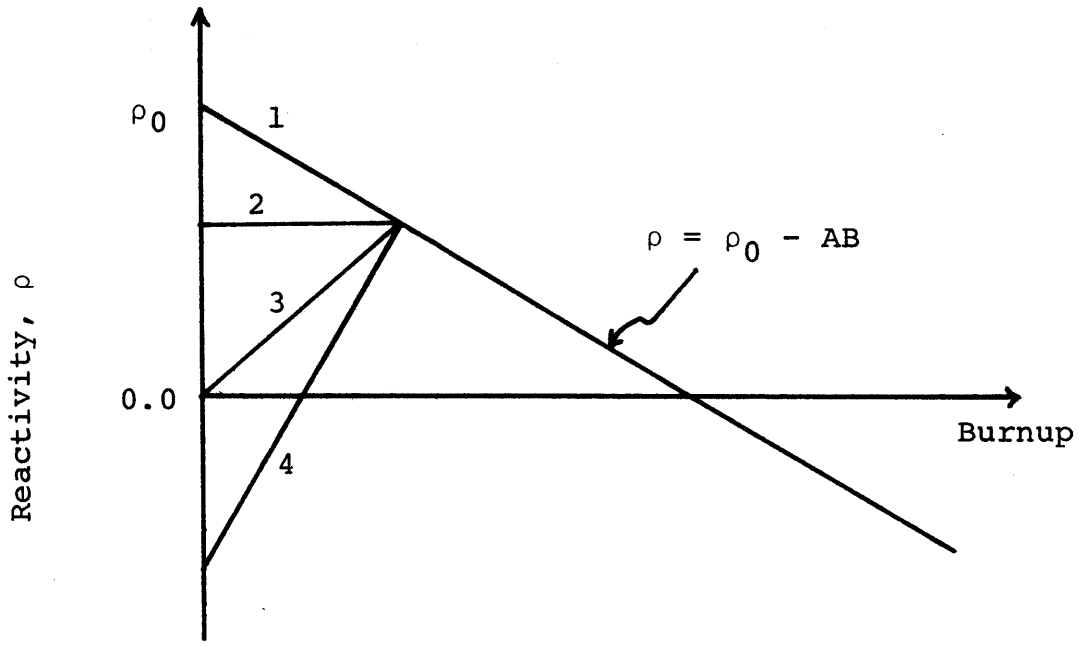

Case 1: No Burnable Poison

Case 2: Constant ρ in the First Cycle

Case 3: Zero ρ at the Beginning of Life

Case 4: All Control via Burnable Poison

Fig. 3.19 Various $\rho(B)$ Traces of Reload Fuel with Burnable Poison

effect on the equal-power-sharing approximation discharge burnup B_o, that is,

$$B_o' = \left(\frac{2n}{n+1}\right)\frac{(\rho_o-\Delta)}{A} \qquad (3.82)$$

Where Δ is the reactivity penalty due to neutron leakage or the presence of chemical shim. Moreover, in cases where burnable poison is employed in the fresh fuel batch, the associated residual poison in this batch of fuel over the remaining cycles can also be accounted for through Δ. However, the results given in Table 3.3 assumed the complete burnout of the burnable poison at the end of cycle.

For the Maine Yankee reactor system, with a 3-batch fuel management scheme (n=3), typical values of ρ_0, θ and A are given below:

$$\rho_0 = 0.22351$$
$$A = 9.2721 \times 10^{-6} \text{ MT/MWD}$$
$$\theta \simeq 1.5$$

The discharge burnups corresponding to the various reactivity versus burnup histories depicted in Fig. 3.19 are given in Table 3.4. As expected, the penalty in discharge burnup due to unequal power sharing among fuel batches is only about 0.5% since it is a second order effect.

A most interesting observation from the results given in Table 3.4 is that the discharge burnups of those cases emp-

TABLE 3.3 ANALYTICAL RESULTS FOR COMMON REACTIVITY HISTORIES

CASE	PRESCRIPTION FOR ε^*
1. No burnable poison	$(\theta\rho_o)^2 \frac{(n-1)}{3(n+1)^2}$
2. Constant ρ in 1st cycle	$-(\theta\rho_o)\frac{(n-1)}{n(n+1)^2} + (\theta\rho_o)^2\frac{(n-1)^2}{3n(n+1)^2}$
3. Zero ρ at BOL	$-(\theta\rho_o)\frac{(n-1)}{2n(n+1)} + (\theta\rho_o)^2\frac{(n-1)^2}{6n(n+1)^2}$
4. All control via burnable poison	$-(\theta\rho_o)\frac{(n-1)}{(n+1)^2}$

---

* Discharge Burnup $B_d = B_o / (1+\varepsilon)$

and B_o = discharge burnup for hypothetical uniform power history

$= (\frac{2n}{n+1})(\frac{\rho_o}{A})$

where n = number of staggered reload batches.

TABLE 3.4 REPRESENTATIVE DISCHARGE BURNUPS CORRESPONDING TO VARIOUS $\rho(B)$ HISTORIES

	CASE	ε	B_d (MWD/MT	% DIFFERENCE* FROM THE FLAT POWER CASE, B_o
1.	No burnable poison	0.005	35978	-0.5
2.	Constant ρ in 1st cycle	-0.011	36560	1.1
3.	Zero ρ at BOL	-0.026	37123	2.7
4.	All control via burnable poison	-0.042	37743	4.4

* $B_d = B_o/(1+\varepsilon)$

and $B_o = \left(\frac{2n}{n+1}\right)\left(\frac{\rho_o}{A}\right) = 36158$ MWD/MT

loying burnable poison are better than that of the flat power case by about 1.0 - 4.4%. Ruling out the case of using burnable poison for all reactivity control as being impracticable, an increase in discharge burnup of about 2.7% over that of the flat power case can be achieved using burnable poison to suppress reactivity in the fresh fuel batch as in case 3 of Fig. 3.19. However, the presence of residual poison may negate the gain in the discharge burnup. We can estimate the residual poison reactivity penalty to break even with respect to discharge burnup compared to the flat power case. From Eq. (3.82), the burnup penalty due to the presence of residual poison can be written as,

$$B_R = \left(\frac{2n}{n+1}\right) \frac{\Delta_R}{A} \qquad (3.83)$$

where Δ_R is the residual poison reactivity.

Thus, the Δ_R which will give breakeven discharge burnup is given by:

$$B_d - B_o = \left(\frac{2n}{n+1}\right) \frac{\Delta_R}{A}$$

or

$$\Delta_R = \left(\frac{n+1}{2n}\right) A \cdot (B_d - B_o)$$

$$= \left(\frac{4}{6}\right)(9.2721 \times 10^{-6})(37123 - 36158)$$

$$= 0.006$$

$$= 0.6\%, \Delta\rho$$

That is, the amount of residual poison which can be tolerated in case 3 without losing discharge burnup compared to the flat power case is $\sim$ 0.6% $\Delta\rho$. Representative residual $\Delta\rho$ values for gadolinium poison in LWR's are typically quoted as $\sim$ 0.5%, which is lower than breakeven, and thus a small gain in burnup and uranium usage can be credited to the poisoned case.

It must be noted that case 3 has the obvious advantage of an additional reactivity control capability through incorporation of burnable poison. This becomes essential if we go to higher enrichment reload fuel to extend burnup.

Although scoping analyses can be done very quickly using the analytical models for discharge burnup derived in this section, more accurate results can be obtained using numerical methods -- which can also be used to check the analytic approximations. This is done in the next chapter. In addition, the numerical methods can handle cases where leakage of neutrons from the core is required to be explicitly modeled, for example, when comparing the low-leakage and out-in/scatter fuel management strategies. Leakage, it will be recognized, is equivalent to a permanent (i.e., non-burnable) shim introduced into a given batch for one cycle only (instead of for all n-cycles, as in the case of burnable poison residual treated above). This case has proven to be too complicated to handle analytically,

at least in terms of extracting a reasonably simple closed form expression.

3.6 CHAPTER SUMMARY

In this chapter a case has been made for the application of the linear reactivity model for current PWR fuel (U-235/UO_2) as well as fuel types comprised of other fissile and fertile materials. The LRM methodology, with the incorporation of features such as the power weighting algorithm and the radial leakage correlation, enables one to determine the discharge burnup of various fuel management schemes more realistically and thus more accurately than previously possible with simple models of this genre. An important component in the development of the LRM improved methodology is the derivation of the power split relation among fuel batches using the "group-and-one-half" diffusion theory model. Analytical models for discharge burnup corresponding to fuel management strategies of contemporary interest were obtained using the LRM methodology. These analytical results allow one to perform fast scoping analyses given only a few important core parameters generated by a minimum number of LEOPARD and PDQ-7 calculations. An extension of the LRM methodology using numerical procedures to further improve its accuracy, to validate the approximations which make the above mentioned analytic treatments practicable and to handle cases which are difficult to model analytically is discussed in the next chapter.

CHAPTER 4

DISCHARGE BURNUP CALCULATIONS

4.1 INTRODUCTION

The analytical expressions derived in the previous chapter permit rapid estimation of discharge burnup for a fuel batch as a function of power history, and thus facilitate quick scoping studies of fuel management strategy. To establish and improve the accuracy of such analyses it is necessary that they be checked against and normalized to more accurate numerical calculations, which is the function of the present chapter. The general methodology employed in the analytical and the numerical approaches are basically similar, except that most of the key approximation of the former can be relaxed in the latter.

A computer program has been developed for the purpose of checking the analytical results and performing more accurate and varied analyses. This code, called DISBURN (for Discharge Burnup), is in many respects an extension as well as a refinement of the ALARM code previously described in Ref. [S-2]. The algorithms together with certain key features of the code are discussed in the next section. Finally, various fuel management strategies (with and without the use of burnable poison) will be simulated and analyzed using the DISBURN code.

4.2 COMPUTER CODE FOR DISCHARGE BURNUP COMPUTATION—DISBURN

The DISBURN code computes the discharge burnup of fuel batches in an n-batch, steady-state reactor core. It is based on the linear reactivity model methodology incorporating features developed in the previous chapter such as the explicit modeling of core leakage in the radial direction and the power weighting of the fuel batch reactivity in determining the system reactivity. The power split equation employed in the code to describe interior as well as peripheral fuel batches was derived from the "group-and-one-half" diffusion theory model.

Although the code, as it is written presently, can only handle linear $\rho(B)$ traces characterizing fuel assemblies in a batch (the input parameters to describe the linear curve being ρ_0—the extrapolated BOL reactivity and A—the slope of the curve), non-linear $\rho(B)$ curves can also be readily evaluated by inserting a simple interpolating routine such as the n^{th} order Lagrangian interpolating routine, into the program; the input in which case will be the ρ versus burnup values (in tabular form) from the assembly spectrum calculation (e.g., LEOPARD or PDQ-7), and interpolation can be performed at each burnup step as required in the computation: this procedure, in fact, is employed in the precursor code, ALARM.

In order to simulate realistic fuel loading patterns, the restriction of having a single type of fuel at the core

periphery is relaxed. Different fractions of the various fuel batches (i.e., subgroups of fuel having different reactivity values) can be placed at the peripheral locations. Table 4.1 gives a summary of the principal features of the code. The algorithm employed in the code is illustrated by the flow chart in Fig. 4.1. A description of the computational procedure is given below:

1. Input data include the extrapolated BOL reactivity ρ_0, the slope of the linear $\rho(B)$ curve, A, the number of batches n, the fractions of a batch in the core interior and on the core periphery, the theta values, θ, the convergence criterion and the time or burnup step size.

   The options available include soluble poison control (alone or in combination with burnable or fixed poison); burnable poison; and fixed (non-burnable) poison shim or radial leakage (which are mathematically equivalent).

2. The beginning of cycle burnup states of the fuel batches $B_{BOC,i}$ are estimated using the equal power sharing approximation. The BOC point for batch i is given by

$$B_{BOC,i} = \frac{2(i-1)}{(n+1)} \frac{\rho_0}{A} \qquad (4.1)$$

3. The batch reactivity ρ_i, batch power fraction f_i,

TABLE 4.1

PRINCIPAL FEATURES OF THE DISBURN CODE

Item	Comment
1. Linear reactivity vs. burnup curve only.	Can easily be adapted to accommodate non-linear $\rho(B)$ traces.
2. Power-weighted reactivity averaging is used.	$\rho_{sys} = \sum_{i=1}^{n} f_i \rho_i$
3. Effect of peripheral leakage is accounted for through a reactivity-power correlation.	$\rho_L = \alpha f_{per} = \alpha \sum_{i=1}^{m} f_i$ m denotes peripheral batches $\therefore \rho_{sys} = \sum_{i=1}^{n-m} f_i \rho_i + \sum_{i=1}^{m} f_i (\rho_i - \alpha)$ interior batches; peripheral batches
4. Batches can be apportioned between core interior and periphery.	User specifies fraction of batch i in core interior ($F_{int,i}$) and core periphery ($F_{per,i}$). $F_{int,i} + F_{per,i} = 1$
5. Interior batch power is computed using the power split equation.	$f_{int,i} = \frac{(F_{int,i})(\frac{1}{1-\theta\rho_i})}{\sum_{i=1}^{n} f_i}$
6. Peripheral batch power is computed using a modified power split equation.	$f_{per,i} = \frac{(F_{per,i})[\frac{1}{1-\theta(\rho_i-\alpha)}]}{\sum_{i=1}^{n} f_i}$ where $f_i = f_{int,i} + f_{per,i}$ (i.e., sum in denominator includes all assemblies in batch i).

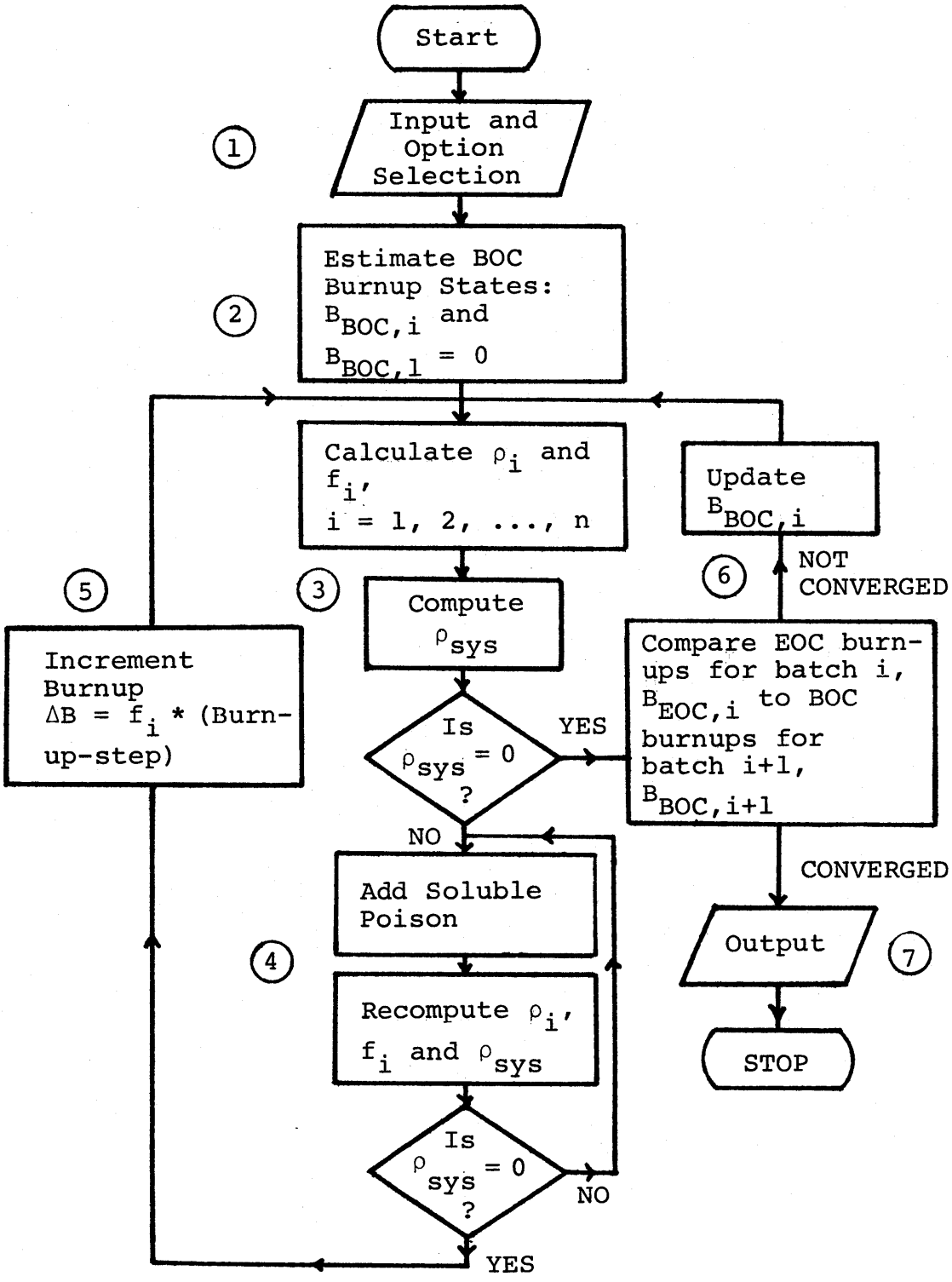

Fig. 4.1 Flowchart for DISBURN COMPUTATIONS

and then the system reactivity ρ_{sys} are computed. The ρ_{sys} is checked to determine whether the EOC point has been reached ($\rho_{sys} = 0$).

4. If the end of cycle point has not been reached (within a certain convergence criterion on ρ_{sys}— a value of ± 0.0001 is presently used in the code), the excess system reactivity is suppressed by means of soluble poison. This is accomplished by adding equal amounts of negative reactivity [$-\Delta\rho_{poison} = \frac{-(\text{Excess system reactivity})}{n}$] to each fuel batch's reactivity value ρ_i. The updated ρ_i and f_i are then used to recompute ρ_{sys}. The process is repeated until criticality is achieved.

   The adding of equal portions of negative reactivity worth to ρ_i (or equivalently, assigning equal soluble boron worth to all the fuel batches irrespective of their different reactivity level) is justified by the fact that the dependence of soluble poison worth on the reactivity levels of the fuel batches is a second order effect. This is evident from the linearity of the plot of reactivity vs. coolant boron concentration for various burnup points, as shown in Fig. 4.2.

5. The next set of burnup points for the fuel batches is obtained by adding the burnup increment $\Delta B_i = (f_i/\bar{f}) \cdot (\text{burnup step})$ to the previous batch burnup

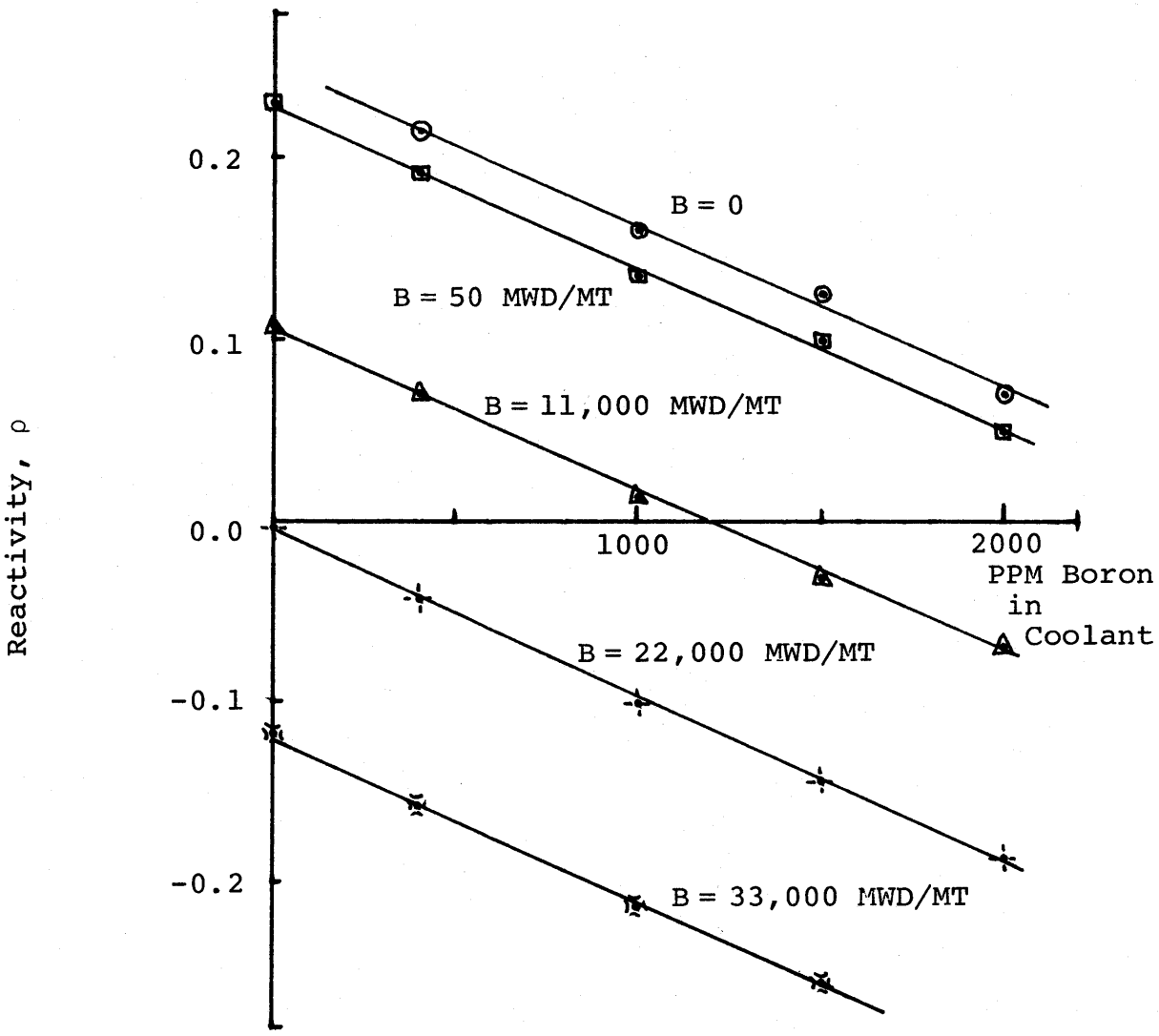

Note linearity, constancy of slope vs. burnup.

Fig. 4.2 Reactivity Worth of Control Poison—Maine Yankee PWR Supercell Calculations

point (initially, the BOC points of the fuel batches). The process (steps 3, 4 and 5) is repeated until the end of cycle point is reached ($\rho_{sys} = 0.0$).

6. The end of cycle parameter values for batch i ($\rho_{EOC,i}$ or $B_{EOC,i}$) are then compared with the beginning of cycle values of batch i+1 ($\rho_{BOC,i+1}$ or $B_{BOC,i+1}$). If convergence (the convergence criterion is user prescribed) is not achieved, the BOC points of the fuel batches are then updated. The outer iteration (comprising steps 3, 4, 5 and 6) is repeated until overall convergence is achieved.
7. The burnup and the cycle-average power fraction for each batch are printed after each outer iteration. The peripheral power fraction and the leakage reactivity are printed as well.

It should be noted that if the extrapolated BOL reactivity, ρ_0, and the slope of the linear $\rho(B)$ curve, A, input to the code come from an infinite medium calculation, the effect of axial leakage can be accounted for by reducing ρ_0. However, this is not necessary if the data come from a PDQ-7 calculation which has included the effect of axial leakage. Similarly, the presence of residual burnable poison in the fuel batch over the remaining cycles can be accounted for by a reduction in ρ_0. The effective extrapolated BOL reactivity in the two situations discussed above is thus given

by

$$\rho_0' = \rho_0 - \Delta \tag{4.2}$$

where Δ represents residual poison reactivity plus the axial leakage reactivity.

A further description of the code, a listing, and a sample problem can be found in Appendix C.

To see how well the code predicts the discharge burnup of fuel batches it was applied to evaluate a five-batch, extended burnup, 'out-in' fuel management scheme and a comparable 'low-leakage' fuel management strategy for the Combusion Engineering System-80 reference design [M-1]. The core has 241 assemblies, 48 of which are located in the core periphery. From available data [M-1] a leakage correlation was developed: the leakage coefficient α, was found to be 0.2846. The reactivity versus burnup values for 4.3 w/o and 4.44 w/o U-235 enriched lattices were generated using the LEOPARD code; from these data the extrapolated BOL reactivity ρ_0 and the slope of the $\rho(B)$ curve A, were determined. The 4.3 w/o enrichment was for the 'out-in' case while the 4.44 w/o value applied to the 'low-leakage' fuel management scheme. The theta (θ) values for the power split equation of the interior and peripheral fuel batches of the core were both set equal to 1.8 (see Fig. 3.15). A residual poison penalty of 0.5% $\Delta\rho$ was assigned to the low-leakage

case to allow for the use of burnable poison in suppressing the radial power peaking associated with the fuel management scheme. Table 4.2 summarizes the relevant parameters for the two cases evaluated using the DISBURN code. The results of the calculations are compared in Tables 4.3a and 4.4a with those obtained using detailed computer analyses, as published in Ref. [M-1]. A parametric study was also performed: the leakage coefficient, α, was varied from a value of 0.2650 to the previously obtained value of 0.2846, and theta values of 1.5 and 2.0 were also analyzed. Tables 4.3 and 4.4 give the results of the calculations for the 'out-in' and 'low-leakage' fuel management schemes, respectively.

The discharge burnups are more sensitive to the leakage coefficient, α, than they are to the theta values used in the calculations. This points to the importance of making an accurate correlation of the leakage reactivity to the peripheral power fraction. The cycle burnups in the two cases analyzed using DISBURN differ by an average of 5.4% from those obtained using detailed computer calculations, the discharge burnup values are in even better agreement. For the 'out-in' fuel management scheme, the discharge burnup (for the reference case of α = 0.2846 and θ = 1.8) was only about 1% less, while for the 'low-leakage' strategy the discharge burnup was approximately 2.8% lower. One possible explanation for the bigger difference in the discharge burnup prediction for the 'low-leakage' scheme is

TABLE 4.2

PARAMETERS USED IN THE EVALUATION OF THE 'OUT-IN' AND 'LOW-LEAKAGE' FUEL MANAGEMENT SCHEMES FOR A 5-BATCH, EQUILIBRIUM CORE

Item	Out-in*	Low-leakage**
Fuel Enrichment, ε w/o	4.30	4.44
Extrapolated BOL Reactivity, ρ_0	0.2632	0.2660
Slope of ρ(B) Curve, MT/MWD	7.063×10^{-6}	6.885×10^{-6}
Leakage Coefficient	0.2846	0.2846
Theta Value θ for both Interior and Peripheral Batches	1.8	1.8
Residual poison $\Delta\rho$ (%)	—	0.5

*All 48 assemblies of batch 1 (fresh fuel) were treated as being on the core periphery.

**8 assemblies of batch 1, 36 of batch 2, and 4 of batch 3 were in peripheral locations.

TABLE 4.3a

COMPARISON OF CYCLE EXPOSURES COMPUTED BY DISBURN AND DETAILED COMPUTER CALCULATIONS FOR THE 'OUT-IN' FUEL MANAGEMENT SCHEME [CONSTANT α]

Cycle of Exposure	C-E* (MWD/MT)	DISBURN, α = 0.2846; (MWD/MT)		
		θ = 1.5	θ = 1.8	θ = 2.0
1	9429	8823	8638	8524
2	12160	12213	12775	13157
3	10842	10631	10735	10772
4	9930	9554	9439	9353
5	8309	8740	8523	8375
Total	50665	49961	50110	50181

*Ref. [M-1].

TABLE 4.3b

COMPARISON OF CYCLE EXPOSURES COMPUTED BY DISBURN AND DETAILED COMPUTER CALCULATIONS FOR THE 'OUT-IN' FUEL MANAGEMENT SCHEME [CONSTANT θ]

Cycle of Exposure	C-E* (MWD/MT)	DISBURN, θ = 1.8; (MWD/MT)		
		α = 0.2650	α = 0.2700	α = 0.2846
1	9429	8977	8885	8638
2	12160	12819	12811	12775
3	10842	10777	10766	10735
4	9930	9479	9470	9439
5	8309	8560	8550	8523
Total	50665	50612	50482	50110

*Ref. [M-1].

TABLE 4.4a

COMPARISON OF CYCLE EXPOSURES COMPUTED BY DISBURN AND DETAILED COMPUTER CALCULATIONS FOR THE 'LOW-LEAKAGE' FUEL MANAGEMENT SCHEME [CONSTANT α]

Cycle of Exposure	C-E* (MWD/MT)	DISBURN, α = 0.2846; (MWD/MT)		
		θ = 1.5	θ = 1.8	θ = 2.0
1	13492	13273	14094	14660
2	8648	9163	8974	8845
3	11068	10613	10639	10633
4	10574	9813	9680	9561
5	9878	8983	8757	8599
Total	53660	51845	52144	52298

*Ref. [M-1].

TABLE 4.4b

COMPARISON OF CYCLE EXPOSURES COMPUTED BY DISBURN AND DETAILED COMPUTER CALCULATIONS FOR THE 'LOW-LEAKAGE' FUEL MANAGEMENT SCHEME [CONSTANT θ]

Cycle of Exposure	C-E* (MWD/MT)	DISBURN, θ = 1.8; (MWD/MT)		
		α = 0.2650	α = 0.2700	α = 0.2846
1	13492	14243	14200	14094
2	8648	9176	9129	8974
3	11068	10699	10687	10639
4	10574	9708	9694	9680
5	9879	8789	8786	8757
Total	53660	52615	52496	52144

*Ref. [M-1].

that the suppression of reactivity in the batch 1 (fresh) fuel by means of burnable poison, which will lead (as shown in the next section) to a slight increase in our calculated discharge burnup, is not simulated here. As will be seen later, the observed difference is of the expected magnitude.

In the present work, we are primarily interested in the relative change in the discharge burnup of a modified fuel management scheme compared to a reference case. Figures 4.3 and 4.4 show the relative difference in discharge burnups between the out-in and low-leakage fuel management schemes as a function of the power sharing parameter theta and the leakage coefficient α, respectively. It can be seen that the differences between the two fuel management strategies and between the DISBURN and C-E results are quite insensitive to both theta and α. This is an important observation since it confirms that the results are not biased in any important way by the details of the methodology used to establish numerical values for the two dominant free parameters in the model. Considering the complexity of the problem involved, the DISBURN code produces satisfactory agreement with the results of detailed state of the art physics analyses.

4.3 SIMULATION OF DIFFERENT FUEL MANAGEMENT STRATEGIES

The DISBURN code was found to be sufficiently accurate for the type of analyses of interest in the present research. Although different fuel management strategies can

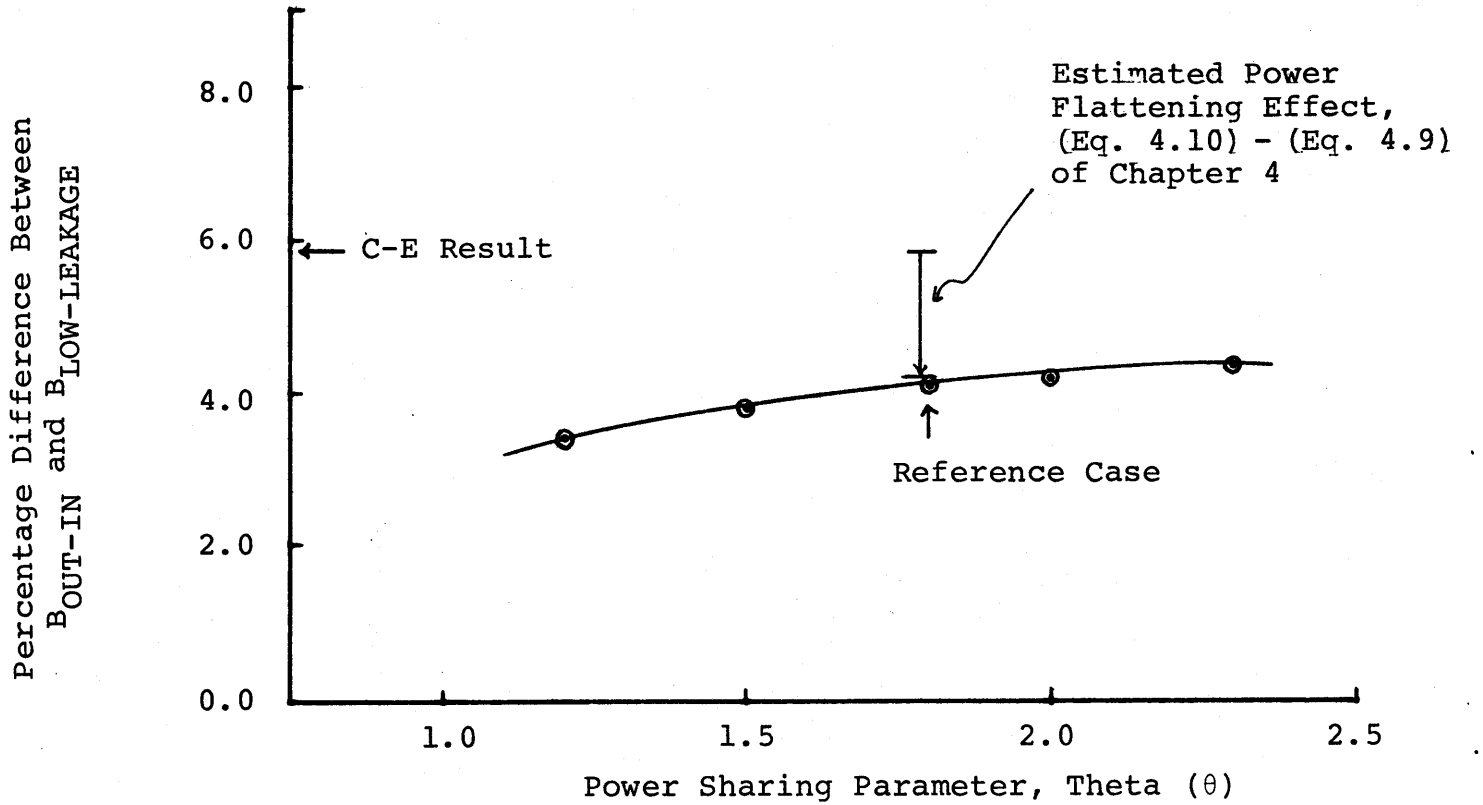

Fig. 4.3 The Percentage Difference between the Discharge Burnup for the Out-in and Low-Leakage Fuel Management Schemes, as a Function of the Power Sharing Parameter Theta

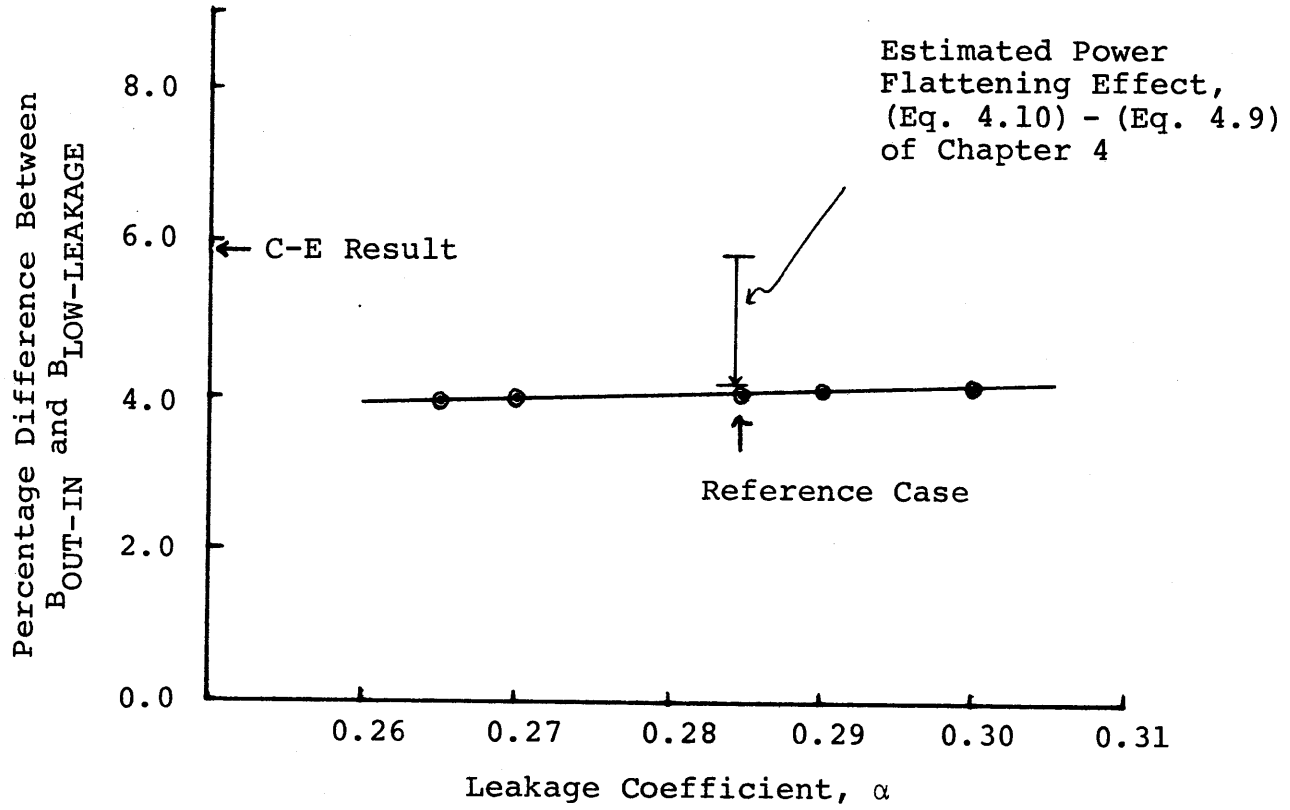

Fig. 4.4 The Percentage Difference between the Discharge Burnup for the Out-In and Low-Leakage Fuel Management Schemes as a Function of the Leakage Coefficient

be simulated and analyzed separately, the ultimate objective of these scoping analyses is the determination of the net improvement (or decrease) in uranium utilization arising from the combination of these common strategies.

The first portion of this section deals with the evaluation of the separate fuel management schemes of contemporary interest such as the use of burnable poison to obtain an optimum power history (with respect to maximizing discharge burnup), the use of low-leakage fuel loading patterns, etc.. In the latter part of this section, the discharge burnup (and hence the uranium utilization) of a synthesis of the various methods for improvement of uranium utilization will be computed.

4.3.1 BURNABLE POISON

The primary objectives of employing burnable poison in the fresh fuel assemblies in the low-leakage fuel management and/or extended burnup/cycle-length strategies are to suppress the power density in these assemblies and to keep soluble boron concentrations at the beginning of cycle sufficiently low to obtain an acceptable (slightly negative) moderator temperature coefficient of reactivity. However, it has apparently not been realized in the past that power shaping using burnable poison can lead to a slight increase in the fuel discharge burnup. This was shown to be the case in Chapter 3 using an analytical approach to derive the discharge burnup of a fuel batch whose power history tra-

jectory was shaped by means of burnable poison. (See Table 3.4). This observation is confirmed in this section using the DISBURN code. Further, an "optimum" (maximum discharge burnup), burnable-poison-shaped power history profile was determined, as well as the residual poison reactivity penalty which can be tolerated to break even with respect to the discharge burnup, as compared to the same case without burnable poison.

The analyses were done for the Main Yankee reactor design—a 3-batch, steady-state core with a reload fuel enrichment of 3 w/o U-235. The parameters associated with the reactivity versus burnup curve which characterize the Main Yankee supercell lattice, and the reactor core configuration are:

Extrapolated BOL reactivity: $\rho_0 = 0.2235$

Slope: $A = 0.9272 \times 10^{-5}$, MT/MWD

Theta value: $\theta = 1.5$

For the moment, the effect of core leakage and the presence of any residual poison were neglected. It was further assumed that the burnable poison was depleted completely just before the end-of-cycle point. Two cases of interest, as shown in Fig. 4.5, were considered: in the first, the reactivity in the first cycle was tailored to increase linearly from a beginning-of-life value, ρ_{BOL}, until it

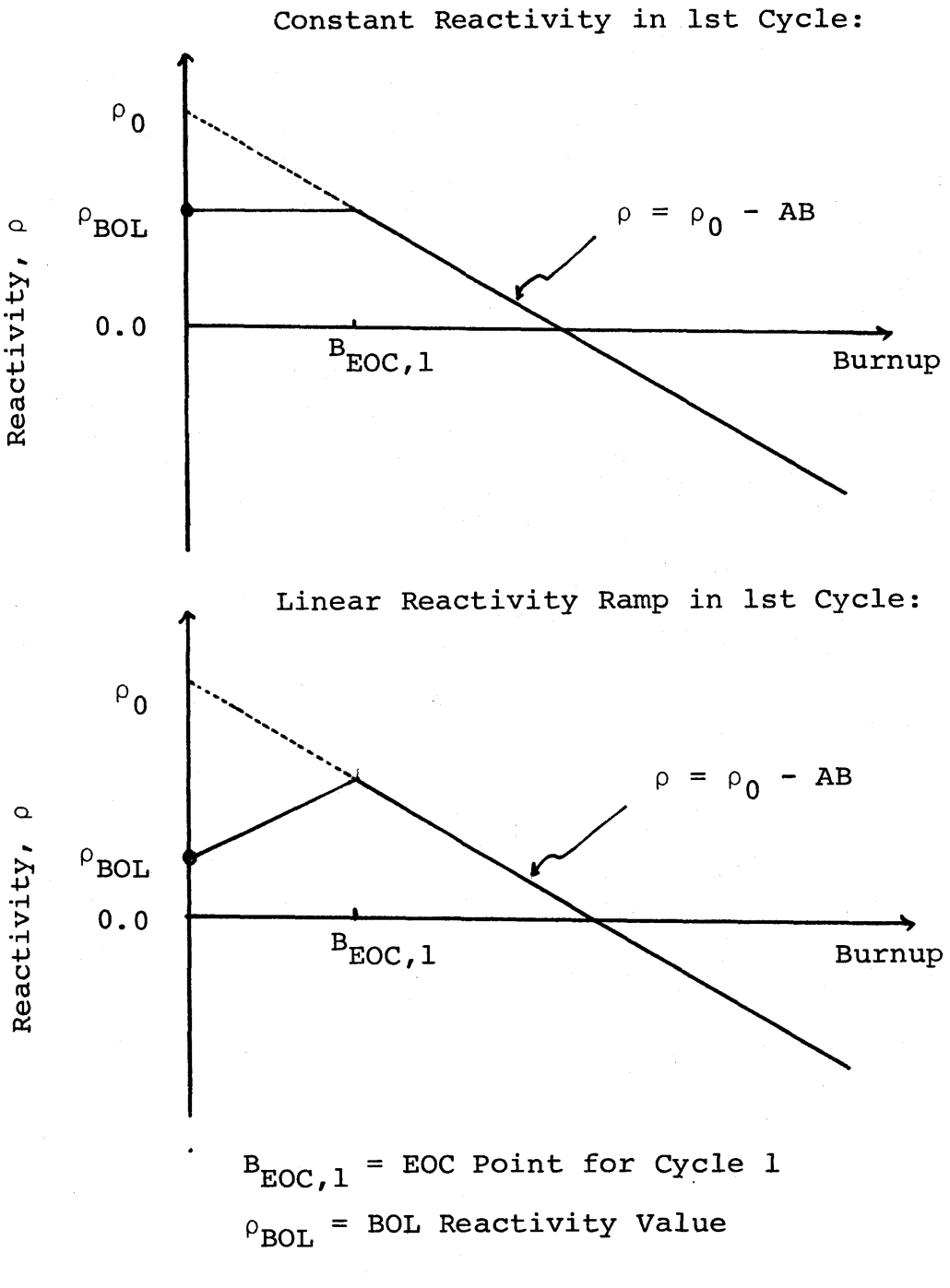

$B_{EOC,1}$ = EOC Point for Cycle 1

ρ_{BOL} = BOL Reactivity Value

Fig. 4.5 Reactivity versus Burnup History Profiles

reaches the burnable poison burnout point, which is also the end of cycle point. In the latter case, ρ_{BOL} was varied in order to determine the "optimum" (maximum discharge burn-up) reactivity versus burnup history profile. The results are shown in Table 4.5. By shaping the power profile history using burnable poison, the discharge burnup was increased by about 2.0% for the case of constant reactivity in the first cycle to approximately 3.5% for the case of a zero beginning-of-life reactivity value. Although the discharge burnup can be further increased by decreasing the BOL reactivity ρ_{BOL}, to a slightly negative value, this option was not investigated in detail for several reasons. In the first place, achieving a negative BOL reactivity value will require a higher concentration of burnable poison and hence higher residual poison, which may negate any additional gain in the discharge burnup compared to those cases with zero or positive BOL reactivity values. The second reason is that we may have to require the burnable poison to deplete at a much faster rate than that readily achievable in real applications. A third practical deterrent is the large relative power swing of the poisoned batch over its first cycle. Finally, when strong negative BOL ρ values are used, DISBURN runs show that the system may encounter premature zero reactivity states part way through a cycle. Thus, the case with a zero BOL reactivity value (case 2(d) in Table 4.5) was taken to be the one having an "optimum" reactivity

TABLE 4.5

INCREASE IN DISCHARGE BURNUP FOR DIFFERENT REACTIVITY VS. BURNUP HISTORY PROFILES

Cases	BOL Reactivity, ρ_{BOL}	EOC Point, $B_{EOC,1}$ MWD/MT	Discharge Burnup, MWD/MT	Increase in Discharge Burnup* Over Case With No Burnable Poison (%)
1. Constant Reactivity in 1st cycle	0.0982	13545	36530	1.95
2. Variable Reactivity in 1st cycle				
2(a)	0.06	13397	36753	2.57
2(b)	0.04	13308	36868	2.89
2(c)	0.02	13228	36973	3.19
2(d)	0.00	13146	37082	3.49
2(e)	-0.02	13085	37168	3.73

*Discharge burnup for the case lacking burnable poison is 35831 MWD/MT; residual poison penalty is not assessed.

versus burnup history profile, and will be referred to as such in the analyses performed in the remaining portion of this section.

The use of burnable poison in the fresh fuel assemblies will always leave a small but finite amount of residual poison reactivity in the subsequent cycles. When gadolinium oxide (Gd_2O_3) is admixed with uranium oxide fuel, the residual reactivity is caused by a quasi-steady-state transmutation of the low cross section even-A gadolinium isotopes into the high cross section odd-A gadolinium isotopes. For boron shim, however, the residual poison reactivity is due to the incomplete depletion of the boron-10 at the end of the first and subsequent cycles: here the residual reactivity will diminish with burnup. The amount of the residual poison reactivity depends upon several factors: among them are (1) the type of burnable poison material used, (2) the burnable poison loading in the fresh fuel assemblies, and (3) the design of the fuel rods containing burnable poison (burnable poison admixed with UO_2), the design of the separate shim rods (lumped burnable poison), and the design of the fuel assemblies which contain burnable poison (i.e., the number of fuel rods with burnable poison, the number of shim rods and the locations in the assembly in which these rods are placed). It has been estimated [M-1, H-3] that for an equilibrium cycle the residual reactivity amounts to about 0.3% - 0.5% $\Delta\rho$ on a core average basis for contemporary

burnable poison materials and designs.

Calculations were performed to determine the residual poison reactivity penalty to break even with respect to the discharge burnup compared to a core without burnable poison. The first set of analyses was done for the case in which the reactivity level in the first cycle remained constant, and the second series of calculations was performed for the "optimum" case. The results are shown in Tables 4.6 and 4.7, respectively. For constant reactivity in cycle 1, the breakeven value of the residual reactivity penalty is about 0.4% $\Delta\rho$, whereas for the optimum $\rho(B)$ profile, the breakeven value is approximately 0.7% $\Delta\rho$. Since the residual reactivity penalty cited for reactivity versus burnup history profiles similar to the former case (i.e., constant reactivity in cycle 1) is in the range of 0.2 - 0.3% $\Delta\rho$ [H-3], there is a net gain in the discharge burnup from suppressing the reactivity of the fresh fuel using burnable poison. The same can be said of the optimum $\rho(B)$ profile case.

The residual poison penalty (particularly when gadolinium is used) should, to first order, be proportional to the amount of poison reactivity initially present: $(\rho_0 - \rho_{BOL})$ in Fig. 4.3. This observation is supported in a recent study by Combustion Engineering [H-3] on the use of gadolinium in PWR extended-burnup cycles, in which it is shown that the residual reactivity holddown was approximately proportional to the weight percent gadolinium oxide loading

TABLE 4.6

DISCHARGE BURNUP FOR THE CASE
OF CONSTANT CYCLE 1 REACTIVITY
AT DIFFERENT RESIDUAL POISON LEVELS

Residual Poison Reactivity (% $\Delta\rho$)	Discharge Burnup MWD/MT	Increase in Discharge Burnup* Over Core Without Burnable Poison (%)
0.0	36530	1.95
0.1	36371	1.51
0.2	36211	1.06
0.3	36038	0.58
0.4	35872	0.11
0.5	35711	-0.33

*Discharge burnup for a core lacking burnable poison is 35831 MWD/MT.

TABLE 4.7

DISCHARGE BURNUP FOR THE "OPTIMUM"
REACTIVITY-BURNUP HISTORY PROFILE
AT DIFFERENT RESIDUAL POISON LEVELS

Residual Poison Reactivity (% $\Delta\rho$)	Discharge Burnup MWD/MT	Increase in Discharge Burnup* Over Core Without Burnable Poison (%)
0.0	37082	3.49
0.1	36919	3.04
0.3	36575	2.08
0.5	36215	1.07
0.7	35875	0.12
0.9	35514	-0.88

*Discharge burnup for a core lacking burnable poison is 35831 MWD/MT.

in the fuel. If this is so, then the more highly poisoned cases, while they improve the power history profile (which improve uranium utilization) also suffer a larger compensating penalty due to residual poison. Assuming a 0.3% $\Delta\rho$ penalty for the constant-reactivity case, and scaling this penalty proportional to $(\rho_0 - \rho_{BOL})$, we find that the net increase in discharge burnup for cases 2(a) - 2(d) is reduced to the point where all burnable poison cases are essentially equivalent. This is shown in Table 4.8. Thus, the "optimum" reactivity versus burnup history profile cited earlier in this section is, in reality, only marginally preferable when the effect of the anticipated residual poison penalty is taken into account. In view of this, a fuel designer can select the poison loading to meet other criteria such as BOC or EOC peak power or power swing over a cycle in or between assemblies.

4.3.2 LOW-LEAKAGE FUEL MANAGEMENT

The DISBURN code has been employed to analyze the effect of low-leakage fuel management on the discharge burnup of the Maine Yankee reactor. The initial analyses were done without the use of burnable poison to shape or suppress the reactivity of the fresh fuel when placed in the core interior as required by this scheme. Later in this section, the additional effect of reactivity suppression in the fresh fuel assemblies located in the core interior by means of burnable poison, on the discharge burnup (and hence, uranium

TABLE 4.8

THE EFFECT OF THE LARGER RESIDUAL POISON REACTIVITY ASSOCIATED WITH A HIGHER BURNABLE POISON LOADING

Case	BOL Reactivity, ρ_{BOL}	Initial Poison* Reactivity, $\rho_0 - \rho_{BOL}$	Residual Poison Reactivity, (% $\Delta\rho$)	Discharge Burnup, (MWD/MT)	Increase in Discharge Burnup** Over Case With No Poison (%)
1. Constant Reactivity in 1st cycle	0.0982	0.1253	0.30	36038	0.58
2. Variable Reactivity in 1st cycle					
2(a)	0.060	0.1635	0.39	36070	0.67
2(b)	0.040	0.1835	0.44	36101	0.75
2(c)	0.020	0.2035	0.49	36108	0.77
2(d)	0.000	0.2235	0.54	36140	0.86

*ρ_0 = 0.2235.

**Discharge Burnup for the case lacking burnable poison is 35831 MWD/MT.

utilization) is discussed.

Three cases were examined. The first case (the reference case) consisted of a reload having 48 of the 72 assemblies of 3.0 w/o U-235 fuel placed on the core periphery (i.e., in a normal out-in/scatter refueling mode, as there are only 48 peripheral locations). In the second and third cases, the same number of assemblies of once- or twice-burned fuel, respectively, were loaded on the core periphery—the former case is designated the 'in-out-in' fuel management scheme while the latter is an 'in-in-out' (or in/scatter-out) scheme; both are commonly referred to as low-leakage schemes. The leakage correlation for the Maine Yankee reactor developed in Chapter 3 was used; the leakage coefficient in this case was $\alpha = 0.1640$. Table 4.9 summarizes the results of this initial analysis. An increase in the discharge burnup of about 3.0% was achieved in going from the current, out-in scheme to the low-leakage strategy. This was also the percentage improvement found for the uranium utilization.

The placing of fresh fuel assemblies in the core interior necessitates the use of burnable poison to maintain the power density below acceptable limits and to keep soluble boron concentrations at the BOC sufficiently low to obtain a slightly negative moderator temperature coefficient of reactivity. However, it was shown in the previous section that the resultant shaping of the reactivity vs.

TABLE 4.9

COMPARISON OF LOW-LEAKAGE FUEL MANAGEMENT
WITH CURRENT, OUT-IN FUEL MANAGEMENT

Case	Discharge Burnup (MWD/MT)	Increase in Discharge Burnup over the Out-In Fuel Management Case (%)
1. Current Out-In	30505	0.0
2. In-Out-In Scheme*, i.e., once-burned fuel on core periphery	30990	1.59
3. In-In-Out Scheme* low-leakage with twice-burned fuel on core periphery	31419	3.00

*Without the incorporation of burnable poison.

burnup history profile due to the incorporation of burnable poison can lead to a slight improvement in the discharge burnup. Analyses were done to determine the net increase in discharge burnup (hence, improvement in uranium utilization) due to the incorporation of burnable poison in the fresh fuel batch for the in-in-out low-leakage fuel management scheme. Two cases were considered: in the first, the reactivity of the fresh fuel was held constant by burnable poison in the first cycle, and in the second case, the reactivity in cycle 1 was tailored by means of burnable poison to increase linearly from a value of $\rho_{BOL} = 0.02$ (case 2(c) in Table 4.5). The reasons for selecting $\rho_{BOL} = 0.02$ as opposed to $\rho_{BOL} = 0.0$ are: there was no significant difference in the net increase in their discharge burnups when their respective residual poison reactivity penalties were taken into account, and in the case with $\rho_{BOL} = 0.0$, we might encounter premature zero reactivity states part way through a cycle, since the leakage of neutrons from the core (which has the effect of lowering the overall system reactivity) was considered in these analyses. The residual poison reactivity penalties associated with the two poisoned $\rho(B)$ profiles adopted in the analyses were taken from Table 4.8. The results are shown in Table 4.10. The additional gain in the discharge burnup of the low-leakage scheme over the out-in scheme due to the employment of the burnable poison in the fresh reload fuel was less than 1%.

TABLE 4.10

THE EFFECT OF USING BURNABLE POISON
IN THE IN-IN-OUT LOW-LEAKAGE
FUEL MANAGEMENT SCHEME

Case	Discharge Burnup, (MWD/MT)	Increase In Discharge Burnup Over the Current Out-In Scheme (%)
Current, Out-In scheme	30505	0.0
Low-Leakage scheme	31419	3.00
Low-Leakage with constant-reactivity in Cycle 1 (no residual poison penalty)	31979	4.83
Low-Leakage with constant-reactivity in Cycle 1 (Residual $\Delta\rho$ = 0.3%)	31479	3.19
Low-Leakage with BOL reactivity value ρ_{BOL} = 0.02 (no residual poison penalty)	32467	6.43
Low-Leakage with BOL reactivity value ρ_{BOL} = 0.02 (Residual $\Delta\rho$ = 0.49%)	31610	3.62

However, the benefit of using burnable poison in the low-leakage fuel management strategy, in addition to benefiting the moderator temperature coefficient of reactivity and the suppression of power peaking, is in the reduction of the radial (global) power peaking factor compared to the case without burnable poison, as shown in Table 4.11. Penalties associated with this factor will be discussed in a subsequent section of this chapter.

4.3.3 EXTENDED CYCLE LENGTH/BURNUP

In recent years, a large number of utilities have seriously considered extending cycle length (18 intead of 12 months) while keeping the number of feed assemblies the same. The primary incentive for this switch is that one refueling outage is eliminated every three years, which allows a higher plant capacity factor, and therefore significant savings in replacement power costs. This strategy can also improve uranium utilization through its inherent reliance upon extended burnup. The steady-state cycle average burnup can be related to the calendar time between startups by:

$$B_c \text{ (MWD/MT)} = \frac{365\ Q_{TH}\ (t-t_R)\ L'}{(A_T)\ (M)} \qquad (4.3)$$

where Q_{TH} = Reactor thermal power rating (MWth)

t = Time between startups (years)

t_R = Downtime for refueling (years)

$t-t_R$ = Time the reactor is producing power (years)

TABLE 4.11

THE EFFECT OF BURNABLE POISON
ON THE GLOBAL, BATCH-AVERAGE
RADIAL POWER PEAKING FACTOR

Item	Relative Radial Power Peaking Factor
1. Current Out-In/Scatter scheme	1.00 (reference value)
2. Low-Leakage In-In-Out scheme without burnable poison	1.15
3. Low-Leakage scheme with constant-reactivity in Cycle 1 (Residual $\Delta\rho$ = 0.3%)	1.09
4. Low-Leakage scheme with BOL reactivity value ρ_{BOL} = 0.02 (Residual $\Delta\rho$ = 0.49%)	1.05

L' = Availablility-based capacity factor

A_T = Total number of assemblies in core

M = Heavy metal loading per assembly (Metric Tons Uranium)

In our previous analyses of the Main Yankee PWR the discharge burnup, under steady-state conditions, for the 3-batch, out-in fuel management scheme, was 30505 MWD/MT (see Table 4.9). If the corresponding time interval between startups is equal to 12 months, then the discharge burnup that must be achieved to extend the cycle length to about 18 months according to Eq. 4.3 is around 46000 MWD/MT. Several analyses were performed to determine the effect of extended cycle length on the busbar and system costs of the plant, and to evaluate the improvement on the uranium utilization of the reactor. For the present purposes, the uranium utilization is defined in terms of MegaWatt-Days per Metric Ton of natural uranium feed (MWD/MTF):

$$U = \frac{B_{dis}}{(F/P)} \quad \text{(MWD/MTF)} \tag{4.4}$$

where B_{dis} is the discharge burnup, and the feed-to-product ratio is given by

$$\frac{F}{P} = \frac{(x_P - x_T)}{(x_F - x_T)} \tag{4.5}$$

with x_P = enrichment of the product (reactor reload

fuel), w/o

x_F = enrichment of the natural uranium feed (= 0.711 w/o)

x_T = enrichment of the tails stream (typically 0.2 w/o)

Equation 4.4 can thus be rewritten as:

$$U \text{ (MWD/MTF)} = \frac{0.511\ B_{dis}}{(x_p - 0.2)} \qquad (4.6)$$

The analyses were again done for the Maine Yankee reactor design, with a reload fuel enrichment of 4.34 w/o U-235. The parameters describing the $\rho(B)$ curve which characterizes the Main Yankee supercell lattice are:

$\rho_0 = 0.2661$

$A = 0.7154 \times 10^{-5}$, MT/MWD

The theta value and the leakage coefficient employed in the analyses remain the same as before ($\theta = 1.5$ and $\alpha = 0.1640$). The results are given in Table 4.12. The use of extended cycle, out-in fuel management results in a 6.3% reduction in uranium requirements. If the extended cycle design is operated in a low-leakage configuration, a saving of 8.8% in uranium usage is obtained.

The analyses were repeated with the incorporation of burnable poison in the low-leakage fuel management scheme.

TABLE 4.12

COMPARISON OF EXTENDED CYCLE AND LOW-LEAKAGE EXTENDED CYCLE FUEL MANAGEMENT WITH CURRENT, THREE-BATCH, OUT-IN/SCATTER FUEL MANAGEMENT

Case	Reload Enrichment, x_P (w/o U-235)	Discharge Burnup (MWD/MT)	U (MWD/MTF)	Uranium Requirement (MTF/MWD)
Current Out-In/Scatter	3.0	30505	5567	1.796×10^{-4}
Extended Cycle, Out-In/Scatter	4.34	48176	5946	1.682×10^{-4}
Extended Cycle, In/Scatter-Out (Low-Leakage)	4.34	49473	6106	1.638×10^{-4}

The appropriate residual poison reactivity penalties were also accounted for in the analyses. Table 4.13 summarizes the results. An improvement in uranium utilization of about 11% is realized in the extended cycle low-leakage fuel management with burnable poison being used to suppress the reactivity of the fresh fuel located in the core interior. Additional economic benefits of the extended cycle low-leakage fuel management scheme are derived from the higher plant capacity factor which significantly affects the system cost of the power plant. Further discussion of the economic benefits of the use of burnable poison in this particular scheme is postponed until later in this chapter.

4.4 COMPARISON OF ANALYTICAL WITH NUMERICAL RESULTS

In Chapter 3, analytical expressions for the discharge burnup of a batch of fuel for various reactivity versus burnup history profiles were derived. In this section, the analytical results are checked against those generated using the DISBURN code. Analytical results which depart significantly from the numerical ones, are normalized to force better agreement.

The discharge burnup equations which were derived analytically were expressed in the form:

$$B_{dis} = B_0 / (1+\varepsilon) \tag{4.7}$$

where B_0 is the discharge burnup for the hypothetical

TABLE 4.13

THE EFFECT OF BURNABLE POISON ON THE URANIUM UTILIZATION OF LOW-LEAKAGE EXTENDED CYCLE FUEL MANAGEMENT

Case	Discharge Burnup (MWD/MT)	Improvement in Uranium Utilization (%)
Current Out-In/Scatter	30505	0.0 (reference case)
Burnable Poison Cases:		
Extended Cycle, Low-Leakage with Constant Reactivity in Cycle 1	50632	12.3
Extended Cycle, Low-Leakage with Constant Reactivity in Cycle 1 (Residual $\Delta\rho$ = 0.3%)	49991	10.8
Extended Cycle, Low-Leakage with ρ_{BOL} = 0.04	51366	13.9
Extended Cycle, Low-Leakage with ρ_{BOL} = 0.04 (Residual $\Delta\rho$ = 0.54%)	50111	11.1

flat power case:

$$= \left(\frac{2n}{n+1}\right)\frac{\rho_0}{A}$$

in which n is the number of batches

ρ_0 is the extrapolated BOL reactivity

A is the slope of the linear $\rho(B)$ curve

and ε is the factor which corrects for the departure of discharge burnup from the flat power case.

The 'ε factors' for the various power history trajectories are available in a closed analytical form (see Table 3.3). These anlytical expressions for the 'ε factor' were compared with the numerically evaluated results, rather than the discharge burnup itself. The transformation between the 'ε factor' and the corresponding discharge burnup is straightforward (Eq. 4.7).

4.4.1 REACTIVITY CONTROL WITH SOLUBLE POISON ONLY

The expression for the 'ε factor' in this case is given by

$$\varepsilon = (\theta\rho_0)^2 \frac{(n-1)}{3(n+1)^2} \qquad (4.8)$$

Figures 4.6 and 4.7 show the analytical and the numerical results for ε. Although the quantitative agreement is apparently poor, it must be noted that the values of ε in this particular case are rather small—a second order effect on B_0. Also, the trends in the variation of ε with both

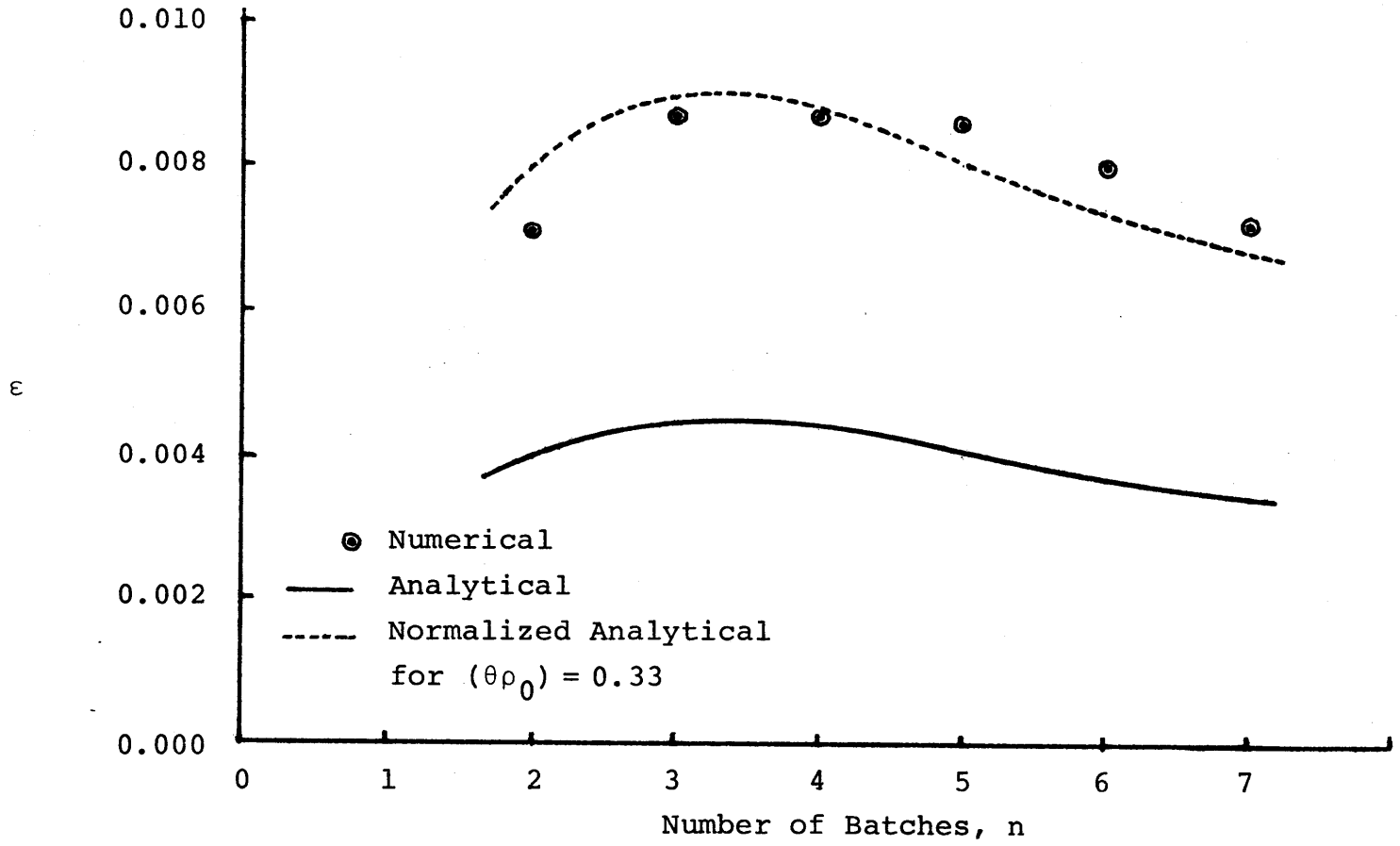

Fig. 4.6 ε as a Function of the Number of Batches for the Case of Reactivity Control by Means of Soluble Poison only

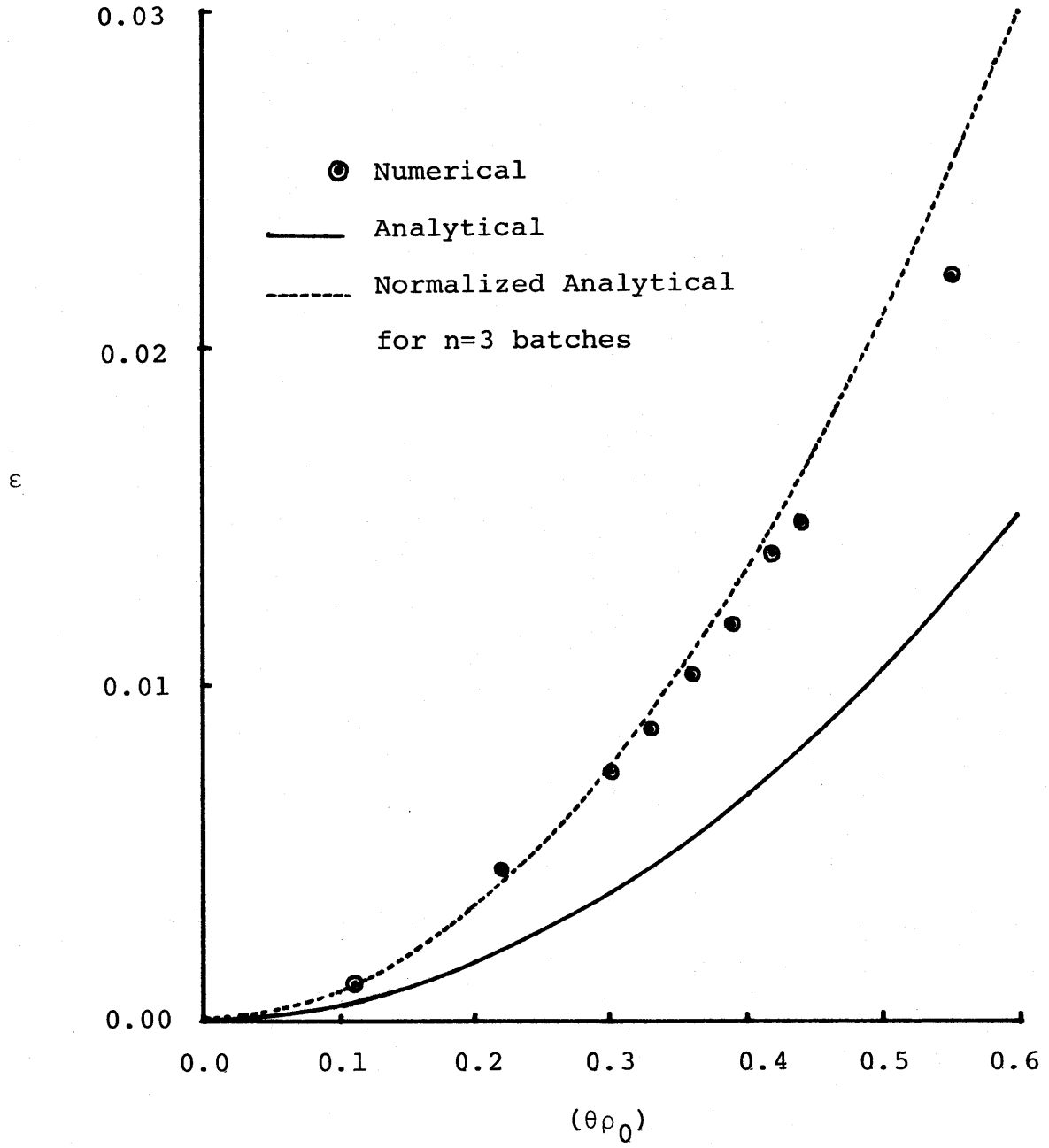

Fig. 4.7 ε as a Function of $(\theta\rho_0)$ for the Case of Reactivity Control by Means of Soluble Poison only

the number of batches n, and $(\theta\rho_0)$ are correctly predicted by the analytical expression of Eq. 4.6. The analytical results were normalized to the accurate numerical ones through the multiplication of Eq. 4.8 by a constant factor of two. The normalized ε factor is thus given by

$$\varepsilon' = \frac{2(\theta\rho_0)^2(n-1)}{3(n+1)^2} \tag{4.9}$$

The normalized results are also plotted in Figs. 4.6 and 4.7; the agreement is quite good.

4.4.2 REACTIVITY CONTROL USING BURNABLE POISON

Two cases of interest were considered in Chapter 3 with regard to the suppression of reactivity in the fresh fuel by means of burnable poison. In the first case, burnable poison was employed to hold the reactivity at a constant value in the first cycle. The expression for the ε factor for this situation is

$$\varepsilon = -(\theta\rho_0)\frac{(n-1)}{n(n+1)^2} + (\theta\rho_0)^2\frac{(n-1)}{3n(n+1)^2} \tag{4.10}$$

Figures 4.8 and 4.9 show good agreement between the results obtained numerically and those from the analytical expression of Eq. 4.10, both in magnitude and in the trend.

In the second case, the reactivity of the fuel batch was tailored by means of burnable poison, to increase linearly from a zero value. The ε factor in this case was

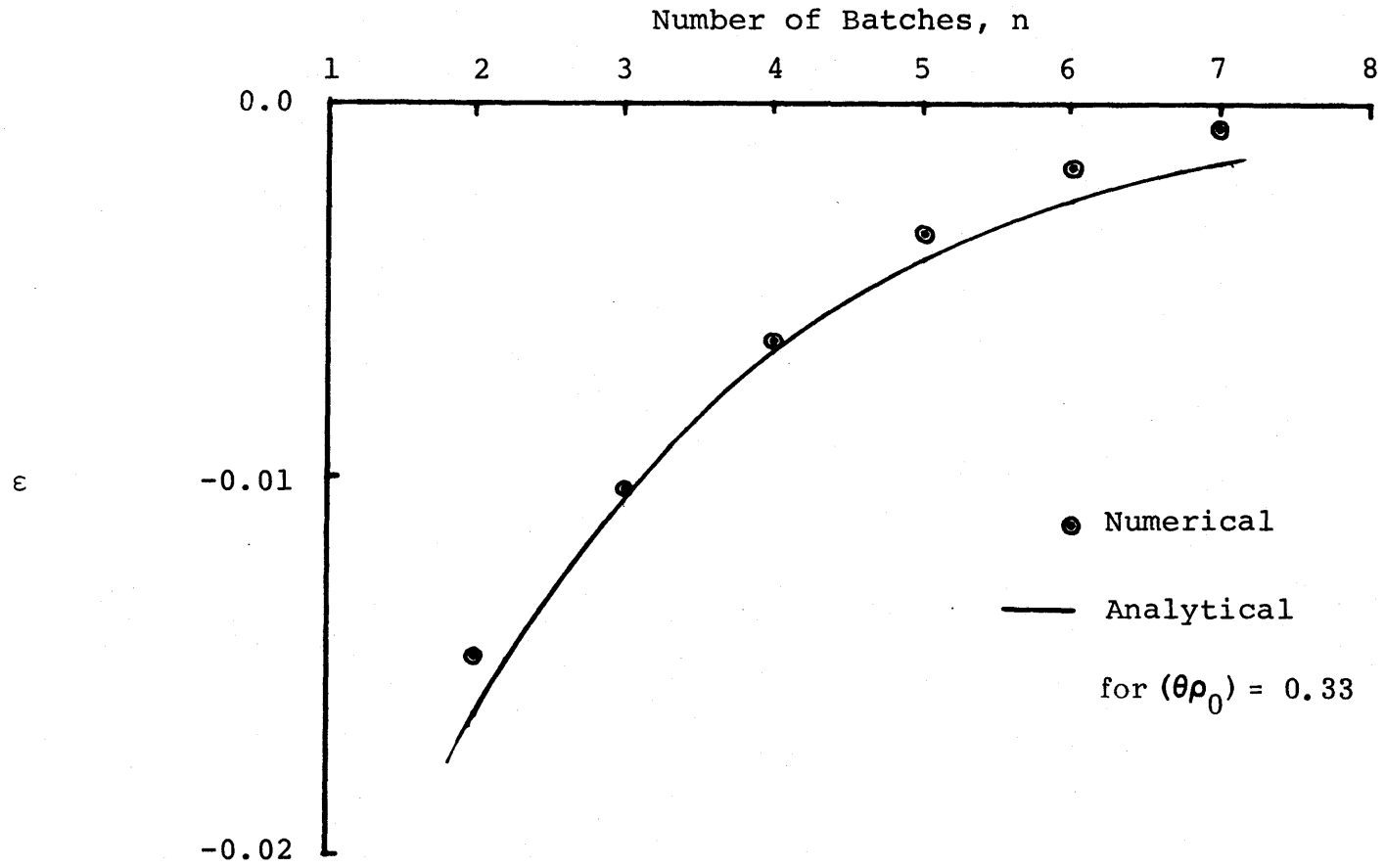

Fig. 4.8 ε as a Function of the Number of Batches, for the case of Constant Reactivity in the First Cycle

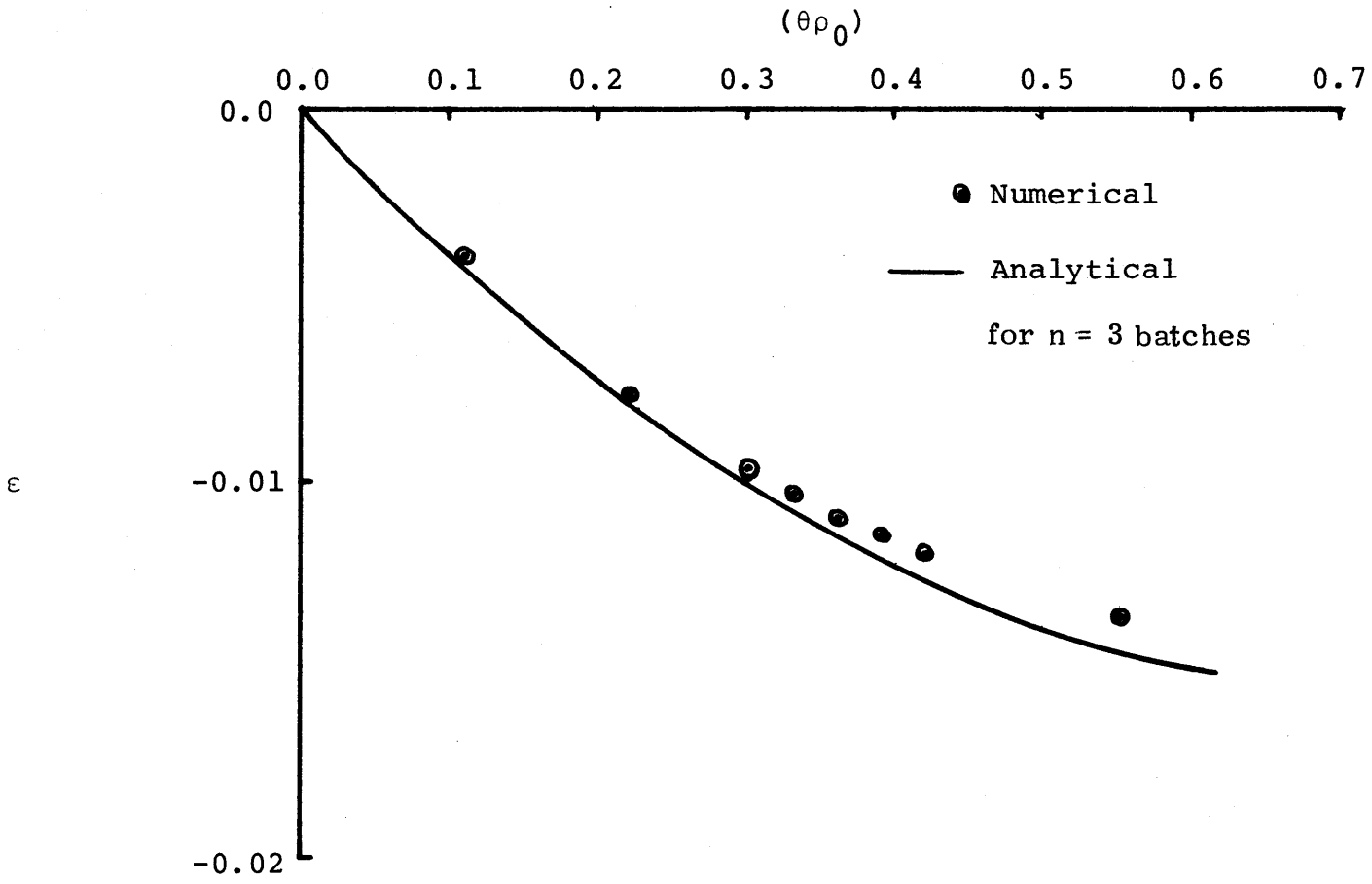

Fig. 4.9 ε as a Function of $(\theta\rho_0)$ for the Case of Constant Reactivity in the First Cycle

given by

$$\varepsilon = - \frac{(\theta\rho_0)(n-1)}{2n(n+1)} + \frac{(\theta\rho_0)^2(n-1)^2}{6n(n+1)^2} \qquad (4.11)$$

Again, the agreement between the analytical and the numerical results was good, as shown in Figs. 4.10 and 4.11. Hence, no empirical normalization is required in these instances.

4.4.3 REACTIVITY CONTROL USING FIXED POISON SHIMS OR LEAKAGE

The insertion of fixed poison shim in a batch of fuel over a given cycle is mathematically equivalent to subjecting the same batch of fuel to a fixed leakage (for example, by placing the fuel batch on the core periphery) since in both cases, the net effect is to impose a fixed reactivity penalty. The situation is depicted in the reactivity versus burnup trace of Fig. 4.12.

It was pointed out in the previous chapter that there was considerable difficulty for this particular reactivity history in deriving an analytical expression for the discharge burnup (and thus, the ε factor) in a closed form. Therefore, numerical computations were performed to determine the functional dependency of the ε factor on parameters such as the number of batches n, the batch or cycle in which the shim is present, j, the reactivity associated with the shim or leakage, etc.. Figures 4.13 to 4.16 show some of

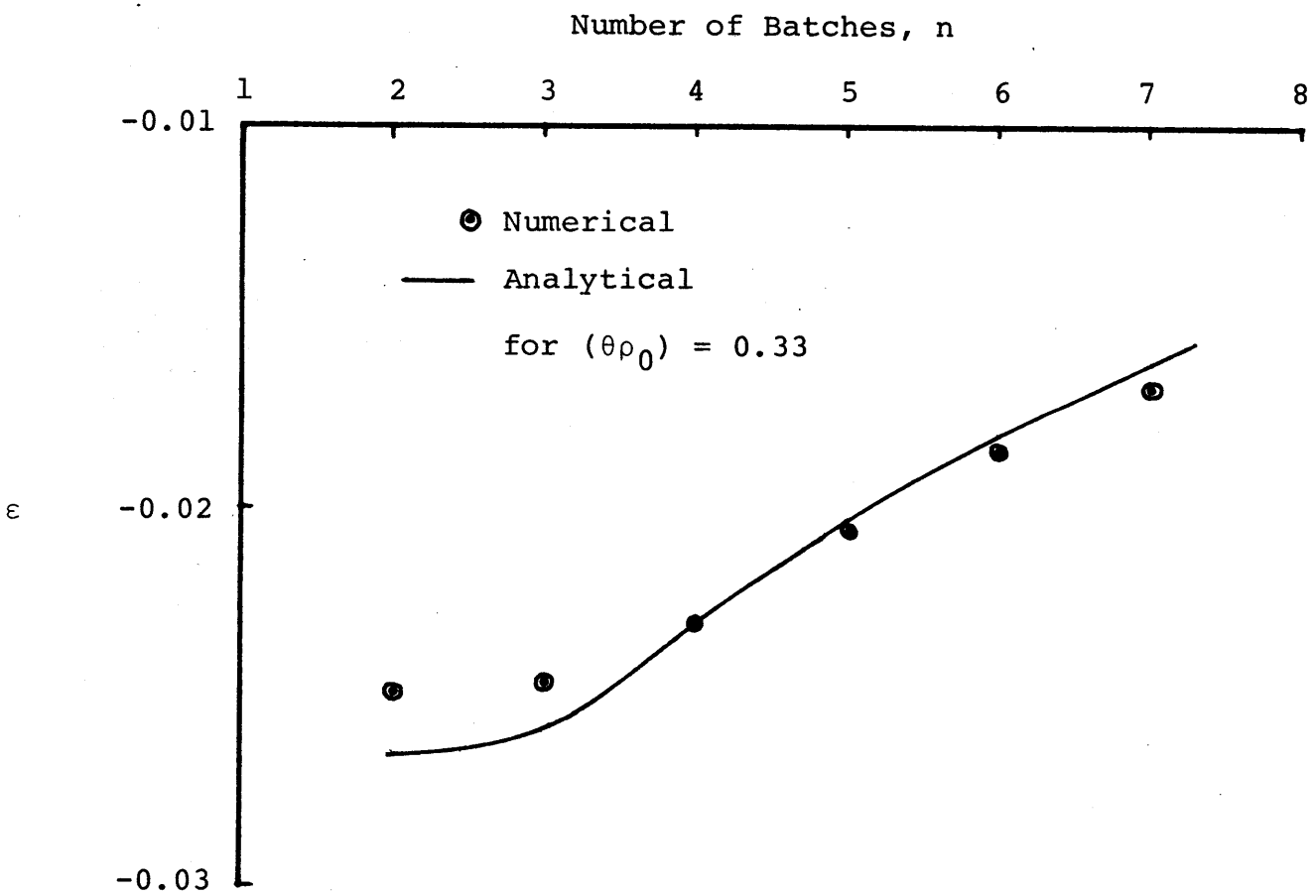

Fig. 4.10 ε as a Function of the Number of Batches for the Case of Reactivity Value at BOL equal to zero ($\rho_{BOL} = 0.0$)

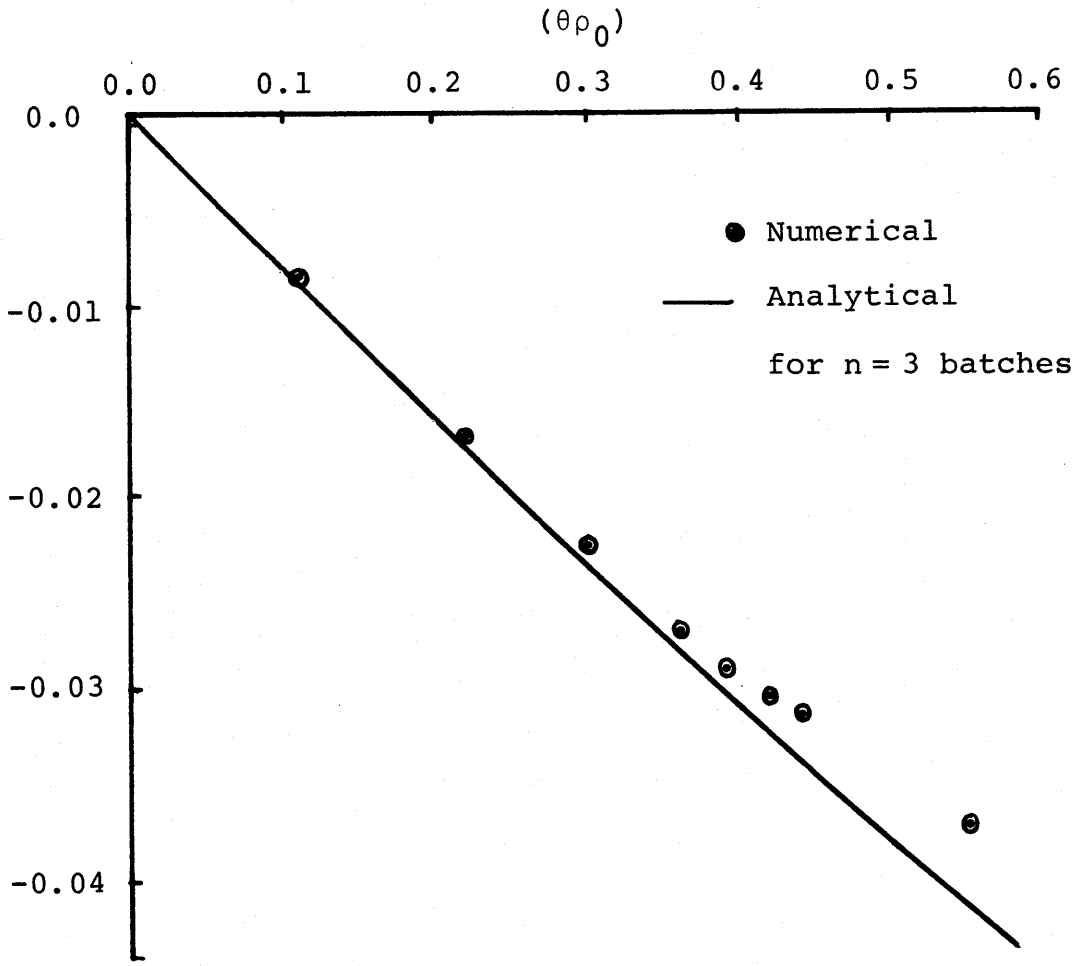

Fig. 4.11 ε as a Function of $(\theta\rho_0)$ for the Case of Reactivity Value at BOL Equal to Zero ($\rho_{BOL} = 0.0$)

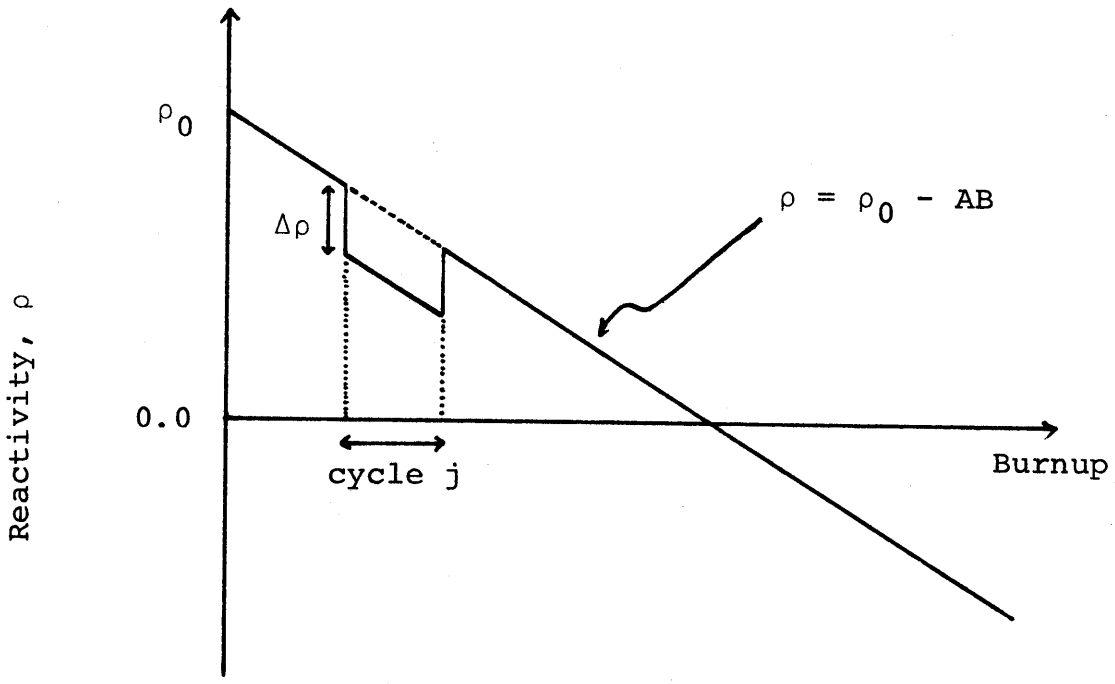

Fig. 4.12 Reactivity versus Burnup Trace for the Case of the Presence of Fixed Poison Shim or Leakage in cycle j

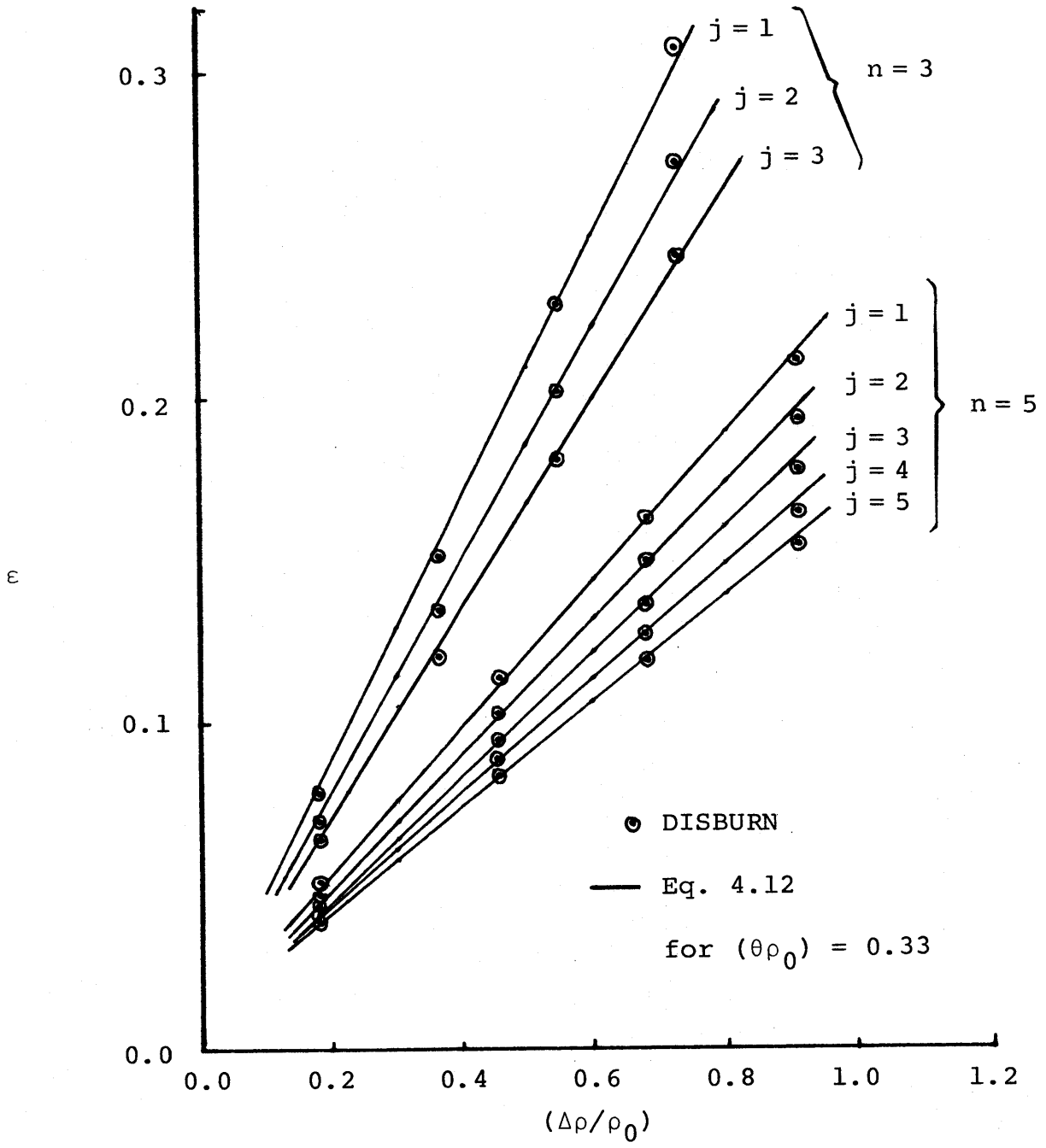

Fig. 4.13 ε as a Function of $(\Delta\rho/\rho_0)$ for the Case of Reactivity Control using Fixed Poison Shim or Leakage in Cycle j

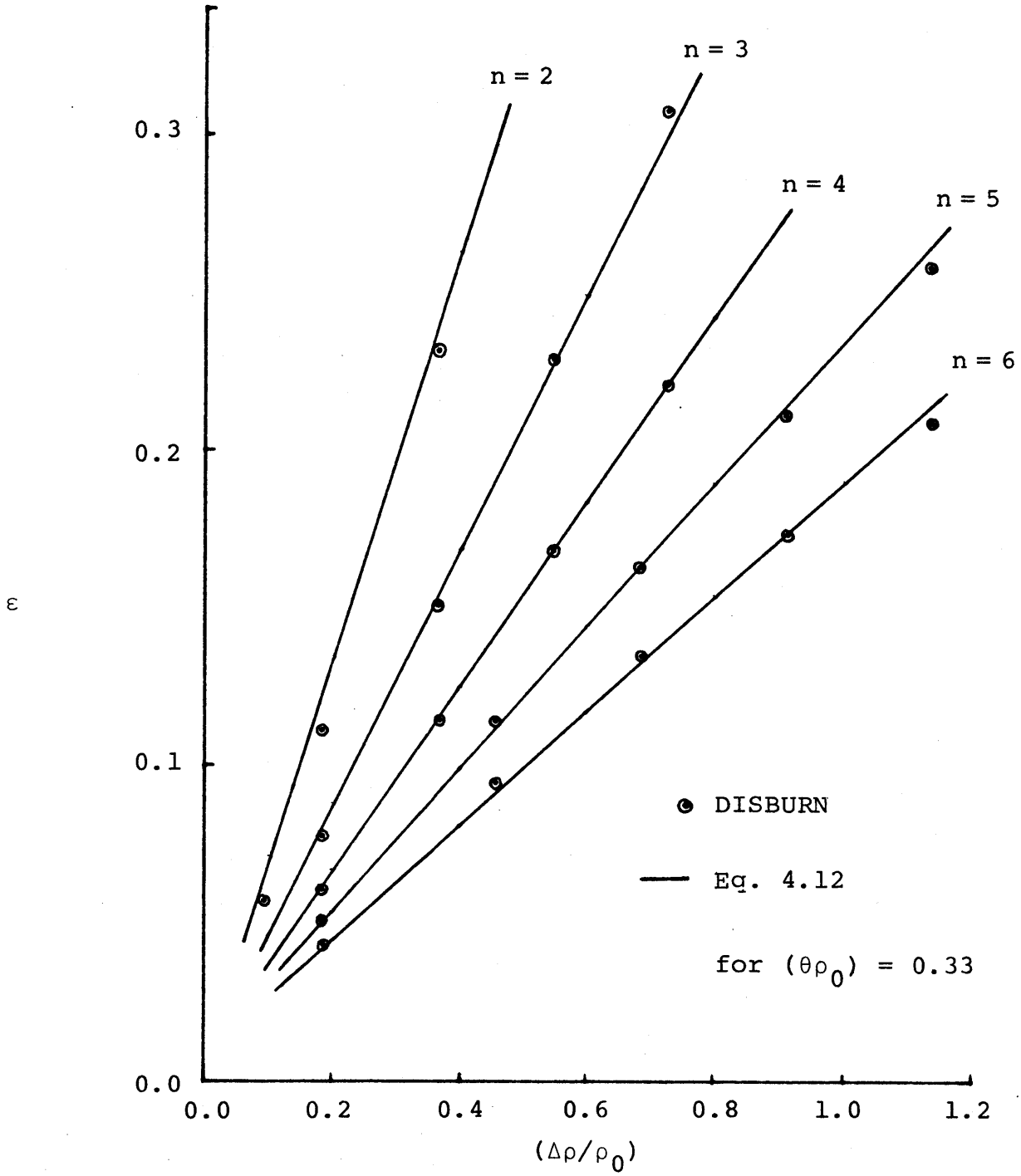

Fig. 4.14 ε as a Function of $(\Delta\rho/\rho_0)$ for the Case of Reactivity Control using Fixed Poison Shim or Leakage in Cycle 1 for Various Numbers of Batches

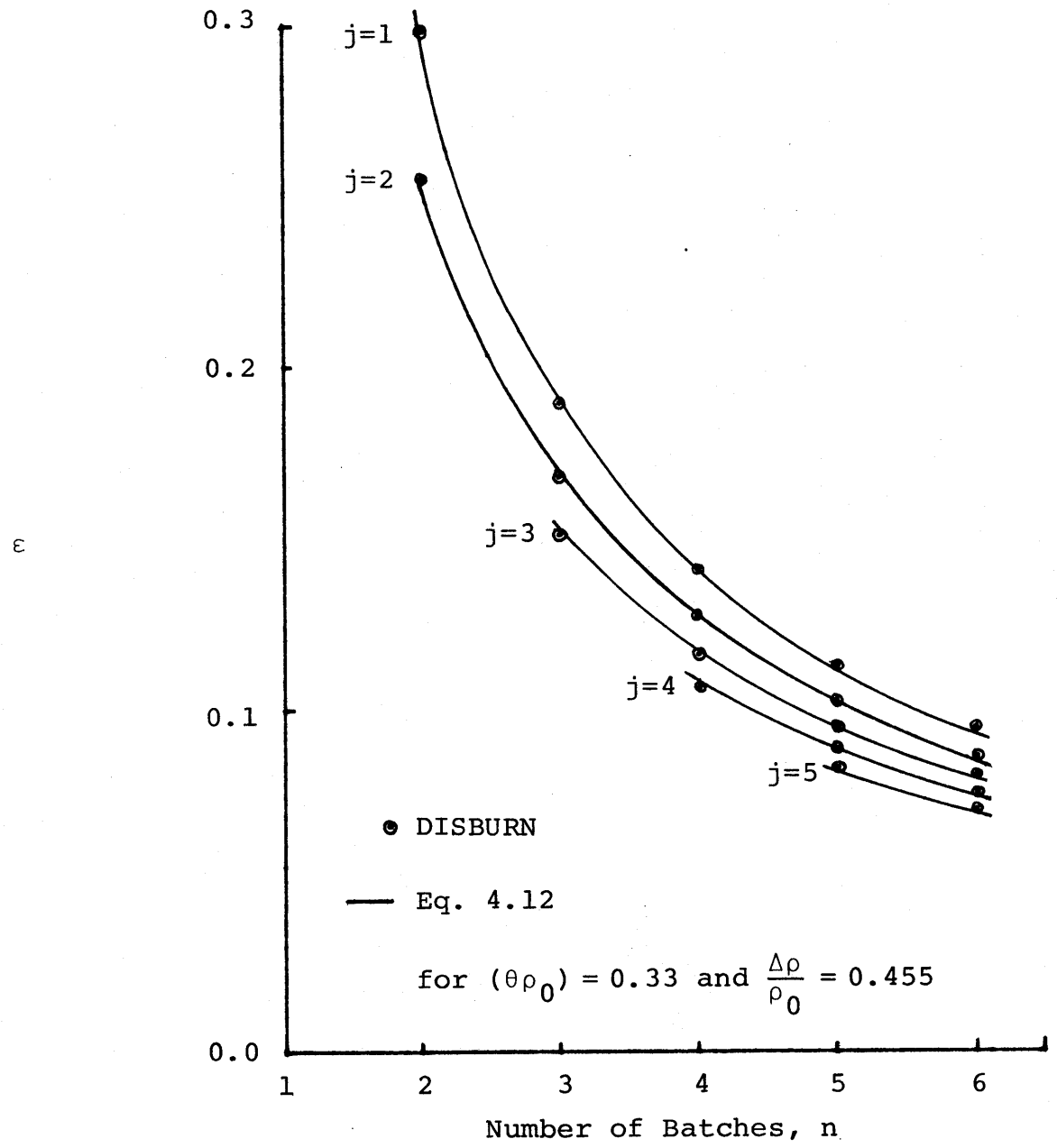

Fig. 4.15 ε as a Function of the Number of Batches for the Case of Reactivity Control by Using Fixed Poison Shim or Leakage in Cycle j

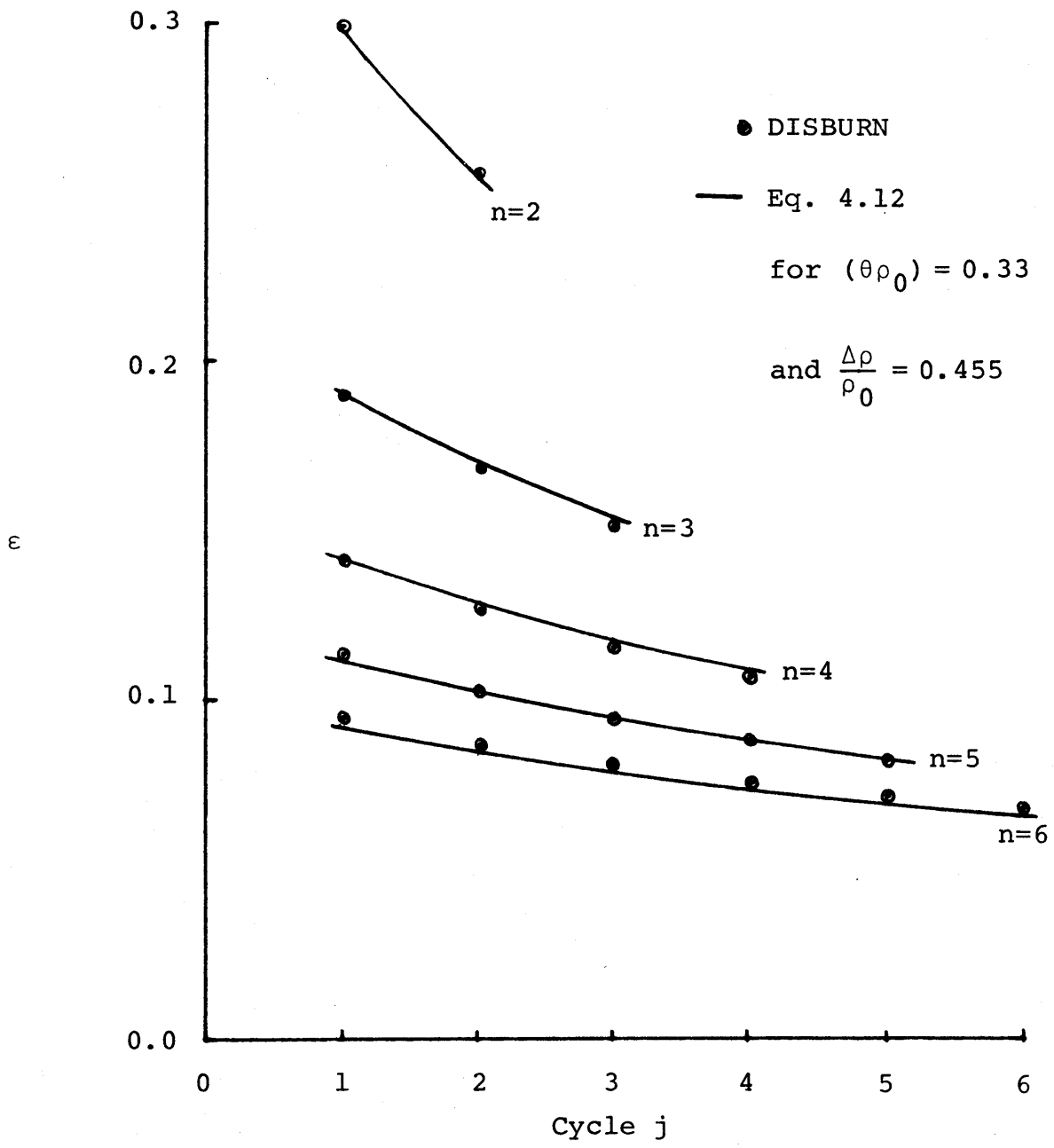

Fig. 4.16 ε as a Function of Cycle j for the Case of Reactivity Control Using Fixed Poison Shim or Leakage for Various Numbers of Batches

the results of these calculations. An empirical correlation for the ε factor was extracted from these results, and is given by

$$\varepsilon = \frac{(15.6-n)(6.8+n)R(\theta\rho_0)}{[(38n-25)+(2n+7)j]} + \frac{2(\theta\rho)^2(n-1)}{3(n+1)^2} \qquad (4.12)$$

where $R = (\Delta\rho / \rho_0)$, the ratio of the shim or leakage reactivity penalty to the initial extrapolated reactivity,

and $j = 1, 2, \ldots, n$.

When no fixed poison shim or leakage is present (i.e., $\Delta\rho = 0.0$), Eq. 4.12 reduces to the case of reactivity control by soluble poison only (i.e., a linear $\rho(B)$ assembly history—without burnable poison or leakage reactivity penalties)—the second term on the right hand side of Eq. 4.12 is the normalized ε factor of the soluble poison case.

We are now in a position to determine the ε factor and the corresponding discharge burnup for any situation involving fixed poison shim or leakage of neutrons from the core, using Eq. 4.12, given just the values of the parameters required in the equation.

4.4.4 SUPERPOSITION OF ANALYTICAL RESULTS

Although the analytical and empirical expressions for the ε factor obtained thus far permit us to calculate the the discharge burnups of a fuel batch with various reacti-

vity versus burnup trajectories; corresponding to individual elements of a fuel management scheme, their utility is still limited in that practical situations involve the combination of the different fuel management strategies—i.e., a reactor core may be operated using a low-leakage loading pattern with burnable poison being employed to suppress the reactivity of the fresh fuel over its first cycle. This and other combinations of fuel management strategies can be readily handled by the DISBURN code, as was demonstrated in the previous sections of this chapter. However, superposition of analytical results for the various individual schemes would, if verified as being sufficiently accurate, allow us to compute the discharge burnup resulting from a synthesis of a wide variety of fuel management tactics. This proposition was examined by considering the discharge burnup of the reference flat power case, B_0. For an individual fuel management scheme, designated subscript ℓ, the penalty or gain in the discharge burnup is given by

$$\Delta B_\ell = B_0 - B_{dis,\ell} \tag{4.13}$$

where $B_{dis,\ell}$ is the discharge burnup for the particular scheme.

Substituting Eq. 4.7 (i.e., in terms of the ε factor) for $B_{dis,\ell}$ into Eq. 4.13, we have

$$\Delta B_\ell = B_0 - \frac{B_0}{(1+\varepsilon_\ell)} = B_0 \left(\frac{\varepsilon_\ell}{1+\varepsilon_\ell}\right) \tag{4.14}$$

Note that the ε factor is a negative number if there is a gain in the discharge burnup.

If we have a combination of m fuel management schemes, the net discharge burnup penalty or gain is

$$\Delta B^m_{net} = \sum_{\ell=1}^{m} \Delta B_\ell$$

$$= B_0 \sum_{\ell=1}^{m} \left(\frac{\varepsilon_\ell}{1+\varepsilon_\ell}\right) \tag{4.15}$$

The corresponding discharge burnup for the synthesis of m of these schemes is (from Eq. 4.13) therefore,

$$B^m_{dis} = B_0 - \Delta B^m_{net} \tag{4.16}$$

Substituting ΔB^m_{net} from Eq. 4.15 into Eq. 4.16 yields

$$B^m_{dis} = B_0 - B_0 \sum_{\ell=1}^{m} \left(\frac{\varepsilon_\ell}{1+\varepsilon_\ell}\right)$$

$$= B_0 \left[1 - \sum_{\ell=1}^{m} \left(\frac{\varepsilon_\ell}{1+\varepsilon_\ell}\right) \right] \tag{4.17}$$

The discharge burnups for a number of combinations of individual fuel management strategies were calculated using the prescription given by Eq. 4.17. These results were compared

to those obtained using the DISBURN code. Tables 4.14 and 4.15 show the differences between the two sets of results. For these cases B_0 = 36184 MWD/MT; hence the total correction factors (bracketed term in Eq. 4.17) were in the range of 4.2 to 13.5%. It can be seen that the discharge burnups calculated using Eq. 4.17 are typically biased—running consistently about 1% less than those computed using the DISBURN code. Hence the relative accuracy case-to-case is very nearly perfect—a highly desirable situation because of the projected use of these relations for strategic comparisons. Considering the simplicity of the prescription developed from the superposition of the analytical expressions for the ε factors and the complexity of the problems involved, its agreement with the more accurate numerical method is rather satisfactory.

The use of superposition should permit evaluation of essentially all combinations of contemporary interest; should schemes be envisioned which cannot be handled in this manner, the DISBURN code can be used.

TABLE 4.14

COMPARISON OF DISCHARGE BURNUPS CALCULATED USING SUPERPOSITION WITH DISBURN RESULTS (BURNABLE POISON USED TO HOLD REACTIVITY IN CYCLE 1 TO A CONSTANT VALUE: LOW-LEAKAGE SCHEME)

Case	Discharge Burnup from Superposition of Analytical Results (MWD/MT)	Discharge Burnup from the DISBURN Code (MWD/MT)	Difference (%)
1. Fixed Poison Shim or leakage in Cycle 2			
1(a) Shim Poison $\Delta\rho$ = 4%	34099	34447	1.0
1(b) Shim Poison $\Delta\rho$ = 10%	31315	31551	0.7
2. Fixed Poison Shim or leakage in Cycle 3			
2(a) Shim Poison $\Delta\rho$ = 3.5%	34537	34874	1.0
2(b) Shim Poison $\Delta\rho$ = 8.0%	32560	32869	0.9

TABLE 4.15

COMPARISON OF DISCHARGE BURNUPS CALCULATED USING SUPERPOSITION WITH DISBURN RESULTS (BURNABLE POISON USED TO TAILOR THE REACTIVITY IN CYCLE 1 TO INCREASE LINEARLY FROM AN INITIAL VALUE OF ZERO)

Case	Discharge Burnup from Superposition of Analytical Results (MWD/MT)	Discharge Burnup from the DISBURN Code (MWD/MT)	Difference (%)
1. Fixed Poison Shim or leakage in Cycle 2			
1(a) Shim Poison $\Delta\rho$ = 4.0%	34672	35025	1.0
1(b) Shim Poison $\Delta\rho$ = 6.0%	33690	34011	0.9
2. Fixed Poison Shim or leakage in Cycle 3			
2(a) Shim Poison $\Delta\rho$ = 5.0%	34425	34759	1.0
2(b) Shim Poison $\Delta\rho$ = 8.0%	33133	33416	0.8

4.5 SOME ELEMENTARY ECONOMIC CONSIDERATIONS

It was pointed out earlier in this chapter that, in addition to benefiting the moderator temperature coefficient of reactivity, the use of burnable poison in the low-leakage fuel management scheme reduces the global radial power peaking factor. Since a nuclear plant must be operated subject to certain thermal constraints, this reduction in the global radial power peaking by means of burnable poison is beneficial with respect to the plant thermodynamic efficiency, its capacity factor and thus the overall economics of the facility.

An approach has been developed to characterize the effects of the thermal limits on the various cost components (e.g., the busbar cost and the system cost) and subsequently, to measure the impact of the global radial power flattening benefits due to the use of burnable poison. In what follows, the economic penalty of system derating will be computed. It is clear that the plant designers/operators would not actually tolerate such penalties, but would take steps to mitigate them. Hence the results developed here should be interpreted as "breakeven avoidance cost": the amount which could be spent on mitigation.

The fuel cycle cost, e_f, the busbar cost, e_b, and the system cost, e_s, are related as follows:

$$e_f = \frac{C}{\eta B} \tag{4.18}$$

$$e_b = \frac{A}{L} + e_f \tag{4.19}$$

$$e_s = e_b L + (1-L)e_r \tag{4.20}$$

where C and A are parameters proportional to fuel and capital costs, respectively, and

η = plant thermodynamic efficiency

B = discharge burnup

L = plant capacity factor

e_r = cost of replacement electricity

For small changes from a reference design, assuming for present purposes that A and C remain unchanged, the following relations hold, to first order:

$$\Delta e_f \simeq \frac{\partial e_f}{\partial \eta} \cdot \Delta\eta + \frac{\partial e_f}{\partial B} \cdot \Delta B \tag{4.21}$$

$$\Delta e_b \simeq \frac{\partial e_b}{\partial L} \cdot \Delta L + \frac{\partial e_b}{\partial e_f} \Delta e_f \tag{4.22}$$

$$\Delta e_s \simeq \frac{\partial e_s}{\partial e_b} \Delta e_b + \frac{\partial e_s}{\partial L} \cdot \Delta L \tag{4.23}$$

The partial derivatives can be calculated given appropriate constraints. The two constraints that have been considered are:

CONSTRAINT (1): Coolant exit enthalpy (temperature)

is limiting. Thus, increased assembly power requires a reduction in exit enthalpy (i.e., a decrease in the mean core exit temperature) with a corresponding decrease in plant efficiency.

CONSTRAINT (2): Local temperature or power peaking are limiting. This requires power level derating at constant thermal dynamic efficiency.

For constraint (1) we have the following relationship between the plant capacity factor, L, and the efficiency, η:

$$\frac{L}{\eta} = \frac{L_0}{\eta_0} \tag{4.24}$$

where the subscript "0" refers to the reference case. For constraint (2), since the efficiency is unchanged, the effect on the capacity factor is directly through the thermal power production:

$$\frac{\Delta L}{L} = \left(\frac{\Delta Q}{Q}\right)_{\text{thermal}} = -\frac{\Delta F}{F} \tag{4.25}$$

where Q is the thermal power and F the radial power peaking factor. Equations 4.24 and 4.25 have been used in conjunction with Eqs. 4.18 through 4.23 to evaluate the relative changes in fuel cycle, busbar, and system costs under the two limiting

constraints. The final expressions are as follows:

CONSTRAINT (1): Exit enthalpy is limiting.

$$\left(\frac{\Delta e_f}{e_f}\right)_1 = -\frac{\Delta\eta}{\eta} - \frac{\Delta B}{B} \tag{4.26}$$

$$\left(\frac{\Delta e_b}{e_b}\right)_1 = -\frac{\Delta\eta}{\eta} - \left(\frac{e_f}{e_b}\right)\frac{\Delta B}{B} \tag{4.27}$$

$$\left(\frac{\Delta e_s}{e_s}\right)_1 = -\frac{e_r L}{e_s}\frac{\Delta\eta}{\eta} - \frac{e_f L}{e_s}\frac{\Delta B}{B} \tag{4.28}$$

CONSTRAINT (2): Local temperature or power peaking are limiting.

$$\left(\frac{\Delta e_f}{e_f}\right)_2 = -\frac{\Delta B}{B} \tag{4.29}$$

$$\left(\frac{\Delta e_b}{e_b}\right)_2 = +\left(1 - \frac{e_f}{e_b}\right)\frac{\Delta F}{F} - \frac{e_f}{e_b}\frac{\Delta B}{B} \tag{4.30}$$

$$\left(\frac{\Delta e_s}{e_s}\right)_2 = +\frac{L(e_r - e_f)}{e_s}\frac{\Delta F}{F} - \frac{e_f}{e_s}\cdot\frac{\Delta B}{B} \tag{4.31}$$

The change in radial power factors and discharge burnups between a reference case and a modified design can be evaluated using the DISBURN code, and the change in efficiency from an expression such as

$$\eta \simeq 1 - \frac{T_c}{T}(1 + u) \tag{4.32}$$

where T_c = mean condenser temperature (assumed constant)

T = mixed mean core exit temperature

u = unavailability (assumed constant)

Again letting the subscript "0" represent the reference (current 3-batch, out-in fuel management) case and subscript "1" the new fuel management scheme, the change in thermodynamic efficiency from the reference case can be obtained from Eq. 4.32:

$$\frac{\Delta\eta}{\eta_0} = \frac{\eta_1 - \eta_0}{\eta_0}$$

$$= -\frac{(1-\eta_0)}{\eta_0}\,\frac{(T_0 - T_1)}{T_1}$$

$$= -\frac{(1-\eta_0)}{\eta_0}\,\frac{(\Delta T)}{T_1} \qquad (4.33)$$

where T_0, T_1 = the mixed mean core exit temperatures of the reference and the new scheme, respectively

ΔT = core exit temperature degradation due to radial power peaking in the new scheme.

Assuming that the inlet core temperatures of both cases have the same constant value, we can write:

$$F_0(T_0 - T_{in}) = F_1(T_1 - T_{in}) \qquad (4.34)$$

where F_0, F_1 = the radial peak/average power ratio of the reference and the new fuel management scheme, respectively

T_{in} = the inlet core temperature of both designs.

Substituting T_1 from Eq. 4.34 into Eq. 4.33, the change in thermodynamic efficiency from the reference case can be expressed in terms of $\Delta F = F_1 - F_0$, and the parameters associated with the reference case, to give:

$$\frac{\Delta\eta}{\eta_0} = - \frac{(1 - \eta_0)}{\eta_0} \left[\frac{\Delta F (T_0 - T_{in})}{\Delta F T_{in} + F_0 T_0} \right] \tag{4.35}$$

The preceding analysis has been applied to evaluate the improvements in the fuel cycle cost, the busbar cost, and the system cost over the reference out-in fuel management scheme due to the implementation of the low-leakage fuel management strategy—in particular, we want to determine the effects of employing burnable poison (to suppress the reactivity of fresh fuel) in the low-leakage scheme, on the fuel cycle, the busbar, and the system cost of the plant. The low-leakage fuel management scheme has been analyzed in an earlier section of this chapter, and Table 4.16 summarizes the results of the analyses. The relevant parameters for the reference base case (current, 3-batch out-in scheme) employed in the cost evaluations are shown in Table 4.17, and Table 4.18 gives the results of the evaluations. Under constraint (1), the positive impact on the fuel cycle, busbar, and system cost due to

TABLE 4.16

BURNUP AND POWER PEAKING CHARACTERISTICS OF LOW-LEAKAGE (IN-IN-OUT) FUEL MANAGEMENT

Case	Increase in Discharge Burnup over the Reference Out-In Scheme (%)	Relative Radial Power Peaking* Factor (BATCH AVERAGE)
Case with No Burnable Poison	3.00	1.15
Burnable Poison Cases:		
Constant Reactivity in Cycle 1 (Residual $\Delta\rho$ = 0.3%)	3.19	1.09
BOL Reactivity Value ρ_{BOL} = 0.02) (Residual $\Delta\rho$ = 0.49%)	3.62	1.05

*Reference Relative Radial Power Peaking Factor is 1.00.

TABLE 4.17

RELEVANT PARAMETERS FOR THE REFERENCE 3-BATCH, OUT-IN FUEL MANAGEMENT CASE USED IN COST CALCULATIONS

Item	Value
Fuel cycle cost, e_f	6.4 mills/kwhr
Busbar cost, e_b	40.0 mills/kwhr
Replacement energy cost, e_r	60.0 mills/kwhr
System cost, e_s	46.0 mills/kwhr
Capacity factor, L_0	0.7
Thermodynamic efficiency, η_0	0.33
Relative radial power peaking factor, F_0	1.00
Inlet core temperature, T_{in}	290°C
Mixed mean core exit temperature, T_0	319°C
Discharge Burnup	30,000 MWD/MT

TABLE 4.18

POTENTIAL CHANGES IN THE FUEL CYCLE, BUSBAR, AND SYSTEM COSTS DUE TO THE IMPLEMENTATION OF LOW-LEAKAGE (IN-IN-OUT) FUEL MANAGEMENT

	$\left(\frac{\Delta e_f}{e_f}\right)^*$ %	$\left(\frac{\Delta e_b}{e_b}\right)^*$ %	$\left(\frac{\Delta e_s}{e_s}\right)^*$ %
CONSTRAINT (1): EXIT ENTHALPY IS LIMITING.			
Case with No Burnable Poison	-1.7	0.8	0.9
Burnable Poison Cases:			
Constant Reactivity in Cycle 1 (Residual $\Delta\rho$ = 0.3%)	-2.4	0.3	0.4
BOL Reactivity Value ρ_{BOL} = 0.02 (Residual $\Delta\rho$ = 0.49%)	-3.1	-0.1	0.1
CONSTRAINT (2): LOCAL POWER PEAKING OR TEMPERATURE IS LIMITING.			
Case with No Burnable Poison	-3.0	-0.4	-0.3
Burnable Poison Cases:			
Constant Reactivity in Cycle 1 (Residual $\Delta\rho$ = 0.3%)	-3.2	-0.4	-0.4
BOL Reactivity Value ρ_{BOL} = 0.02 (Residual $\Delta\rho$ = 0.49%)	-3.6	-0.5	-0.5

*All increments are relative to use of the same fuel without burnable poison in a conventional out-in/scatter fuel management scheme. A negative value represents a savings.

the reduction of the global radial power peaking factor by means of burnable poison in the low-leakage scheme can be observed. Whereas under constraint (2), which requires thermal power reduction at constant thermodynamic efficiency, because power peaking is limiting, the impact of the burnable poison is less significant, but still beneficial.

Thus the use of burnable poison can be assessed in terms of avoidance costs. For purposes of comparison, note that:

- 1% in fuel cycle cost corresponds to roughly 10 $/kg HM in fuel fabrication costs, and
- 1% in busbar cost corresponds to roughly 2×10^6 $/yr in the cost of electricity.

On this basis one could afford to implement the use of burnable poison if it increased fuel assembly costs by as much as 5 to 10%. These estimates are only approximate, of course, and much more specific analyses should be done on a case-by-case basis.

4.6 CHAPTER SUMMARY

In this chapter, the DISBURN code was evaluated as a tool for computing the fuel discharge burnup for a given fuel management scheme. It was shown to predict the relative changes in the discharge burnup due to modifications in a reference design quite accurately, and not biased to any significant degree by the details of the method used to obtain the two most important free parameters of the model, i.e., the leakage coefficient, α, and the power sharing parameter, θ.

Analyses performed using the DISBURN code have indicated that proper shaping of the reactivity versus burnup trace of a fuel batch by means of burnable poison can improve the discharge burnup by as much as 3.5%; this value is reduced to roughly 1% when the anticipated residual poison reactivity penalty is also considered. When burnable poison is employed in conjunction with a low-leakage fuel management strategy and cycle length extension, the global radial power peaking factor of the core is significantly reduced. The avoidance costs of plant derating or efficiency degradation appear sufficient to cover the added expenses of poison use.

The overall improvement in the uranium utilization for the standard cycle length low-leakage fuel management scheme with the incorporation of burnable poison, and accounting for the anticipated residual poison reactivity penalty, was about 3.6%, while the corresponding uranium utilization increase for an extended cycle length low-leakage fuel management scheme was approximately 11.1% over the reference case.

Finally, the discharge burnups resulting from synthesis of a variety of fuel management strategies, calculated using superposition of analytical expressions for the ε factors for the various individual schemes, were found to be in good agreement with values obtained using the DISBURN code. Hence, quick scoping analyses can be performed using the analytical expressions for the ε factors developed in the present work.

CHAPTER 5

SUMMARY, CONCLUSIONS, AND RECOMMENDATIONS

5.1 INTRODUCTION

In recent years, considerable interest in the achievement of higher fuel burnup in light water reactors has been generated by a number of factors: a need for resource conservation due to the delay in the commercialization of nuclear fuel reprocessing and the development of breeder reactors, a desire by utilities to extend the cycle length of reactor operation in order to increase plant capacity factor and to improve the overall economics of their systems.

Recent M.I.T. work, including that reported here, has been concerned with the self-consistent evaluation of ways to facilitate the realization of high burnup and improved neutron economy. An important part of the present effort is the development and improvement of a simple model which has a sound theoretical basis and is capable of evaluating the effects of small changes in core design and fuel management schemes on a consistent basis. Another major focus of the present work has been on the development of an optimum strategy for the use of a generalized burnable poison to alleviate the power peaking which typically characterizes higher burnup assembly designs and core arrangements, and in the process further improve the discharge burnup of a fuel batch through the shaping of its power history profile.

The work described in this report was undertaken as part of the D.O.E.'s LWR Technology Program for Improved Uranium Utilization.

5.2 THE LINEAR REACTIVITY MODEL

The linear reactivity model (LRM) is based on the observation that the reactivity, ρ, of a PWR fuel lattice varies linearly with burnup within the current range of interest with respect to fuel lattice parameters. As a point of interest, we also found that the LRM methodology is applicable to other fuel types (combinations of other fissile and fertile isotopes such as U-233, Pu-239, Pu-241 and Th-232), since quite linear $\rho(B)$ traces are also observed for these lattices (with the exception of Pu/Th-232 lattice: see Figs. 5.1 and 5.2).

To analyze fuel management strategies of contemporary interest, two important features which reflect the actual behavior of PWR cores were incorporated into the methodology. The first was the appropriate algorithm for the combination of the reactivity of fuel batches in a core—a power-reactivity weighting scheme; the system reactivity is thus given by

$$\rho_{sys} = \sum_{i=1}^{n} f_i \rho_i \qquad (5.1)$$

The discharge burnup of the fuel batch can be obtained by performing a reactivity balance for an n-batch, steady-state core:

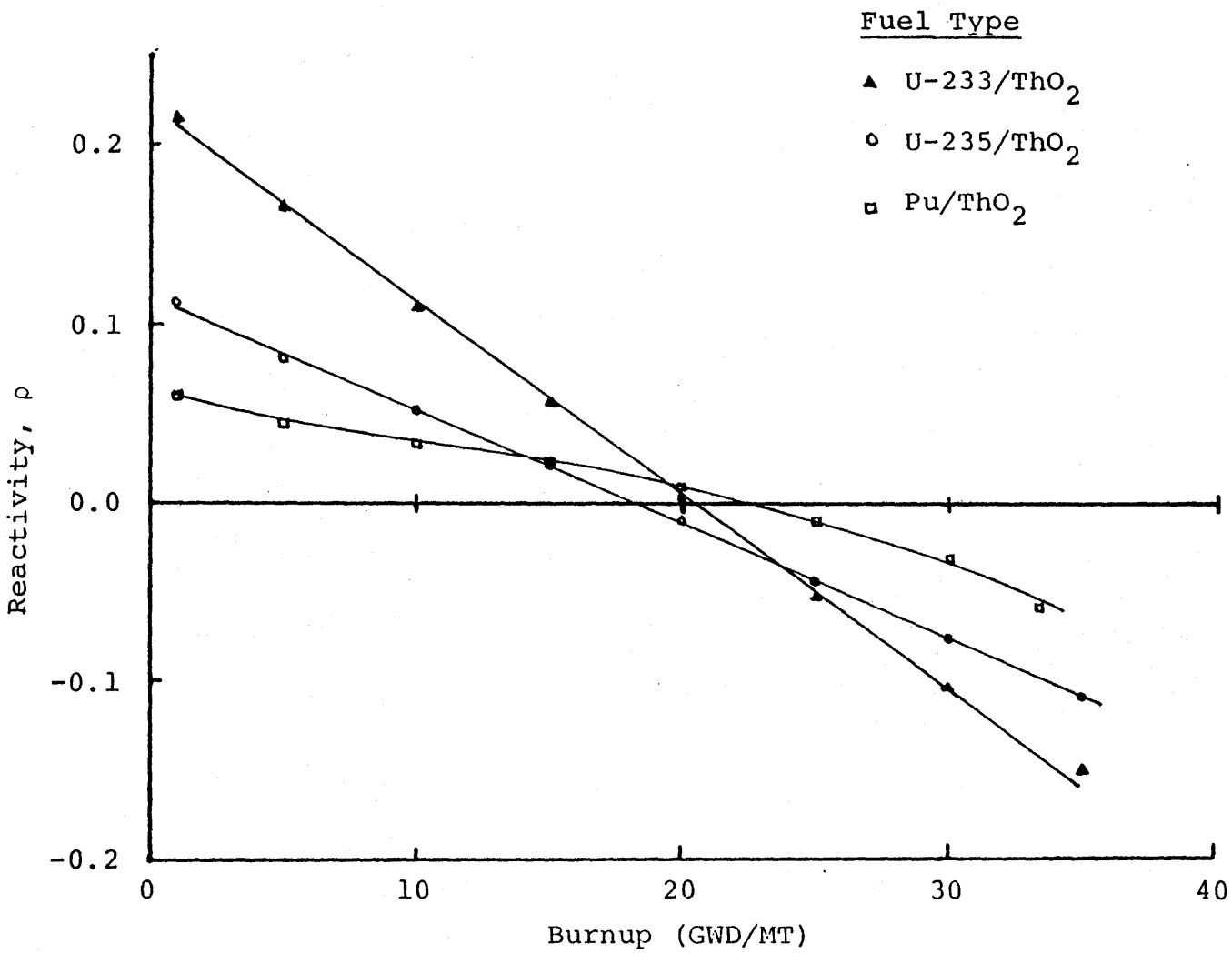

Fig. 5.1 Reactivity versus Burnup for Various Fissile Materials in ThO_2

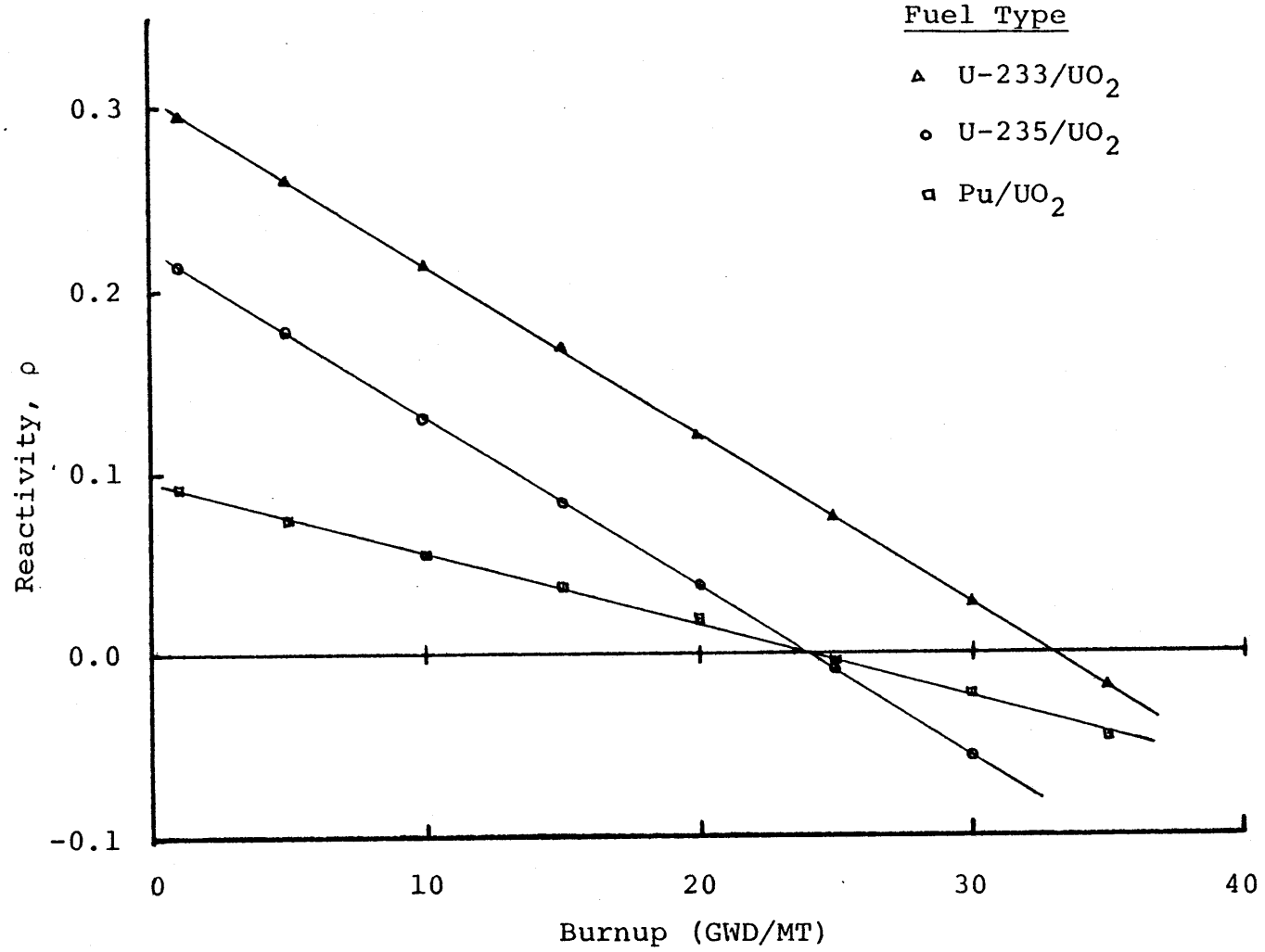

Fig. 5.2 Reactivity versus Burnup for Various Fissile Materials in UO_2

$$\rho_1 = \rho_0 - AB_{dis}\bar{f}_1$$

$$\rho_2 = \rho_0 - AB_{dis}(\bar{f}_1 + \bar{f}_2)$$

$$\vdots$$

$$\rho_n = \rho_0 - AB_{dis}(\bar{f}_1 + \bar{f}_2 + \ldots + \bar{f}_n) \qquad (5.2)$$

where ρ_0 is the extrapolated beginning-of-life reactivity

A is the slope of the linear $\rho(B)$ curve, MT/MWD

B_{dis} is the discharge burnup, MWD/MT

and assuming that the batch i cycle burnup is proportional to its average power level $\bar{f}_i$. At end-of-cycle (reactivity-limited condition), and with thermal power fraction f_i at EOC, one will have

$$B_{dis} = \frac{\rho_0}{A\left[\sum_{i=1}^{n}\sum_{j=1}^{i} f_i\bar{f}_j\right]} \qquad (5.3)$$

The second feature introduced into the methodology accounts for neutron leakage from a core. The effect of leakage on the system's reactivity is given by

$$\rho_{sys} = \sum_{i=1}^{n} f_i\rho_i - \rho_L \qquad (5.4)$$

where the reactivity associated with leakage is defined as:

$$\rho_L = \frac{A_{ex\text{-}core}}{\sum_{i=1}^{n} \nu F_i} \tag{5.5}$$

with $A_{ex\text{-}core}$ = neutron absorption rate in the ex-core region

$\sum_{i=1}^{n} \nu F_i$ = total neutron production rate in the core

The corresponding discharge burnup is thus,

$$B_{dis} = \frac{\rho_0 - \rho_L}{A\left[\sum_{i=1}^{n} \sum_{j=1}^{i} f_i \bar{f}_j\right]} \tag{5.6}$$

The leakage effect was found to be most prominent within the last few migration lengths of the core periphery, and it was found that the radial leakage reactivity can be correlated with the peripheral assemblies' power:

$$\rho_L = \alpha f_{per} \tag{5.7}$$

where f_{per} is the peripheral power fraction

and α is the leakage coefficient, a constant.

The remaining ingredient necessary for the implementation of the LRM methodology is a power sharing relationship for the fuel batches in a PWR core. This relation was derived using the "group-and-one-half" theory (which neglects thermal leakage):

Fast Group (>0.6 eV)

$$-D_1\nabla^2\phi_1 + \Sigma_{a1}\phi_1 + \Sigma_{12}\phi_1 - \frac{1}{k}(\nu\Sigma_{f1}\phi_1 + \nu\Sigma_{f2}\phi_2) = 0 \qquad (5.8)$$

leakage; absorption; down-scatter; fission source

Thermal Group

$$\Sigma_{a2}\phi_2 - \Sigma_{12}\phi_1 = 0 \qquad (5.9)$$

absorption; in-scatter

With the additional assumptions that the energy released per fission (κ), the migration area (M^2), and the fast diffusion coefficient (D_1) do not vary with position within the core, one obtains

$$f_i = \frac{(\frac{V_i}{V_s})(\frac{\overline{f}}{k_\infty})_s}{1 - \theta\rho_i} \qquad (5.10)$$

where $\theta = 1 + \frac{\gamma h^2}{M^2}$

h = size of the node (width of an assembly)

V_i/V_s = volume of the node/that of all the surrounding nodes

γ = constant

and subscripts 'i' and 's' denote the node and its surroundings, respectively.

For a fuel batch, in a critical core, we can use the form:

$$f_i \cong \frac{\bar{f}}{1 - \theta\rho_i} \tag{5.11}$$

where $\bar{f}$ is the average power fraction (equal to $\frac{1}{n}$ for an n-batch core). This power split relation was verified using data from whole core analyses. Figure 5.3 shows the plot for assemblies grouped into a batch in the Main Yankee Cycle 4 reload core design.

The power split relation was extended to include the peripheral batches/assemblies of a core through the leakage reactivity:

$$\rho_L = \alpha f_{per}$$

$$= \alpha \sum_{i=1}^{m} f_i \tag{5.12}$$

where $f_{per} = \sum_{i=1}^{m} f_i$ is the power fraction of the core's peripheral batches, m in number. At the EOC ($\rho_{sys} = 0.0$), we have

$$\underbrace{\sum_{i=1}^{n-m} f_i\rho_i}_{\substack{\text{Interior} \\ \text{batches}}} + \underbrace{\sum_{i=1}^{m} f_i(\rho_i - \alpha)}_{\substack{\text{Peripheral} \\ \text{batches}}} = 0 \tag{5.13}$$

The generalized power split equation which is compatible with Eq. 5.13 is,

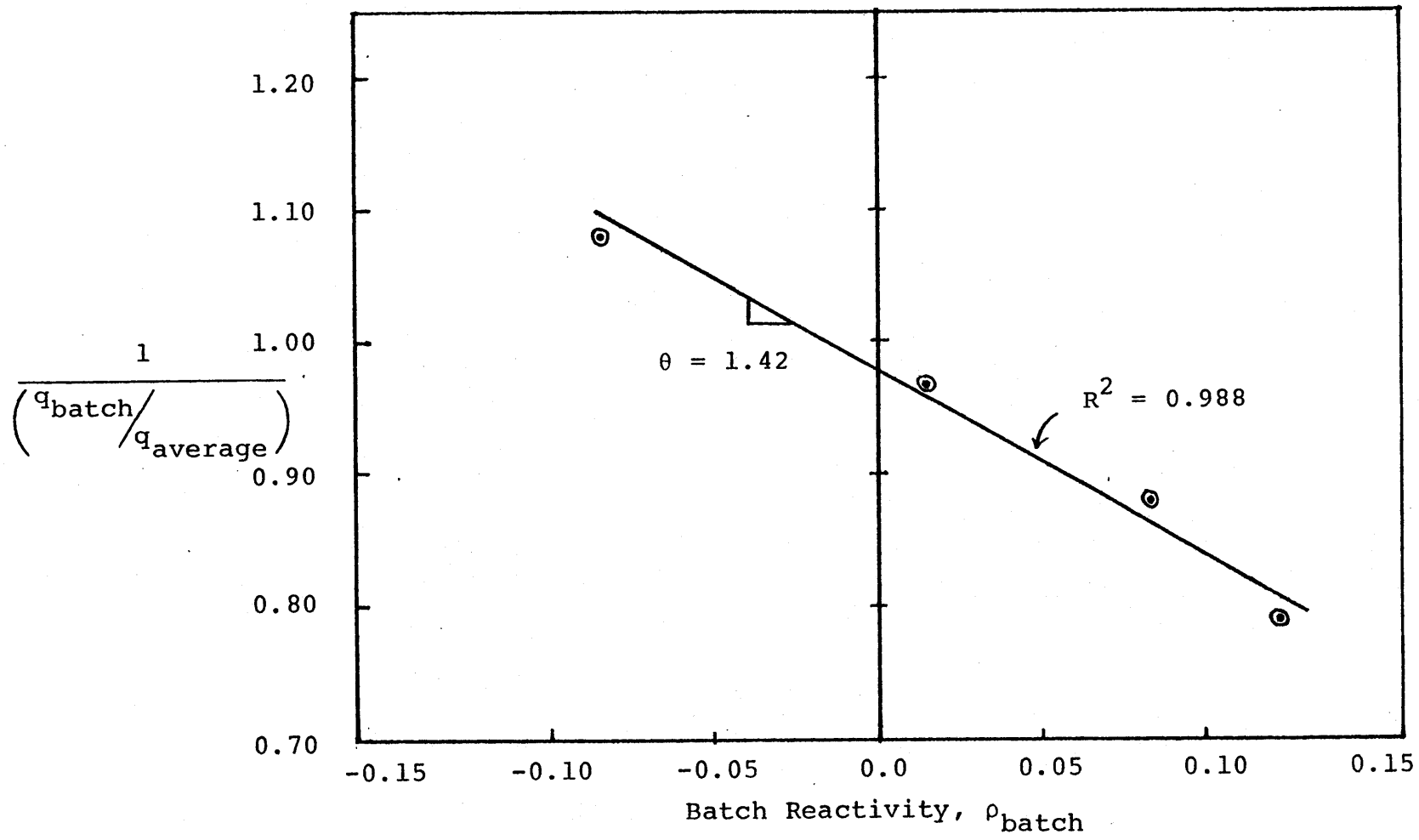

Fig. 5.3 Regression Line of Power vs. Reactivity for Main Yankee Fuel Batches

$$f_i = \frac{\bar{f}}{1 - \theta(\rho_i - \alpha)} \tag{5.14}$$

where $\alpha = \begin{cases} \alpha \text{ for peripheral batches} \\ 0 \text{ for interior batches} \end{cases}$

One of the important constraints which the generalized power split equation satisfies is the summation of batch power fraction to unity,

$$\sum_{i=1}^{n} f_i = 1 \tag{5.15}$$

5.3 THE DISBURN CODE

The LRM methodology has been sufficiently developed to permit the accurate computation of the discharge burnup for various cases of fuel management strategies of contemporary interest. An automated procedure has been developed, and a computer code called DISBURN (for Discharge Burnup) programmed to facilitate its application. Table 5.1 gives a summary of the main features of the code, and the algorithms employed in DISBURN are illustrated by the flow chart in Fig. 5.4.

The code was applied to evaluate a five-batch, extended burnup, 'out-in' fuel management scheme and a comparable 'low-leakage' fuel management strategy for the C-E System-80 reference design [M-1]. The two key parameters essential for the analyses (the power split parameter, θ, and the leakage coef-

TABLE 5.1

PRINCIPAL FEATURES OF THE DISBURN CODE

Item	Comment
1. Linear reactivity vs. burnup curve only.	Can easily be adapted to accommodate non-linear $\rho(B)$ traces.
2. Power-weighted reactivity averaging is used.	$\rho_{sys} = \sum_{i=1}^{n} f_i \rho_i$
3. Effect of peripheral leakage is accounted for through a reactivity-power correlation.	$\rho_L = \alpha f_{per} = \alpha \sum_{i=1}^{m} f_i$ m denotes peripheral batches $\therefore \rho_{sys} = \sum_{i=1}^{n-m} f_i \rho_i + \sum_{i=1}^{m} f_i (\rho_i - \alpha)$ interior batches; peripheral batches
4. Batches can be apportioned between core interior and periphery.	User specifies fraction of batch i in core interior ($F_{int,i}$) and core periphery ($F_{per,i}$). $F_{int,i} + F_{per,i} = 1$
5. Interior batch power is computed using the power split equation.	$f_{int,i} = \frac{(F_{int,i})(\frac{1}{1-\theta\rho_i})}{\sum_{i=1}^{n} f_i}$
6. Peripheral batch power is computed using a modified power split equation.	$f_{per,i} = \frac{(F_{per,i})[\frac{1}{1-\theta(\rho_i-\alpha)}]}{\sum_{i=1}^{n} f_i}$ where $f_i = f_{int,i} + f_{per,i}$ (i.e., sum in denominator includes all assemblies in batch i).

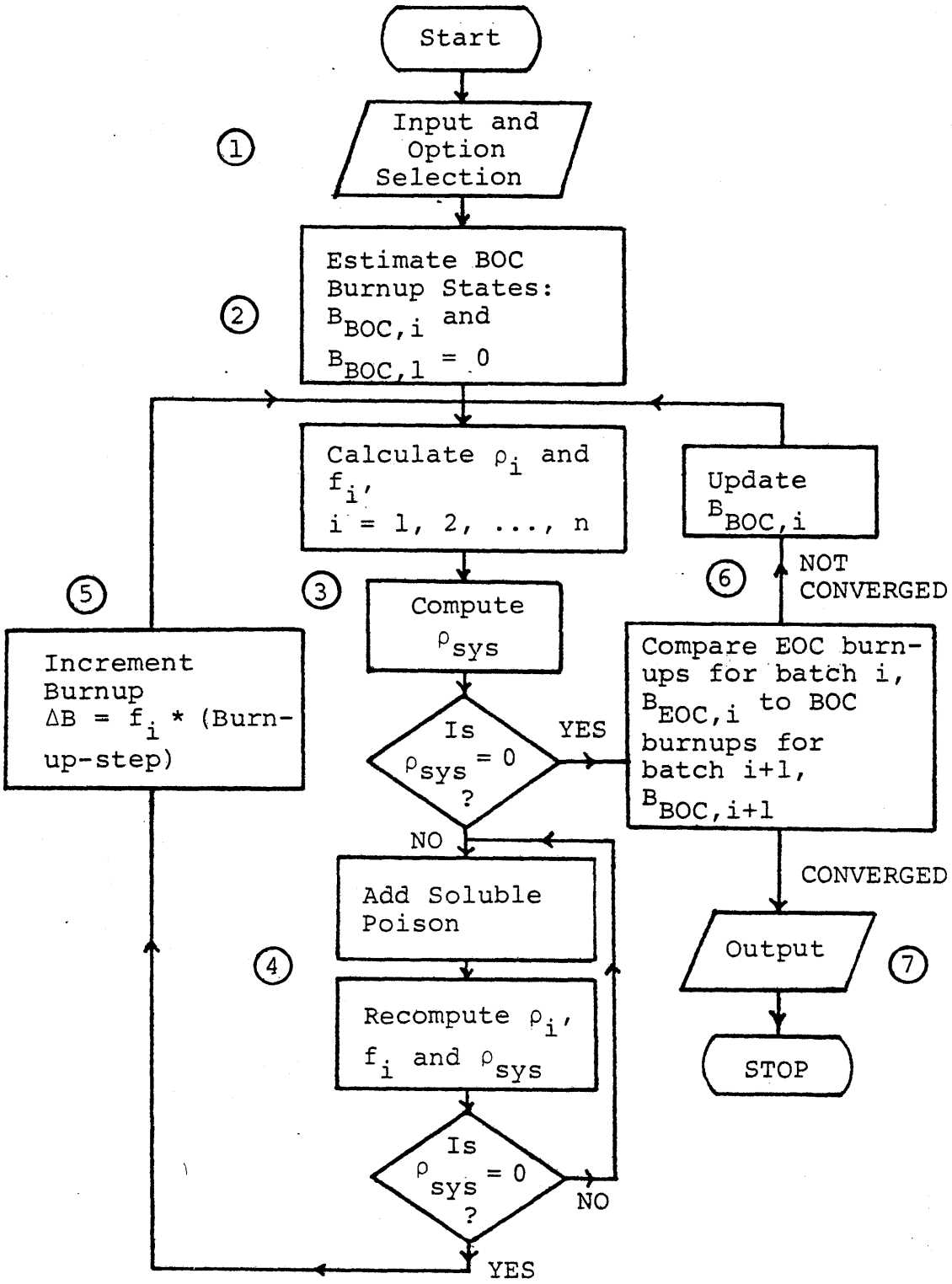

Fig. 5.4 Flowchart for DISBURN Computations

ficient, α) were derived from data published in Ref. [M-1]. The analyses revealed that the difference between the two fuel management strategies and between the DISBURN and C-E results are quite insensitive to both theta and α, and the overall agreement between the two sets of results is good, considering the complexity of the problem involved.

5.4 ANALYSES OF DIFFERENT FUEL MANAGEMENT STRATEGIES

The DISBURN code was employed to evaluate separate fuel management schemes of contemporary interest such as the use of burnable poison to shape the power history profile, the use of low-leakage fuel loading patterns, etc. The analyses were also extended to include combinations of these schemes.

5.4.1 BURNABLE POISON

It is shown in the present work that the use of burnable poison in the fresh reload fuel batch in a low-leakage fuel loading can lead to a slight increase in the fuel discharge burnup (in addition to benefiting the moderator temperature coefficient of reactivity and suppressing the power density in the fuel) through the shaping of the cycle-by-cycle power history profile of the fuel batch. Two cases of interest were considered: in the first, the as-poisoned reactivity value in the first cycle was taken to be constant, and in the second, the reactivity in the first cycle was tailored to increase linearly from a BOL value $\rho_{BOL} = 0.0$, until it reaches the EOC point, where it burns out completely. Neglecting, for the

moment, the leakage effect and the presence of any residual poison, an increase of about 2% and 3.5% in the discharge burnup can be realized for the constant Cycle 1 reactivity case and the $\rho_{BOL} = 0.0$ case, respectively. However, when the anticipated residual poison reactivity penalties were taken into account, the net increase in the discharge burnup for both cases was only about 1%.

5.4.2 LOW-LEAKAGE FUEL MANAGEMENT

It was found that low-leakage fuel management (an In-In-Out scheme) for a representative core (3-batch fuel management) improves steady state discharge burnup (hence uranium utlization) by about 3%. When burnable poison was incorporated in the fresh reload fuel batch in this fuel management scheme, and when the anticipated residual poison reactivity penalty is accounted for, the discharge burnup was increased by a further 0.6%. However, the major benefit in the employment of burnable poison in the fresh fuel batch in the low-leakage fuel management scheme, was the significant reduction ($\sim$10%) of the global radial (batch average) power peaking factor. This factor would have otherwise affected the overall plant economics negatively.

5.4.3 EXTENDED CYCLE LENGTH/BURNUP

The use of extended cycle, out-in/scatter fuel management results in a 6.8% improvement in uranium utilization over the out-in/scatter fuel management scheme common in current prac-

tice. When the extended cycle design is instead operated in a low-leakage configuration, an increase of 9.7% in uranium utilization was obtained. When burnable poison was incorporated in the low-leakage fuel management scheme, and with the appropriate residual poison reactivity penalty taken into account, a uranium utilization improvement of about 11% was realized. However, it must again be noted that a more important consequence of the use of burnable poison in this situation is the supression of the global radial power peaking factor by as much as 10%.

5.5 ANALYTICAL MODELS FOR DISCHARGE BURNUP

Analytical models were developed to calculate the fuel discharge burnup for several common fuel management tactics based upon the LRM methodology. To facilitate the derivation of the discharge burnup equations for different power history profiles, a linearized version of the power split equation (which fits core map data equally well) was employed:

$$f_{batch} = \bar{f}(1 + \theta\rho_{batch}) \tag{5.16}$$

After considerable algebra, the discharge burnups for the different power history trajectories were cast in the form:

$$B = B_0 / (1 + \varepsilon) \tag{5.17}$$

where B_0 is the discharge burnup for the hypothetical flat

power case:

$$B_0 = \left(\frac{2n}{n+1}\right)\frac{\rho_0}{A}$$

in which n is the number of batches

ρ_0 is the extrapolated BOL reactivity

A is the slope of the linear $\rho(B)$ curve

and ε is the factor which corrects for the departure of discharge burnup from the flat power case.

In the particular case of when a fixed poison shim was included in a batch of fuel over a given cycle (mathematically equivalent to subjecting the same batch of fuel to a fixed leakage penalty—e.g., by placing the fuel batch on the core periphery), it was difficult to obtain an expression for the discharge burnup in a closed form. Thus an empirical correlation for the 'ε factor' was determined from numerical results. Table 5.2 shows the various power history trajectories and their corresponding ε factors. Figure 5.5 compares the analytical and DISBURN results for a case of particular interest: constant first cycle reactivity induced through the use of burnable poison.

Superposition of analytical results for the various individual schemes would, if verified as being sufficiently accurate, allow one to compute the discharge burnup resulting from a synthesis of a variety of fuel management strategies.

TABLE 5.2

ANALYTICAL RESULTS FOR COMMON REACTIVITY HISTORIES

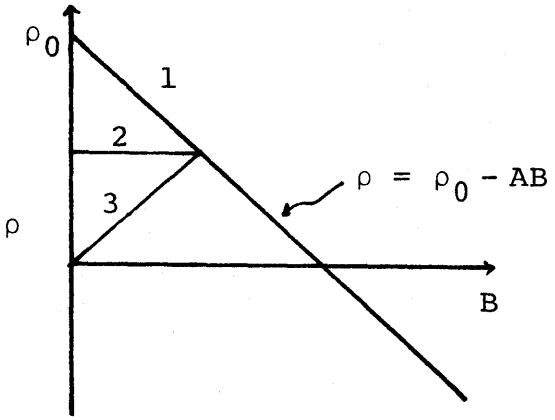

Burnable Poison in Reload Fuel

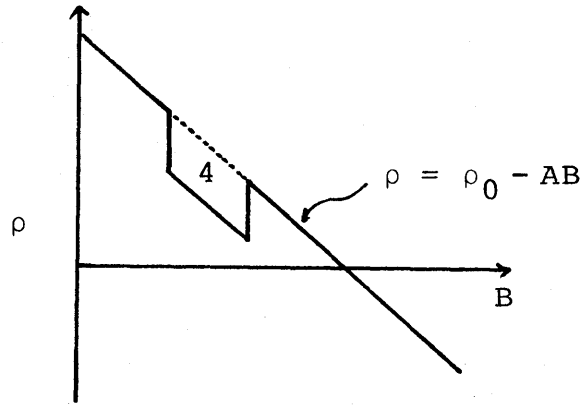

Shim or Peripheral Leakage in Cycle j

Case*	Prescription for ε
1. (no burnable poison)**	$2(\theta\rho_0)^2 \frac{(n-1)}{3(n+1)^2}$
2. (constant ρ in 1st Cycle)	$-(\theta\rho_0)\frac{(n-1)}{n(n+1)^2} + (\theta\rho_0)^2\frac{(n-1)^2}{3n(n+1)^2}$
3. (zero ρ at BOL)	$-(\theta\rho_0)\frac{(n-1)}{2n(n+1)} + (\theta\rho_0)^2\frac{(n-1)^2}{6n(n+1)^2}$
4. (shim or leakage in Cycle j)	$\frac{(15.6-n)(6.8+n)R(\theta\rho_0)}{[(38n-25)+(2n-7)j]} + 2(\theta\rho_0)^2\frac{(n-1)}{3(n+1)^2}$

where $R = \frac{\text{(shim or leakage reactivity penalty, } \Delta\rho)}{\rho_0}$

*Case number corresponds to those in the figure.

**Factor of 2 in prescription for ε is an empirical normalization.

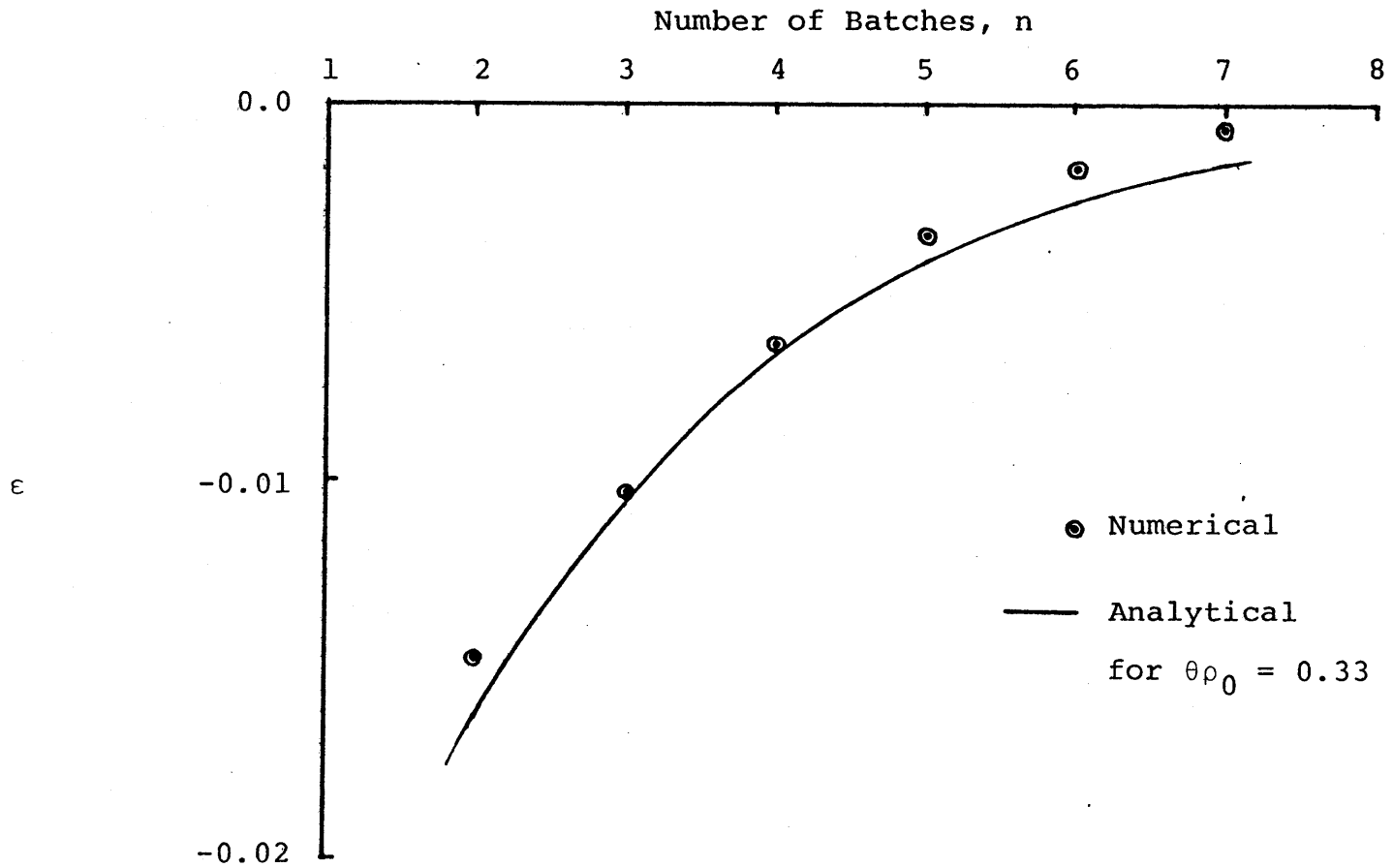

Fig. 5.5 ε as a Function of the Number of Batches, for the case of Constant Reactivity in the First Cycle

The discharge burnup for the synthesis of m of these schemes is given by

$$B_{dis}^{m} = B_0 \left[1 - \sum_{\ell=1}^{m} \left(\frac{\varepsilon_\ell}{1+\varepsilon_\ell} \right) \right] \tag{5.18}$$

For a number of combinations of individual fuel management strategies, the discharge burnups calculated using the prescription given by Eq. 5.18 were typically biased—running consistently about 1% less than those computed using the DISBURN code. Hence the relative accuracy case-to-case is extremely good—a highly desirable situation because of the projected use of these relations for strategic comparisons. Therefore, fast analyses for scoping purposes can be performed using the analytical expressions for the ε factors developed in the present work.

5.6 CONCLUSIONS

While a considerable investment of time and effort went into model development, the underlying objective of the present work remained the evaluation of the consequences of using burnable poison in PWRs on the uranium utilization. In this regard it was found that the use of burnable poison in conjunction with low-leakage fuel management can increase the discharge burnup by an additional 1%—that is over and above the gain due to the low-leakage nature of the fuel loading scheme. We can therefore conclude that the use of burnable poison does not penalize the discharge burnup (or the conse-

quent uranium utilization) despite nominal amounts of residual poison in the fuel batch.

5.7 RECOMMENDATIONS

The LRM methodology, with the incorporation of features such as the power weighting algorithm and a radial leakage correlation, permits one to compute accurately the discharge burnup of fuel for various cases of fuel management strategies of current interest. It is also capable of evaluating the effects of small changes in core design and fuel management tactics on a consistent basis. Although the present methodology utilizes a power split relation which has a sound theoretical basis (developed from a $1\frac{1}{2}$ group diffusion theory model) and the key features incorporated within it were thoroughly benchmarked against results generated with detailed state-of-the-art computer analyses, further improvements in the model can still be made, as follows:

1) A more detailed treatment of the peripheral fuel assemblies/batches should be investigated. In the present work, only the gross effects of leakage were correlated with the peripheral power fraction; finer effects such as the number of assembly faces exposed to the reflector, and the interaction of the peripheral batch with the next interior ring of fuel should be studied. These 'second order' effects may be important when one has quite different types of fuel on the core periphery, such as reconstituted assemblies having a different lattice pitch than the rest of the core, or thorium fueled blankets in a uranium core, and the like.

2) Although the generalized power split relation (Eq. 5.4) handles the interior and peripheral fuel batches rigorously in that important constraints were satisfied by the relation, the application of the equation at the core periphery needs to be examined in more detail, and, if necessary, modified to agree with the results generated using detailed state-of-the-art computer analyses. In particular, the most appropriate value of the parameter θ for peripheral assemblies may be different from the value applied to interior assemblies.

3) The relation of the power sharing algorithm used in the present work to those used in so-called nodal codes such as FLARE and its successors, should be further explored.

4) Efforts should be continued to develop a closed form analytic solution for the case of a fixed shim or leakage reactivity decrement in cycle j, to either substantiate or supplant the empirical expression arrived at by fitting numerical results in the present report.

5) The effect of the deliberate retention (or introduction) of some burnable poison in the second and subsequent burnup cycles should be studied to investigate the costs and benefits of such operations.

Finally, attention is called to the companion effort by A. Kamal [K-2], in which further substantiation of the linear reactivity model is documented, and in which a wide variety of additional applications of this methodology are discussed.

APPENDIX A

NON-LINEAR REACTIVITY VS. BURNUP DEPENDENCE

Although we have confirmed that reactivity varies very nearly linearly with burnup for PWR lattices, one can introduce even extreme non-linearity without much complication.

Let us assume a polynomial curve fit of the form:

$$\rho = \rho_o - A_1 B - A_2 B^2 - A_3 B^3 - A_4 B^4 - \ldots \qquad (A.1)$$

An end-of-cycle reactivity balance can be constructed; consider cycles of length B_c and an n-batch core:

newest batch $\quad \rho_o - A_1 \cdot B_c - A_2 B_c^2 - A_3 B_c^3 - A_4 B_c^4$

next batch $\quad \rho_o - A_1 \cdot 2\, B_c - A_2 (2B_c)^2 - A_3 (2B_c)^3 - A_4 (2B_c)^4$

.

.

.

oldest batch $\quad \rho_o - A_1 \cdot n\, B_c - A_2 (nB_c)^2 - A_3 (nB_c)^3 - A_4 (nB_c)^4$

$$\text{Sum} = 0 = n\rho_o - A_1 B_c \sum_{j=1}^{n} j - A_2 \cdot B_c^2 \sum_{j=1}^{n} j^2 - A_3 \cdot B_c^3 \cdot$$

$$\sum_{j=1}^{n} j^3 - A_4 \cdot B_c^4 \sum_{j=1}^{n} j^4$$

The required sums can be evaluated in closed form [M-4]:

$$\sum_{j=1}^{n} j = \frac{1}{2} n(n+1) \qquad \sum_{j=1}^{n} j^3 = \frac{1}{4} n^2 (n+1)^2$$

$$\sum_{j=1}^{n} j^2 = \frac{1}{6} n(n+1)(2n+1) \qquad \sum_{j=1}^{n} j^4 = \frac{1}{30} n(n+1)(2n+1)(3n^2+3n+1)$$

Thus our equation for cycle burnup becomes the polynomial:

$$B_c^4 + a B_c^3 + b B_c^2 + c B_c - d = 0 \qquad (A.2)$$

where

$$a = \frac{15n(n+1)}{2(2n+1)(3n^2+3n-1)} \left(\frac{A_3}{A_4}\right), \quad c = \frac{15}{(2n+1)(3n^2+3n-1)} \left(\frac{A_1}{A_4}\right)$$

$$b = \frac{5}{(3n^2+3n-1)} \left(\frac{A_2}{A_4}\right), \quad d = \frac{30\rho_o}{n(n+1)(2n+1)(3n^2+3n-1)A_4}$$

This equation can be solved for B_c, and discharge burnup $n \cdot B_c$, using numerical methods.

Note that the equation correctly reduces to two limiting cases:

(a) $n = 1$, single batch core, Eq. (A.2) becomes $\rho(B) = 0$, where $\rho(B)$ is given by Eq. (A.1)

(b) $n = \infty$, Eq. (A.2) yields the same result as would be obtained by setting the integral of Eq. (A.1) equal to zero, i.e.:

$$\int_o^B \rho(B)\, dB = 0$$

Finally, since one can sum <u>any</u> power of sequential integers, $\sum_{k=0}^{n} k^m$, (Eq. A.6) p. 58, of Ref. [M-4], a polynomial of arbitrarily high order could be used in lieu of Eq. (A.1), and therefore any non-pathological $\rho(B)$ curve could be fit and its implied cycle burnup computed.

Of particular interest here is the use of the above development to estimate the error in discharge burnup incurred by use of the linear approximation in the bulk of the present work.

Consider the reactivity-burnup data of a U-235/UO_2 (enrichment $\varepsilon \sim 3.0$w/o) supercell lattice generated by the LEOPARD program. A linear curve-fit (using the least squares method) to these data gives the following relation (for burn-up in MWD/MTHM):

$$\rho = \rho_o - AB \qquad (A.3)$$

with $\rho_o = 0.223508$

$A = 9.27205 \times 10^{-6}$

The same data fit to a quadratic yields:

$$\rho = \rho_o' - aB - bB^2 \qquad (A.4)$$

with $\rho_o' = 0.222936$

$a = 9.1728106 \times 10^{-6}$

$$b = 2.977847 \times 10^{-12}$$

For an n-batch core at steady state, the discharge burnup using the linear curve is

$$B_d = \left(\frac{2n}{n+1}\right) \frac{\rho_o}{A} \tag{A.5}$$

Whereas, the discharge burnup employing the quadratic curve is determined as follows. The EOC reactivity balance gives

$$0 = n\rho_o' - aB_c \sum_{j=1}^{n} j - bB_c^2 \sum_{j=1}^{n} j^2 \tag{A.6}$$

Rearranging Eq. (A.5) and substituting the sums by their evaluated forms, we have

$$\alpha B_c^2 + \beta B_c - \rho_o' = 0 \tag{A.7}$$

where $\alpha = \frac{b}{6}(n+1)(2n+1)$

and $\beta = \frac{a}{2}(n+1)$

Solving Eq. (A.6), and noting that $B_c > 0$, we have

$$B_c = \frac{-\beta + \sqrt{(\beta^2 + 4\alpha\rho_o')}}{2\alpha} \tag{A.8}$$

and the corresponding discharge burnup can then be calculated.

If we assume that the quadratic fit of the data is "exact," then the error in the discharge burnup incurred by the use of the linear model is given below (for different n):

n	B_d ("exact")	B_d (linear model)	% error
2	32126	32141	-0.05
3	36126	36158	-0.09
4	38525	38569	-0.11
5	40123	40176	-0.13

From these results, we conclude that the "error" in using the linear reactivity model is rather insignificant.

The worst case, with regard to the linearity of the $\rho(B)$ trace, encountered in this work is that of the Pu/ThO_2 system lattice (see Fig. 3.3 and Table 3.2). A third order polynomial fit to the corresponding data gives

$$\rho = \rho_o'' - a'B + b'B^2 - C'B^3 \qquad (A.9)$$

with $\rho_o'' = 0.060659$

$a' = 3.27659 \times 10^{-6}$

$b' = 7.69132 \times 10^{-11}$

$c' = 2.33005 \times 10^{-15}$

Again, performing the EOC reactivity balance, substituting the appropriate summations and rearranging the resulting

equation yields:

$$\alpha' B_c^3 - \beta' B_c^2 + \gamma' B_c - \rho_o'' = 0 \qquad \text{(A.10)}$$

where $\alpha' = \frac{c'n}{4}(n+1)^2$

$$\beta' = \frac{b'}{b}(n+1)(2n+1)$$

$$\gamma' = \frac{a'}{2}(n+1)$$

Equation A.10 can be solved readily using numerical methods. The results are given below:

n	B_c (MWD/MT)	B_d (MWD/MT)
2	14134	28268
3	10385	31155
4	8215	32860
5	6798	33990

A linear fit to the same set of data for the Pu/ThO_2 system lattice gives

$$\rho = \rho_o''' - A''' B$$

with $\rho_o''' = 0.06566$

$$A''' = 3.270 \times 10^{-6}$$

The corresponding discharge burnup can be computed using Eq. (A.5). The error in the discharge burnup incurred by the use of this linear approximation is given below:

n	B_d (3rd order fit), MWD/MT	B_d (linear model), MWD/MT	ΔB %
2	28268	26773	5.3
3	31155	30119	3.3
4	32860	32127	2.2
5	33990	33466	1.5

The results show that for small n, the use of the LRM to evaluate the discharge burnup of the Pu/Th_2O system is not adequate and therefore, a higher order ($\simeq$ 3) fit of the reactivity-burnup data and the method of calculating the discharge burnup discussed in this section, must be adopted. However, for higher values of n ($\simeq$ 5) the LRM may be employed. The accuracy of the LRM improves with n because as the number of EOC points at which $\rho(B)$ is sampled increases, the more one tends to have compensation between over and under-estimates of the true $\rho(B)$ and its linear approximation. Indeed one could improve the accuracy of the LRM for small n by restricting the curve fit to data points near the estimated EOC $\rho(B)$ values for batches 1, 2, ..., n.

APPENDIX B

REACTIVITY CONTROL USING BURNABLE POISON ONLY

A limiting case has been identified for assessment vis-à-vis burnable poison control, namely a core controlled entirely by burnable poison in the fresh fuel without the need for soluble poison. Although this approach will probably result in over-compensation as regards power suppression in fresh fuel, and may require a faster-than-practicable poison burn, it will serve to define the outer envelope for fuel management strategies.

Using the linear reactivity model of assembly behavior, the conceptual picture of this type of operation can be sketched on a $\rho(B)$ map as shown in Fig. B.1. The assembly without poison would follow the linear trace starting at ρ_o when B=0; with poison it would start at the (negative) reactivity value $\rho_{1,BOC}$, burn out completely and linearly in one cycle to $\rho_{1,EOC}$, then follow the unpoisoned trace to its discharge value at the end of n cycles, $\rho_{n,EOC}$.

One can show that $\rho_{1,BOC} = \rho_{n,EOC}$ as follows. We require that the power-weighted reactivity sum to zero at both BOC and EOC, thus:

$$\sum_{i=1}^{n} f_{i,BOC}\ \rho_{i,EOC} = \sum_{i=1}^{n} f_{i,EOC}\ \rho_{i,EOC} \qquad (B.1)$$

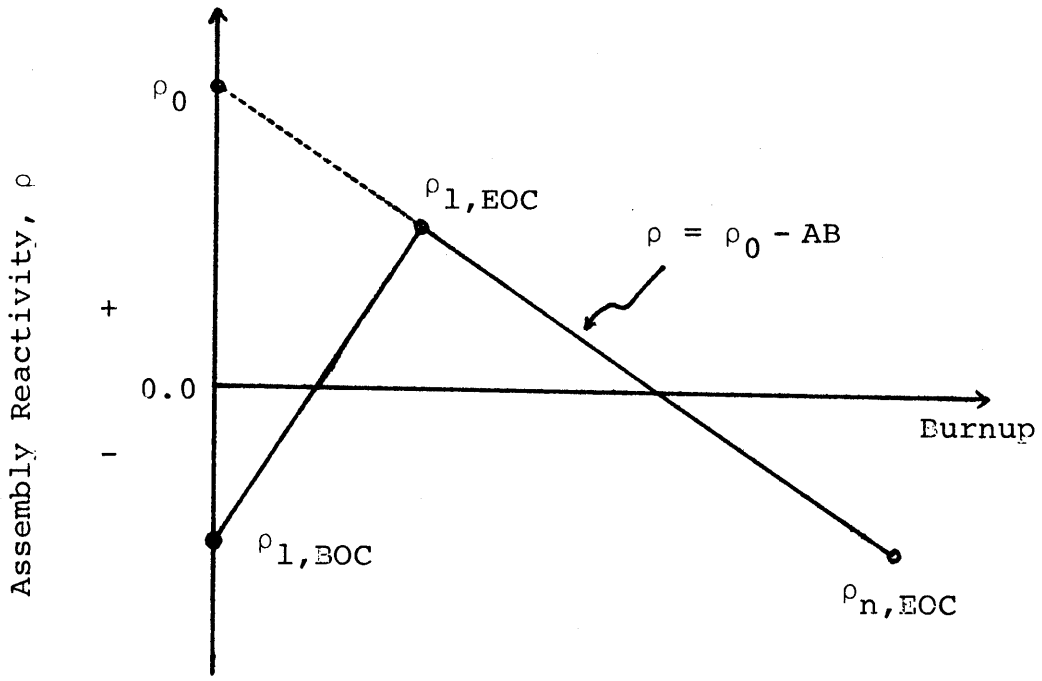

Fig. B.1 The Reactivity versus Burnup Trace for the Case of a Core Controlled Entirely by Burnable Poison

But since there is no soluble poison,

$$\rho_{i,EOC} = \rho_{i+1,BOC} \tag{B.2}$$

The power sharing prescription derived in chapter 3 is given by

$$f_i = \frac{\bar{f}}{1-\theta\,\rho_i} = \frac{1}{n}\left(\frac{1}{1-\theta\,\rho_i}\right) \tag{B.3}$$

Or f_i is a function only of ρ_i, since θ is a constant.

This means that in Eq. (B.1) all terms except the first on the LHS and the last on the RHS are identical (by Eq. B.2) and therefore cancel; the remaining terms yield directly;

$$\rho_{1,BOC} = \rho_{n,EOC} \tag{B.4}$$

In other words, the reload assembly has the same negative BOL reactivity (as poisoned) as it does when fully burned.

APPENDIX C

DISBURN CODE INPUT DESCRIPTION, LISTING, AND SAMPLE PROBLEM

C.1 CODE DESCRIPTION

The DISBURN (Discharge Burnup) code enables one to compute accurately, the discharge burnup for various cases of fuel management strategies of contemporary interest. The methodology employed in DISBURN is based on the linear reactivity model, and incorporates important features such as power-reactivity weighting and allowance for the effects of neutron leakage. The principal features of the DISBURN code and the algorithms employed in the code have been shown in Table 4.1 and Fig. 4.1 of Chapter 4.

The code is written in FORTRAN (see listing in Table C.2), but can easily be translated into the BASIC language for use with minicomputers. Although the present version of the code is written to be used in an interactive mode at a computer terminal, it can be run in a batch job mode by putting the input data on a separate data file and then appropriately defining the input data file. Table C.1 lists the instructions for input preparation.

The sample problem concerns the evaluation of the low-leakage fuel management scheme for the Maine Yankee reactor system (see Section 4.3.2 of Chapter 4). In this problem, burnable poison was used in the fresh reload fuel to tailor the reactivity in Cycle 1 to increase linearity from a value

of $\rho_{BOL} = 0.02$, and with no residual poison at the EOC. Table C.3 is a listing of the terminal session for the problem.

TABLE C.1

INPUT SPECIFICATIONS

Card Set 1 (one card)

J: number of batches

TSTEP: burnup-step size (MWD/MT)

CONVRG: convergence criterion (MWD/MT)

FORMAT (8x, I2, 2F10.5)

Card Set 2 (one card)

THETAI: interior batch θ value

THETAP: peripheral batch θ value

FORMAT (2F10.5)

Card Set 3 (one card

RHOINT: extrapolated BOL reactivity value for the linear $\rho(B)$ curve - ρ_0

A: slope of the linear $\rho(B)$ curve, $(MWD/MT)^{-1}$

FORMAT (F10.5, E10.5)

Card Set 4 (one card)

OPTION SPECIFIED BY 'N'

N=1: no burnable poison used

N=2: burnable poison used

FORMAT (3x, I2)

Card Set 5 (one card)

(used only when N=2, i.e., case with burnable poison)

TABLE C.1 (continued)

OPTION SPECIFIED BY 'NN'

NN=1: constant reactivity in Cycle 1

NN=2: sloping (i.e., ramp) reactivity in Cycle 1

FORMAT (3x, I2)

Card Set 6 (one card)

(used only when NN=1, i.e., constant reactivity in Cycle 1)

BI: enter estimated poison burnout point (PBP), MWD/MT, for EOC 1

FORMAT (F1.02)

Note: Code will optimize PBP to match EOC point.

Card Set 7 (one card)

(used only when NN=2, i.e., sloping reactivity in Cycle 1)

RHOLBOL: BOL reactivity value

BI: estimated poison burnout point (PBP), MWD/MT, for EOC 1

FORMAT (F1.05, F10.2)

Note: Code will optimize PBP to match EOC point.

Card Set 8 (one card)

OPTION SPECIFIED BY 'NNN'

NNN=1: use fixed poison shim over a cycle or model leakage explicitly

NNN=2: if neither

FORMAT (x3, I2)

TABLE C.1 (continued-3)

Card Set 9 (one card)

(used only when NNN=1, i.e., using shim or leakage)

SHIM: amount of shim poison, $\Delta\rho$, or leakage coefficient, α.

FORMAT (F10.5)

Card Set 10 (one or more cards)

(used only when NNN=1)

APER(I), I = 1 to J: fraction of batch (I) on core periphery or fraction of batch (I) with fixed shim poison

FORMAT (8F10.5)

Card Set 11 (one or more cards)

(used only when NNN=1)

AINT(I), I = 1 to J: fraction of batch (I) in core interior or fraction of batch (I) without fixed shim poison

FORMAT (8F10.5)

Card Set 12 (one card)

OPTION SPECIFIED BY 'NNNN'

NNNN=0: for end of computation

NNNN=1: for the next case

FORMAT (x3, I2)

TABLE C.2

DISBURN CODE LISTING

```
CCCCCCCCCCCCCCCCCCCCCCCCCCCCCCCCCCCCCCCCCCCCCCCCCCCCCCCCCCCCCCCCCCCCCCCCCCCC  LRM00010
C                                                                          C  LRM00020
C                    DISBURN CODE                                          C  LRM00030
C                                                                          C  LRM00040
CCCCCCCCCCCCCCCCCCCCCCCCCCCCCCCCCCCCCCCCCCCCCCCCCCCCCCCCCCCCCCCCCCCCCCCCCCCC  LRM00050
      IMPLICIT  REAL*8(A-H, O-Z) , REAL*8(K)                               LRM00060
      DIMENSION DONE(10), B(10), F(10), RHO(10), FA(10),FAVG(10)           LRM00070
      DIMENSION AINT(10), APER(10), PINT(10), PPER(10),RHOP(10)            LRM00080
C                                                                          LRM00090
C                                                                          LRM00100
C                                                                          LRM00110
C       J     NUMBER OF BATCHES                                            LRM00120
C CONVRG      CONVERGENCE CRITERION IN MWD/MT                              LRM00130
C  TSTEP      TIME STEP OR BURNUP INCREMENT IN MWD/MT                      LRM00140
C RHOINT      EXTRAPOLATED BOL REACTIVITY                                  LRM00150
C RHOBOL      BOL REACTIVITY VALUE                                         LRM00160
C       A     SLOPE OF THE LINEAR REACTIVITY-BURNUP TRACE, MT/MWD          LRM00170
C      BI     ESTIMATED POISON BURNOUT POINT NEAR EOC 1, MWD/MT            LRM00180
C THETAI      INTERIOR THETA VALUE                                         LRM00190
C THETAP      PERIPHERAL THETA VALUE                                       LRM00200
C   SHIM      FIXED POISON SHIM REACTIVITY PENALTY                         LRM00210
C  ALPHA      LEAKAGE COEFFICIENT                                          LRM00220
C   AINT      FRACTION OF INTERIOR ASSEMBLIES IN EACH BATCH                LRM00230
C   APER      FRACTION OF PERIPHERAL ASSEMBLIES IN EACH BATCH              LRM00240
C                                                                          LRM00250
C                                                                          LRM00260
   10 WRITE(6,4000)                                                        LRM00270
      READ(5,2000) J, TSTEP, CONVRG                                        LRM00280
      WRITE(6,4005)                                                        LRM00290
      READ(5,2050) THETAI, THETAP                                          LRM00300
C                                                                          LRM00310
       ALPHA=0.0                                                           LRM00320
       SHIM=0.0                                                            LRM00330
       NUMR=0                                                              LRM00340
       JLESS=J-1                                                           LRM00350
       STORE=TSTEP                                                         LRM00360
       BI=1000.0                                                           LRM00370
       NN=3                                                                LRM00380
      DO 110 I=1,J                                                         LRM00390
      AINT(I)=1.0                                                          LRM00400
      APER(I)=0.0                                                          LRM00410
  110 CONTINUE                                                             LRM00420
C                                                                          LRM00430
      WRITE(6,4010)                                                        LRM00440
      READ(5,2010) RHOINT, A                                               LRM00450
```

```
      RHOBOL=RHOINT                                                    LRM00460
  111 WRITE(6,4020)                                                    LRM00470
      READ(5,2020) N                                                   LRM00480
C                                                                      LRM00490
C   N=1 : OPTION WITHOUT BURNABLE POISON                               LRM00500
C   N=2 : OPTION WITH BURNABLE POISON                                  LRM00510
C                                                                      LRM00520
      IF (N.EQ.1) GOTO 113                                             LRM00530
      IF (N.EQ.2) GOTO 1110                                            LRM00540
      GOTO 111                                                         LRM00550
C                                                                      LRM00560
C                                                                      LRM00570
C     CASE WITH BURNABLE POISON                                        LRM00580
C                                                                      LRM00590
C      NN=1: CONSTAN REACTIVITY IN CYCLE 1                             LRM00600
C      NN=2: SLOPE REACTIVITY IN CYCLE 1                               LRM00610
C                                                                      LRM00620
C                                                                      LRM00630
 1110 WRITE(6,4035)                                                    LRM00640
      READ(5,2020)NN                                                   LRM00650
C                                                                      LRM00660
      IF (NN.EQ.1) GOTO 1115                                           LRM00670
      IF (NN.EQ.2) GOTO 112                                            LRM00680
      GOTO 1110                                                        LRM00690
C                                                                      LRM00700
C     CONSTANT REACTIVITY IN CYCLE 1                                   LRM00710
C                                                                      LRM00720
 1115 WRITE(6,4025)                                                    LRM00730
      READ(5,2035) BI                                                  LRM00740
      GOTO 113                                                         LRM00750
C                                                                      LRM00760
C     SLOPE REACTIVITY IN CYCLE 1                                      LRM00770
C                                                                      LRM00780
  112 WRITE(6,4030)                                                    LRM00790
      READ(5,2030) RHOBOL, BI                                          LRM00800
C                                                                      LRM00810
C                                                                      LRM00820
C     CASE WITH AND WITHOUT BURNABLE POISON                            LRM00830
C                                                                      LRM00840
C     NNN=1: USE FIXED POISON SHIM OR MODEL LEAKAGE                    LRM00850
C            EXPLICITLY OVER A CYCLE                                   LRM00860
C     NNN=2: IF NEITHER                                                LRM00870
C                                                                      LRM00880
C                                                                      LRM00890
  113 WRITE(6,4040)                                                    LRM00900
```

```
      READ(5,2020) NNN                                                  LRM00910
      IF(NNN.EQ.1) GOTO 114                                             LRM00920
      IF(NNN.EQ.2) GOTO 117                                             LRM00930
      GOTO 113                                                          LRM00940
C                                                                       LRM00950
  114 WRITE(6,4041)                                                     LRM00960
      READ(5,2030) SHIM                                                 LRM00970
      GOTO 116                                                          LRM00980
C                                                                       LRM00990
  116 WRITE(6,4043)                                                     LRM01000
      READ(5,2050) (APER(I), I=1,J)                                     LRM01010
      WRITE(5,4044)                                                     LRM01020
      READ(5,2050) (AINT(I), I=1,J)                                     LRM01030
  117 CONTINUE                                                          LRM01040
      WRITE(6,3000)                                                     LRM01050
C                                                                       LRM01060
C                                                                       LRM01070
  118 DO 119 I=1,J                                                      LRM01080
      FA(I)=0.0                                                         LRM01090
  119 CONTINUE                                                          LRM01100
      FAP=0.0                                                           LRM01110
      TSTEP=STORE                                                       LRM01120
      ADD=0.0                                                           LRM01130
C                                                                       LRM01140
C                                                                       LRM01150
C     ESTIMATE CYCLE BURNUP                                             LRM01160
C                                                                       LRM01170
      BEST=2.0*RHOINT/((J+1)*A)                                         LRM01180
C                                                                       LRM01190
C                                                                       LRM01200
C     ESTIMATE BOC POINTS                                               LRM01210
C                                                                       LRM01220
C                                                                       LRM01230
      DONE(1)=0.0                                                       LRM01240
      DO 120 I=1,J                                                      LRM01250
      W=I-1                                                             LRM01260
      DONE(I)=W*BEST                                                    LRM01270
  120 CONTINUE                                                          LRM01280
C                                                                       LRM01290
C                                                                       LRM01300
  190 DO 200  I=1,J                                                     LRM01310
      B(I)=DONE(I)                                                      LRM01320
  200 CONTINUE                                                          LRM01330
C                                                                       LRM01340
C                                                                       LRM01350
```

```
C     COMPUTE THE REACTIVITY VALUES CORRESPONDING TO THE                LRM01360
C     DIFFERENT BURNUP POINTS FOR DEFFERENT OPTIONS                    LRM01370
C                                                                      LRM01380
C                                                                      LRM01390
  330 DO 370 I=1,J                                                     LRM01400
      IF (NN.EQ.1) RHOBOL=RHOINT-A*BI                                  LRM01410
      IF (B(I).LE.BI)                                                  LRM01420
     $    RHO(I)=RHOBOL+(RHOINT-RHOBOL)*B(I)/BI - A*B(I)               LRM01430
      IF (B(I).GT.BI)                                                  LRM01440
     $    RHO(I)=RHOINT-A*B(I)                                         LRM01450
          RHOP(I)=RHOINT-A*B(I)                                        LRM01460
  370 CONTINUE                                                         LRM01470
C                                                                      LRM01480
C                                                                      LRM01490
C     CALCULATE THE BATCH POWER FRACTION                               LRM01500
C                                                                      LRM01510
C                                                                      LRM01520
      FSUM=0.0                                                         LRM01530
      DO 371 I=1,J                                                     LRM01540
      PPER(I)=APER(I)/(J*(1.0-THETAP*(RHOP(I)-SHIM)))                  LRM01550
      PINT(I)=AINT(I)/(J*(1.0-THETAI*RHO(I)))                          LRM01560
      F(I)=PPER(I)+PINT(I)                                             LRM01570
      FSUM=FSUM+F(I)                                                   LRM01580
  371 CONTINUE                                                         LRM01590
C                                                                      LRM01600
C       CALCULATE PERIPHERAL POWER FRACTION                            LRM01610
C                                                                      LRM01620
      FPER=0.0                                                         LRM01630
      DO 372 I=1,J                                                     LRM01640
      FPER=FPER+PPER(I)/FSUM                                           LRM01650
  372 CONTINUE                                                         LRM01660
C                                                                      LRM01670
C                                                                      LRM01680
C       CALCULATE SYSTEM REACTIVITY                                    LRM01690
C                                                                      LRM01700
C                                                                      LRM01710
      RHOSYS=0.0                                                       LRM01720
      DO 390  I=1,J                                                    LRM01730
      PPER(I)=PPER(I)/FSUM                                             LRM01740
      PINT(I)=PINT(I)/FSUM                                             LRM01750
      RHOSYS=RHOSYS+(PPER(I)*(RHOP(I)-SHIM) + PINT(I)*RHO(I))          LRM01760
  390 CONTINUE                                                         LRM01770
C                                                                      LRM01780
C                                                                      LRM01790
C     IF SYSTEM REACTIVITY HAS NOT CONVERGED, SOLUBLE POISON IS        LRM01800
```

```
C     ADDED UNTIL CONVERGENCE IS ACHIEVED AND THE BATCH BURNUP          LRM01810
C     IS INCREMENTED.                                                   LRM01820
C     IF EOC POINT IS REACHED THE OUTER CONVERGENCE CRITERION           LRM01830
C     IS CHECK                                                          LRM01840
C                                                                       LRM01850
C                                                                       LRM01860
C                                                                       LRM01870
      IF (RHOSYS.GE.0.0)GOTO 391                                        LRM01880
      IF (RHOSYS.LT.0.0)GOTO 410                                        LRM01890
  391 IF (RHOSYS.LE.0.0001)  GOTO 460                                   LRM01900
      IF (RHOSYS.GT.0.0001)  GOTO 392                                   LRM01910
C                                                                       LRM01920
C                                                                       LRM01930
  392 DELTA=RHOSYS/J                                                    LRM01940
      FSUM1=0.0                                                         LRM01950
      DO 395 I=1,J                                                      LRM01960
      RHOP(I)=RHOP(I)-DELTA                                             LRM01970
      RHO(I)=RHO(I)-DELTA                                               LRM01980
      PPER(I)=APER(I)/(J*(1.0-THETAP*(RHOP(I)-SHIM)))                   LRM01990
      PINT(I)=AINT(I)/(J*(1.0-THETAI*RHO(I)))                           LRM02000
      F(I)=PPER(I)+PINT(I)                                              LRM02010
      FSUM1=FSUM1+F(I)                                                  LRM02020
  395 CONTINUE                                                          LRM02030
C                                                                       LRM02040
C                                                                       LRM02050
      FPER=0.0                                                          LRM02060
      DO 396 I=1,J                                                      LRM02070
      FPER=FPER+PPER(I)/FSUM1                                           LRM02080
  396 CONTINUE                                                          LRM02090
C                                                                       LRM02100
      RHOSYS=0.0                                                        LRM02110
      DO 397 I=1,J                                                      LRM02120
      PPER(I)=PPER(I)/FSUM1                                             LRM02130
      PINT(I)=PINT(I)/FSUM1                                             LRM02140
      RHOSYS=RHOSYS+(PPER(I)*(RHOP(I)-SHIM) + PINT(I)*RHO(I))           LRM02150
  397 CONTINUE                                                          LRM02160
C                                                                       LRM02170
C                                                                       LRM02180
      IF (RHOSYS.LE.0.0001)  GOTO 417                                   LRM02190
      IF (RHOSYS.GT.0.0001)  GOTO 392                                   LRM02200
C                                                                       LRM02210
C                                                                       LRM02220
C                                                                       LRM02230
  410 DO 415 I=1,J                                                      LRM02240
      B(I)=B(I)-F(I)*TSTEP                                              LRM02250
```

```
      FA(I)=FA(I)-F(I)*TSTEP                                          LRM02260
  415 CONTINUE                                                        LRM02270
      FAP=FAP-FPER*TSTEP                                              LRM02280
C                                                                     LRM02290
      ADD=ADD-TSTEP                                                   LRM02300
      TSTEP=TSTEP/2.0                                                 LRM02310
C                                                                     LRM02320
C                                                                     LRM02330
  417 DO 420 I=1,J                                                    LRM02340
      B(I)=B(I)+F(I)*TSTEP                                            LRM02350
      FA(I)=FA(I)+F(I)*TSTEP                                          LRM02360
  420 CONTINUE                                                        LRM02370
      FAP=FAP+FPER*TSTEP                                              LRM02380
      ADD=ADD+TSTEP                                                   LRM02390
      GOTO 330                                                        LRM02400
C                                                                     LRM02410
C                                                                     LRM02420
  460  CONTINUE                                                       LRM02430
  540 IF (J.EQ.1)  GO TO 560                                          LRM02440
C                                                                     LRM02450
C     CHECK FOR CONVERGENCE AT CYCLE END-POINTS                       LRM02460
C                                                                     LRM02470
  550 DO 560 I=1,JLESS                                                LRM02480
      M=I+1                                                           LRM02490
      TELL=B(I)-DONE(M)                                               LRM02500
      IF (DABS(TELL).GT.CONVRG) GO TO 210                             LRM02510
  560 CONTINUE                                                        LRM02520
C                                                                     LRM02530
  210 CONTINUE                                                        LRM02540
      FAVGS=0.0                                                       LRM02550
      FPAVGS=FAP/ADD                                                  LRM02560
      DO 211 I=1,J                                                    LRM02570
      FAVG(I)=FA(I)/ADD                                               LRM02580
      FAVGS=FAVGS+FAVG(I)                                             LRM02590
  211 CONTINUE                                                        LRM02600
      DO 2110 I=1,J                                                   LRM02610
      FAVG(I)=FAVG(I)/FAVGS                                           LRM02620
 2110 CONTINUE                                                        LRM02630
      FPAVGS=FPAVGS/FAVGS                                             LRM02640
      IF(N.EQ.2) GOTO 212                                             LRM02650
      NUMB = NUMB + 1                                                 LRM02660
      WRITE(6,3070)NUMB                                               LRM02670
      RHOL=SHIM*FPAVGS                                                LRM02680
      WRITE(6,3095) FPAVGS,RHOL                                       LRM02690
      WRITE(6,3090) (B(I),I=1,J)                                      LRM02700
```

```
      WRITE (6,3100) (FAVG(I),I=1,J)                                    LRM02710
  212 IF(DABS(TELL).LE.CONVRG) GO TO 990                                LRM02720
C                                                                       LRM02730
C                                                                       LRM02740
C     REINITIALIZE AND UPDATE BOC POINTS                                LRM02750
C                                                                       LRM02760
C                                                                       LRM02770
      DO 213 I=1,J                                                      LRM02780
      FA(I)=0.0                                                         LRM02790
  213 CONTINUE                                                          LRM02800
      FAP=0.0                                                           LRM02810
                                                                        LRM02820
      ADD=0.0                                                           LRM02830
      TSTEP = STORE                                                     LRM02840
      S=0.0                                                             LRM02850
  220 DO 230  I=1,J                                                     LRM02860
      L=I-1                                                             LRM02870
      IF (I.NE.1)  DONE(I)=B(L)                                         LRM02880
  230 CONTINUE                                                          LRM02890
      GO TO 190                                                         LRM02900
C                                                                       LRM02910
  990 IF (N.EQ.1) GOTO 999                                              LRM02920
      BDELTA=DABS(B(1)-BI)                                              LRM02930
      NUMB=NUMB+1                                                       LRM02940
      WRITE(6,3070) NUMB                                                LRM02950
      WRITE(6,3090) (B(I),I=1,J)                                        LRM02960
      WRITE(6,3100) (FAVG(I),I=1,J)                                     LRM02970
      WRITE (6,3090)BI                                                  LRM02980
      IF (BDELTA.LE.50.0) GOTO 999                                      LRM02990
      BI=BI+BDELTA/5.0                                                  LRM03000
      GOTO 118                                                          LRM03010
C                                                                       LRM03020
  999 WRITE(6,4060)                                                     LRM03030
      READ(5,2020)NNNN                                                  LRM03040
C                                                                       LRM03050
C     NNNN=0: STOP                                                      LRM03060
C     NNNN=1: NEXT CASE                                                 LRM03070
C                                                                       LRM03080
      IF(NNNN.EQ.0) GOTO 919                                            LRM03090
      IF(NNNN.EQ.1) GOTO 10                                             LRM03100
      GOTO 999                                                          LRM03110
  919 STOP                                                              LRM03120
CCCCCCCCCCCCCCCCCCCCCCCCCCCCCCCCCCCCCCCCCCCCCCCCCCCCCCCCCCCCCCCCCCCCCC  LRM03130
C                                                                   C   LRM03140
C       FORMATS FOR INPUT AND OUTPUT STATEMENTS                     C   LRM03150
```

```
C                                                                       C    LRM03160
CCCCCCCCCCCCCCCCCCCCCCCCCCCCCCCCCCCCCCCCCCCCCCCCCCCCCCCCCCCCCCCCCCCCCCC    LRM03170
 2000 FORMAT(8X,I2,2F10.5)                                                  LRM03180
 2010 FORMAT(F10.5,E10.5)                                                   LRM03190
 2020 FORMAT(3X,I2)                                                         LRM03200
 2030 FORMAT(F10.5,F10.2)                                                   LRM03210
 2035 FORMAT(F10.2)                                                         LRM03220
 2040 FORMAT(8X,I2,F10.5)                                                   LRM03230
 2050 FORMAT(8F10.5)                                                        LRM03240
 3000 FORMAT(1X///4X,' THE VALUES OF BATCH BURNUP B(I) IN MWD/MT,'/         LRM03250
     $      4X,' THE POISON BURNOUT POINT BI (EOC POINT) ,'/                LRM03260
     $       4X,' PERIPHERAL POWER FRACTION, LEAKAGE REACTIVITY AND'/       LRM03270
     $       4X,' BATCH POWER FRACTION F(I) ARE ARRANGED IN'/               LRM03280
     $       4X,' THE FOLLOWING ORDER AFTER EACH ITERATION'///              LRM03290
     $         13X,4HFPER,9X,4HRHOL/                                        LRM03300
     $       13X,4HB(1),9X,4HB(2),9X,4HB(3),9X,4HB(4),9X,4HB(5),            LRM03310
     $       6X,3HETC/13X,4HF(1),9X,4HF(2),9X,4HF(3),9X,                    LRM03320
     $       4HF(4),9X,4HF(5),6X,3HETC/13X,2HBI///)                         LRM03330
 3070 FORMAT(/3X,I3,2X,F10.4)                                               LRM03340
 3080 FORMAT(5X,F10.2,F10.5)                                                LRM03350
 3090 FORMAT(5X,8(3X,F10.1))                                                LRM03360
 3095 FORMAT(5X,2(3X,F10.5))                                                LRM03370
 3100 FORMAT(5X,8(3X,F10.4)/1H )                                            LRM03380
 4000 FORMAT(1X//' INPUT NUMBER_OF_BATCHES, BURNUP_INCREMENT(MWD/MT),'/     LRM03390
     $       ' AND CONVERGENCE CRITERION.'/                                 LRM03400
     $       ' FORMAT(8X,I2,2F10.4)'/)                                      LRM03410
 4005 FORMAT(1X//' INPUT INTERIOR THETA AND PERIPHERAL THETA'/              LRM03420
     $       ' FORMAT(2F10.5)'/)                                            LRM03430
 4010 FORMAT(1X//' INPUT RHO_INTERCEPT AND SLOPE OF TRACE.'/                LRM03440
     $       ' FORMAT(F10.5,E10.5)'/)                                       LRM03450
 4020 FORMAT(1X//' WITH SOLUBLE POISON ONLY: INPUT 1'/                      LRM03460
     $       ' WITH BURNABLE POISON    : INPUT 2'/                          LRM03470
     $       ' FORMAT(3X,I2)'/)                                             LRM03480
 4025 FORMAT(1X//' CONSTANT REACTIVITY IN CYCLE 1 :'/                       LRM03490
     $   ' INPUT POISON BURNOUT POINT(PBP)'/                                LRM03500
     $     ' CODE WILL OPTIMIZE PBP TO MATCH EOC POINT'/                    LRM03510
     $      ' FORMAT(10.2)'/)                                               LRM03520
 4030 FORMAT(1X//' SLOPE REACTIVITY IN CYCLE 1 :'/                          LRM03530
     $ ' INPUT BOL_RHO AND POISON BURNOUT POINT(PBP)'/                      LRM03540
     $  ' CODE WILL OPTIMIZE PBP TO MATCH EOC POINT'/                       LRM03550
     $ ' FORMAT(F10.5,F10.2)'/)                                             LRM03560
 4035 FORMAT(1X//' BURNABLE POISON CASE:'/                                  LRM03570
     $   ' FOR CONSTANT REACTIVITY IN CYCLE 1, INPUT 1'/                    LRM03580
     $ ' FOR SLOPE REACTIVITY IN CYCLE 1, INPUT 2'/                         LRM03590
     $    ' FORMAT(3X,I2)'/)                                               LRM03600
```

```
4040 FORMAT(1X//' USING FIXED POISON SHIM OVER A CYCLE OR'/                LRM03610
     $       ' MODEL LEAKAGE EXPLICITLY: INPUT 1'/                        LRM03620
     $       ' IF NEITHER: INPUT 2'/                                      LRM03630
     $       ' FORMAT(3X,I2)'/)                                           LRM03640
4041 FORMAT(1X//' INPUT AMOUNT OF SHIM POISON OR LEAKAGE'/                LRM03650
     $       ' COEFFICIENT: ALPHA'/                                       LRM03660
     $       ' FORMAT(F10.5)'/)                                           LRM03670
4043 FORMAT(1X//' INPUT FRACTION OF BATCH (I) IN PERIPHERY OR'/           LRM03680
     $       ' FRACTION OF BATCH WITH SHIM POISON: I=1,2,..,N '/          LRM03690
     $       ' FORMAT(8F10.5)'/)                                          LRM03700
4044 FORMAT(1X//' INPUT FRACTION OF BATCH (I) IN INTERIOR OR'/            LRM03710
     $       ' FRACTION OF BATCH WITHOUT SHIM: I=1,2,...,N '/             LRM03720
     $       ' FORMAT(8F10.5)'/)                                          LRM03730
4060 FORMAT(1X//' END OF COMPUTATION'////                                 LRM03740
     $       ' FOR THE NEXT CASE, INPUT 1'/                               LRM03750
     $       ' FOR END OF COMPUTATION, INPUT 0'/                          LRM03760
     $       ' FORMAT(3X,I2)'/)                                           LRM03770
      END                                                                 LRM03780
```

TABLE C.3

SAMPLE PROBLEM

```
 FORTGI DISBURN
G1 COMPILER ENTERED
ISOURCE ANALYZED
PROGRAM NAME = MAIN
*  NO DIAGNOSTICS GENERATED
R; T=1.29/1.65 15:26:24

.GLOBAL TXTLIB FORTMOD2
R; T=0.01/0.02 15:26:35

.LOAD DISBURN
R; T=0.09/0.20 15:26:47

.START
EXECUTION BEGINS...


INPUT NUMBER_OF_BATCHES, BURNUP_INCREMENT(MWD/MT),
AND CONVERGENCE CRITERION.
FORMAT(8X,I2,2F10.4)

.          3     100.0      20.0


INPUT INTERIOR THETA AND PERIPHERAL THETA
FORMAT(2F10.5)

.        1.5       1.5
```

```
INPUT RHO_INTERCEPT AND SLOPE OF TRACE.
FORMAT(F10.5,E10.5)

.    0.2235 0.9272E-5


WITH SOLUBLE POISON ONLY: INPUT 1
WITH BURNABLE POISON    : INPUT 2
FORMAT(3X,I2)

.    2


BURNABLE POISON CASE:
FOR CONSTANT REACTIVITY IN CYCLE 1, INPUT 1
FOR SLOPE REACTIVITY IN CYCLE 1, INPUT 2
FORMAT(3X,I2)

.    2


SLOPE REACTIVITY IN CYCLE 1 :
INPUT BOL_RHO AND POISON BURNOUT POINT(PBP)
CODE WILL OPTIMIZE PBP TO MATCH EOC POINT
FORMAT(F10.5,F10.2)

.    0.0200   11000.0


USING FIXED POISON SHIM OVER A CYCLE OR
MODEL LEAKAGE EXPLICITLY: INPUT 1
IF NEITHER: INPUT 2
FORMAT(3X,I2)

.    1
```

```
INPUT AMOUNT OF SHIM POISON OR LEAKAGE
COEFFICIENT: ALPHA
FORMAT(F10.5)

.     0.1640


INPUT FRACTION OF BATCH (I) IN PERIPHERY OR
FRACTION OF BATCH WITH SHIM POISON: I=1,2,..,N
FORMAT(8F10.5)

.        0.0        0.0      0.667


 INPUT FRACTION OF BATCH (I) IN INTERIOR OR
 FRACTION OF BATCH WITHOUT SHIM: I=1,2,...,N
 FORMAT(8F10.5)

.        1.0        1.0      0.333
```

THE VALUES OF BATCH BURNUP B(I) IN MWD/MT,
THE POISON BURNOUT POINT BI (EOC POINT) ,
PERIPHERAL POWER FRACTION, LEAKAGE REACTIVITY AND
BATCH POWER FRACTION F(I) ARE ARRANGED IN
THE FOLLOWING ORDER AFTER EACH ITERATION

	B(1)	B(2)	B(3)	B(4)	B(5)	ETC
	F(1)	F(2)	F(3)	F(4)	F(5)	ETC
	BI					
1						
	11935.2	23554.1	32379.8			
	0.3683	0.3591	0.2726			
	11000.0					
2						
	11916.3	23557.9	32396.8			
	0.3677	0.3595	0.2728			
	11187.0					
3						
	11910.7	23562.1	32412.4			
	0.3673	0.3598	0.2729			
	11332.9					
4						
	11899.2	23567.7	32421.9			
	0.3669	0.3600	0.2730			
	11448.5					

5

11899.7	23573.9	32437.1
0.3667	0.3602	0.2731
11538.6		

6

11891.9	23571.8	32438.4
0.3664	0.3604	0.2732
11610.8		

7

11885.7	23569.7	32438.4
0.3662	0.3605	0.2732
11667.1		

8

11881.9	23577.4	32446.6
0.3661	0.3606	0.2733
11710.8		

9

11878.5	23583.6	32440.7
0.3660	0.3606	0.2733
11745.0		

10

11885.3	23583.5	32454.8
0.3659	0.3607	0.2733
11771.7		

11

11873.8	23583.3	32455.9
0.3659	0.3608	0.2734
11794.4		

```
   12
          11872.1        23581.6        32460.9
           0.3658         0.3608         0.2734
          11810.3

   13
          11871.1        23582.1        32467.4
           0.3658         0.3608         0.2734
          11822.7


END OF COMPUTATION


FOR THE NEXT CASE, INPUT 1
FOR END OF COMPUTATION, INPUT 0
FORMAT(3X,I2)

.    0
R; T=51.83/56.18 15:33:14

.
```

APPENDIX D

RESULTS OF 3 X 3 - FUEL BUNDLE PDQ-7 CALCULATIONS

The power split relation (derived from a $1\frac{1}{2}$ group diffusion theory model) for a two-region problem such as that shown in Fig. 3.8 of Chapter 3, can be written as

$$f_1 = \frac{(\frac{V_1}{V_2})(\overline{\frac{f}{k_\infty}}_2)}{1 - \theta\rho_1} \qquad (D.1)$$

where subscripts '1' and '2' correspond to the interior test assembly and the surrounding assemblies, respectively. Equation D.1 can be rearranged into a form through which the power split relation can be easily tested:

$$\frac{(\frac{V_1}{V_2})(\overline{\frac{f}{k_\infty}}_2)}{f_1} = 1 - \theta\rho_1 \qquad (D.2)$$

A series of two-group PDQ-7 calculations were performed for the assembly arrangement given in Fig. 3.8 of Chapter 3. Three successive constant values of k_2 (0.9, 1.0, 1.2) were employed, and the values of k_1 ($= \frac{1}{1-\rho_1}$) were varied over a wide range of enrichments, burnups, fuel-to-moderator ratios and boron concentrations. The basic assembly and pincell composition and configuration were those of the Maine Yankee Reactor (see Tables 2.3 and 2.4 of Chapter 2), and all cross sections were prepared using LEOPARD supercell computations.

Table D.1 lists the results of the analyses. These data points were plotted in Fig. 3.10 of Chapter 3.

TABLE D.1

RESULTS OF PDQ-7 CALCULATIONS FOR 3 X 3 ROD BUNDLES

$$y = \frac{(\frac{V_1}{V_2})(\frac{\overline{f}}{k_{\infty}})_2}{f_2}$$

Variables	$x = \rho_1$	k_2=1.2	k_2=1.0	k_2=0.9
1a) Variation in Burnup, MWD/MT (ε = 4.3 w/o)				
150	0.2892	0.6870	0.6141	0.5631
10000	0.2295	0.7385	0.6619	0.6078
25000	0.1261	0.9126	0.8229	0.7584
1b) Variation in Burnup, MWD/MT (ε = 3.0 w/o)				
15000	0.0875	1.0313	0.9111	0.8638
25000	-0.0021	1.1970	1.0812	1.0033
35000	-0.0929	1.3532	1.2384	1.1531
2) Variation in Boron Concentration, PPM				
0	0.2515	0.7948	0.7139	0.6564
100	0.2425	0.8039	—	—
200	0.2335	0.8131	0.7309	0.6724
400	0.2157	0.8312	0.7479	0.6884
500	0.2068	0.8402	—	—
600	0.1979	—	0.7766	0.7044
800	0.1802	—	0.7817	0.7204
900	0.1714	0.8762	—	—

TABLE D.1 (continued

Variables	$x = \rho_1$	$y = \frac{(\frac{V_1}{V_2})(\frac{\overline{f}}{k_{\infty 2}})}{f_2}$ k_2=1.2	k_2=1.0	k_2=0.9
3) Variation in Enrichment, w/o U-235				
4.3	0.2884	0.6893	0.6162	0.5650
4.0	0.2821	—	0.6333	0.5810
3.5	0.2684	0.7486	—	0.6162
3.0	0.2515	0.7948	0.7139	0.6564
2.5	0.2269	—	—	0.7157
2.0	0.1900	0.9610	0.8698	0.8036
4) Variation in Pitch, in.				
0.500	0.1922	0.8757	0.7903	0.7278
0.575	0.2494	0.7898	0.7160	0.6583
0.580	0.2515	—	—	0.6566
0.600	0.2680	0.7873	0.7074	—

*Unless stated, otherwise: fuel enrichment $\varepsilon = 3.0$ w/o U-235,
burnup point = 0 MWD/MT,
boron concentration = 0 PPM,
pitch = 0.580 in

APPENDIX E

RELATION OF POWER SHARING ALGORITHM TO NODAL METHODS

We have developed a power sharing prescription using the differential form of the neutron balance equation as a starting point. There has been considerable work in the past along similar lines starting from integral equation formulations—the classical 'nodal' approach (FLARE and its successors). Since both deal with the same phenomena, it should be possible to manipulate both into similar forms.

The general approach in FLARE-type calculations is as follows:

The neutron production rate, S_j, and absorption rate, A_j, in node j (part-of, or an entire assembly) are coupled by the multiplication factor, $k_{\infty j}$,:

$$S_j = \lambda^{-1} k_{\infty j} A_j \tag{E.1}$$

where λ is the eigenvalue needed to achieve system criticality.

Nodes are coupled by the kernel:

$$\begin{aligned} A_j &= \sum_m W_{mj} S_m \\ &\equiv \sum_{m \neq j} W_{mj} S_m + W_{jj} S_j \end{aligned} \tag{E.2}$$

where W_{mj} is the probability that a neutron born at node m is

ultimately absorbed at node j.

Substituting A_j of Eq. E.2 into Eq. E.1, the source in node j is then

$$S_j = \lambda^{-1} k_{\infty j} \sum_{m \neq j} W_{mj} S_m + \lambda^{-1} k_{\infty j} W_{jj} S_j \qquad (E.3)$$

or

$$S_j = \frac{\lambda^{-1} k_{\infty j} \sum_{m \neq j} W_{mj} S_m}{1 - \lambda^{-1} k_{\infty j} W_{jj}} \qquad (E.4)$$

This is the basic FLARE equation.

Starting with Eq. E.4, consider a critical system, $\lambda \equiv 1.0$, and normalizing by total power, we obtain

$$f_j = \frac{k_{\infty j} \sum_{m \neq j} W_{mj} f_m}{1 - k_{\infty j} W_{jj}} \qquad (E.5)$$

But $k = 1/(1-\rho)$; thus

$$f_j = \frac{\sum_{m \neq j} W_{mj} f_m}{1 - W_{jj} - \rho_j} \qquad (E.6)$$

or

$$f_j = \frac{\sum_{m \neq j} \left(\frac{W_{mj}}{1 - W_{jj}} \right) f_m}{1 - \left(\frac{1}{1 - W_{jj}} \right) \rho_j} \qquad (E.7)$$

which has a numerator characterizing the "surroundings" and a denominator of the form "$(1 - \theta\rho_j)$". Equation E.7 is, there-

fore, similar in structure to the power split relation derived from the $1\frac{1}{2}$ group diffusion theory model in the present work: Eq. 3.46 of Chapter 3.

APPENDIX F

DATA FOR THE CASE OF FIXED POISON SHIM IN CYCLE J

An empirical expression for the ε factor for the case of fixed poison shim in cycle j has been formulated based on the results generated using the DISBURN code (see Table F.1). The formula is given by Eq. 4.12 in Chapter 4, and the plots for the data are shown in Figs. 4.12 through 4.16 in the same chapter. Tne following values were used in the computations:

extrapolated BOL reactivity, $\rho_0 = 0.22$

slope of the linear $\rho(B)$ curve = 0.912×10^{-5}, MT/MWD

theta value (θ) = 1.5

TABLE F.1

VALUES OF THE ε FACTOR FOR THE CASE OF FIXED POISON SHIM IN CYCLE J

Poison Shim Reactivity, $\Delta\rho$	ε Factor (DISBURN)					
	j = 1	j = 2	j = 3	j = 4	j = 5	j = 6
n = 2						
0.02	0.0574	0.0511	—	—	—	—
0.04	0.1113	0.0975	—	—	—	—
0.08	0.2315	0.1995	—	—	—	—
0.10	0.2986	0.2555	—	—	—	—
0.12	0.3706	0.3166	—	—	—	—
n = 3						
0.04	0.0777	0.0699	0.0638	—	—	—
0.08	0.1512	0.1347	0.1213	—	—	—
0.10	0.1894	0.1679	0.1508	—	—	—
0.12	0.2287	0.2023	0.1811	—	—	—
0.16	0.3080	0.2718	0.2440	—	—	—
n = 4						
0.04	0.0611	0.0557	0.0515	0.0482	—	—
0.08	0.1145	0.1027	0.0944	0.0874	—	—
0.10	0.1409	0.1269	0.1156	0.1068	—	—
0.12	0.1676	0.1509	0.1372	0.1269	—	—
0.16	0.2209	0.1992	0.1810	0.1668	—	—

TABLE F.1—Cont.

Poison Shim Reactivity, Δρ	ε Factor (DISBURN)					
	j = 1	j = 2	j = 3	j = 4	j = 5	j = 6
n = 5						
0.04	0.0509	0.0468	0.0438	0.0409	0.0389	—
0.10	0.1139	0.1027	0.0953	0.0886	0.0838	—
0.15	0.1632	0.1489	0.1372	0.1276	0.1196	—
0.20	0.2115	0.1933	0.1776	0.1653	0.1555	—
0.25	0.2575	0.2359	0.2177	0.2029	0.1905	—
n = 6						
0.04	0.0438	0.0404	0.0378	0.0358	0.0341	0.0327
0.10	0.0953	0.0872	0.0812	0.0759	0.0719	0.0686
0.15	0.1347	0.1238	0.1153	0.1075	0.1024	0.0972
0.20	0.1730	0.1591	0.1485	0.1390	0.1313	0.1251
0.25	0.2087	0.1929	0.1796	0.1683	0.1591	0.1515

REFERENCES

A-1 Andrews, J. B., et al., "Development of an Extended Burnup Mark B Design, First Semi-Annual Progress Report: July-December 1978," BAW-1546-1, (1979).

A-2 Adamsam, E. G., et al., "Computer Methods for Utility Reactor Physics Analysis," Reactor and Fuel-Processing Technology, Vol. 12, No. 2, (Spring 1969).

A-3 Amster, H. and Suarez, R., "The Calculation of Thermal Constants Averaged over a Wigner-Wilkins Flux Spectrum: Description of the SOFOCATE Code," WAPD-TM-39, (January 1957).

A-4 Atefi, B., "A Two-Lumped Fission Product Model for Fast Reactor Analysis," Trans. Am. Nucl. Soc., 38, 659-660, (June 1981)

B-1 Bowling, M. L. and Miller, J. G., "Core Design, Operation and Economics of 18-Month Fuel Cycles," Trans. Am. Nucl. Soc., 30, 279-280, (November 1978).

B-2 Bowling, M. L., Smith, M. L. and Franklin, C. B., "Development of a Fuel Management Scheme for Extended Burnup at VEPCO," Trans. Am. Nucl. Soc., 33, 392-393, (November 1979).

B-3 Barry, R. F., "LEOPARD—A Spectrum Dependent Non-Spatial Depletion Code," WCAP-3269-26, (September 1973).

B-4 Bohl, H., Gelbard, E. and Ryan, G., "MUFT-4-Fast Neutron Spectrum Code for the IBM-704," WAPD-TM-72, (July 1957).

B-5 Breen, R. J., "A One-Group Model for Thermal Activation Calculations," Nucl. Sci. Eng., 9, 91, (1961).

C-1 Correa, F., Driscoll, M. J. and Lanning, D. D., "An Evaluation of Tight-Pitch PWR Cores," MIT Energy Laboratory Report No. MIT-EL-79-022, (August 1979).

C-2 Coleman, T. A., et al., "Qualification of the B & W Mark B Fuel Assembly for High Burnup, First Semi-Annual Progress Report: July-December 1978," BAW-1546-1, (1979).

C-3 Chang, Y. I., et al., "Alternative Fuel Cycle Options: Performance Characteristics and Impact on Nuclear Power Growth Potential," RSS-TM-4, Argonne National Laboratory, Argonne, Illinois, (January 1977).

C-4 Chernick, J., "Status of Reactor Physics Calculations for U.S. Power Reactors," Reactor Technology, Vol. 13, No. 4, (Winter 1970-1971).

C-5 Cadwell, W. R., "PDQ-7 Reference Manual," WAPD-TM-678, (January 1967).

D-1 Driscoll, M. J., Fujta, E. K. and Lanning, D. D., "Improvement in PWRs on the Once-Through Fuel Cycle," Trans. Am. Nucl. Soc., 30, 280-281, (November 1978).

D-2 Driscoll, M. J., Lecture Notes, Subject 22.35: Nuclear Fuel Mangement, Dept. of Nucl. Eng., M.I.T., 1981.

D-3 Driscoll, M. J., Pilat, E. E. and Correa, F., "Routine Coastdown in LWRs as an Ore Conservation Measure," Trans. Am. Nucl. Soc., 33, 399, (November 1979).

E-1 Eich, W. J., "LWR Assembly Reaction Rate Representation," Presented at Conf. Nuclear Data Problems for Thermal Reactor Applications, Brookhaven National Laboratory, (May 22-24, 1978).

F-1 Fujita, E. K., Driscoll, M. J. and Lanning, D. D., "Design and Fuel Management of PWR Cores to Optimize the Once-Through Fuel Cycle," M.I.T. Energy Laboratory Report No. MIT-EL-78-017, (August 1978).

F-2 Flipot, A. J., et al., "Burnable Poison Dispersion in UO_2 Fuel," Nuclear Engineering International, Vol. 15, No. 167, (April 1970).

G-1 Garel, K. C., et al., "A Comparative Assessment of the PWR, SSCR, and PHWR Concepts," Trans. Am. Nucl. Soc., 30, 301, (November 1978).

G-2 Ghahramani, K. and Driscoll, M. J., "Ore Price Escalation in Fuel Cycle Economic Analyses," Trans. Am. Nucl. Soc., 28, 383-384, (June 1978).

G-3 Graves, H. W., Nuclear Fuel Management, John Wiley & Sons, Inc., (1979).

H-1 Hove, C. M., Robichaud, G. C. and Tulenko, J. S., "PWR Once-Through Fuel Cycle Improvements," Trans. Am. Nucl. Soc., 30, 275-276, (November 1978).

H-2 Hofman, P. L., Busselman, G. J. and Holeman, R. H., "Nuclear Characteristics of Some Compact, Water Moderated Plutonium Burners," HW-79977, (April 1964).

H-3 Harris, R. P., "Use of Gadolinium in PWR Extended Burnup Fuel Cycles," Interim Report, CEND-391, Combustion Engineering Power Systems, Windsor, Connecticut, (September 1981).

H-4 Ho, A., "Design Evaluation of Westinghouse 15 x 15 Fuel Lumped Burnable Poison," PNE-FM-M-81-1, School of Nucl. Eng., Purdue University, (May 23, 1981).

J-1 Jonsson, A., Rec., J. R. and Singh, U. N., "Verification of a Fuel Assembly Spectrum Code Based on Integral Transport Theory," TIS-5815, Combustion Engineering Power Systems, Windsor, Connecticut, (June 1978).

K-1 Kamal, A., "The Effect of Axial Power Shaping on Ore Utilization in Pressurized Water Reactors," S.M. Thesis, Dept. of Nucl. Eng., M.I.T., (January 1980).

K-2 Kamal, A., "The Selective Use of Thorium and Heterogeneity in Uranium-Efficient Pressurized Water Reactors," Ph.D. Thesis, Dept. of Nucl. Eng., M.I.T., (Expected, June 1982).

L-1 Lang, P. M., "Development of Improvements to the Light Water Reactor Fuel Cycle," Paper Presented at the ANS Fuel Cycle and Waste Management Division Topical Meeting on 'Technical Bases for Nuclear Fuel Cycle Policy,' at Newport, Rhode Island, (September 1981).

L-2 Lan, J. S., "Assessment of the Prevailing Physics Codes: LEOPARD, LASER, and EPRI-CELL," Trans. Am. Nucl. Soc., 38, 685-687, (June 1981).

L-3 Littlechild, J. E., Buttler, G. G. and Lester, G. W., "The Production of Burnable Poison Oxide Fuel," Proc. Int. Conf. on Nuclear Fuel Performance, BSNE, No. 65, (October 1973).

M-1 Matzie, R. A., et al., "Uranium Resource Utilization Improvements in the Once-Through PWR Fuel Cycle," CEND-380, Combustion Engineering Power Systems, Windsor, Connecticut, (April 1980).

M-2 MacNabb, W. V., "Two Near-Term Alternatives for Improved Nuclear Fuel Utilization," Trans. Am. Nucl. Soc., 33, 398, (November 1979).

M-3 Momsen, B. F., "An Analysis of Plutonium Recycle Fuel Elements in San Onofre-1," Nucl. Eng. Thesis, Dept. of Nucl. Eng., M.I.T., (May 1974).

M-4 Mangulis, V., Handbook of Series for Scientists and Engineers, Academic Press, New York, (1965).

Q-1 Quan, B. L., Malone, J. P. and Pilat, E. E., "Yankee Atomic Experience with Coastdown," YAEC-1270, (May 1981).

R-1 Robbins, T., "Preliminary Evaluation of a Variable Lattice Fuel Assembly and Reactor Design Concept," Draft Report Under Subcontract No. 11Y13576V for Oak Ridge National Laboratory, Pickard, Lowe and Garrick, Inc., Washington, D.C., (February 1979).

S-1 Shapiro, N. L. and Lin, Y., "Improvement of Fuel Utilization for Once-Through PWR Cycles," Trans. Am. Nucl. Soc., 30, 276-277, (November 1978).

S-2 Sefcik, J. A., Driscoll, M. J. and Lanning, D. D., "Analysis of Strategies for Improving Uranium Utilization in Pressurized Water Reactors," M.I.T. Energy Laboratory Report No. MIT-EL-80-132, (January 1981).

S-3 Sider, F. M., "An Improved Once-Through Fuel Cycle for Pressurized Water Reactors," TIS-6529, Combustion Engineering Power Systems, Windsor, Connecticut, (June 1980).

S-4 Smith, M. L., Franklin, C. B. and Schleicher, T. W., "Extended Burnup and Extended Cycle Design," Trans. Am. Nucl. Soc., 34, 389-390, (June 1980).

S-5 Schweiger, R. G., "Managing Nuclear Fuel, A Special Report," POWER, (December 1969).

S-6 Spierling, H., "The Value of Recycle Plutonium in Pressurized Water Reactors," Ph.D. Thesis, Dept. of Nucl. Eng., M.I.T., (February 1972).

S-7 Solan, G. M., Handschuh, J. A. and Bergeron, P. A., "Maine Yankee Cycle 4 Design Report," YAEC-1171, (January 1979).

T-1 Turner, S. E., Elgin, W. J. and Mowery, A. L., "Historical Survey of U.S. LWR Fuel Utilization," Trans. Am. Nucl. Soc., 33, 390-391, (November 1979).

W-1 Williamson, E. A., Terney, W. B. and Huber, D. J., "Interactive Fuel Management Using a CRT," Trans. Am. Nucl. Soc., 30, 341, (November 1978).